Fall 12-17-2011

Self-Assemblies Driven by the Hydrophobic Effect

Haiying Gan
joycegan2005@yahoo.com

Self-Assemblies Driven by the Hydrophobic Effect

A Dissertation

Submitted to the Graduate Faculty of the
University of New Orleans
in partial fulfillment of the
requirements for the degree of

Doctor of Philosophy
in
Chemistry

by

Haiying Gan

B.S. Northwest University of China, 2001

December, 2011

ACKNOWLEDGEMENTS

It is my pleasure to express appreciation to my advisor, Professor Bruce C. Gibb, who continually supports and guides my research with his immense knowledge. I would like to thank the members of my research committee, Dr. Mark Trudell, Dr. Guijun Wang, Dr. Steven Rick, and Dr. John Wiley for their assistance and guidance.

I owe my gratitude to Corinne Gibb for passing to me her knowledge and extensive experience of NMR and ITC. I am indebted to my many colleagues of the Gibb research group who supported me.

I give special appreciation to the entire chemistry faculty of the University of New Orleans for their guidance. I also would like to thank the University of Michigan and University of Texas, Austin who supported me as a visiting student after hurricane Katrina.

I also give my hearty appreciation to Mr. and Mrs. Harvey Vredeveld, Mr. and Mrs. Jim Carlson for their kindness, caring, and generous help after hurricane Katrina. All my Ph.D work and this dissertation would have remained a dream had it not been for the love, encouragement, and support of my husband Bradley Vredeveld.

TABLE OF CONTENTS

List of Figures

List of Schemes

List of Tables

ABSTRACT

Water is a simple molecule but is an essential part of life. One key aspect of the properties of water is the hydrophobic effect, and whilst there is an appreciation of this phenomenon at the macro-scale (raindrops falling off leaves) and the micro-scale (the structure of cellular systems), a complete understanding at the molecular level still eludes science. Addressing this issue, our studies involve synthetic supramolecular compounds that assemble in water via the hydrophobic effect.

First of all, a novel water-soluble deep-cavity cavitand was synthesized. It possesses four *endo* methyl groups on top rim of the cavitand, eight water-solubilizing carboxylic acid groups coated on the cavitand exterior, and a relatively large hydrophobic interior. Compared to a previous well-studied water-soluble deep-cavity cavitand octa-acid (OA), this novel cavitand (TEMOA) possesses a non-monotonic assembly profile in the presence of a homologous series of straight-chain alkanes. Three supramolecular species were observed: 1:1, 2:2, and 2:2 and they are approximately isoenergetic. Second, we examined the guest-controlled self-sorting in assemblies. A mixture of OA and TEMOA formed hetero-capsular complex driven by the hydrophobic effect. The extent of homo- or hetero-dimerization is intimately tied to the size of the guest being encapsulated. TEMOA is less predisposed to dimerize than OA, thus TEMOA possesses the ability to form various self-assembled states, such as tetrameric and hexameric assemblies. Furthermore, we also discussed our observation of how external stimuli such as changing the nature or concentration of a co-solute salt influences a unique, unusual transition from one assembled state to another.

Keyword: self-assembly, hydrophobic effect, diffusion constant, hydrodynamic volume, salt

I. Introduction

1.1 Non-covalent Interactions in Water

Non-covalent interactions, which can make molecules "stick" together, play an essential role in the structures of DNA, proteins, and other biomolecules. They are also the dominant type of bonds in supramolecular chemistry. In contrast to covalent bonds, non-covalent interactions refer to attractive intermolecular forces. In this introduction we will focus on a few typical non-covalent interactions prevalent in water: ion-pairing interactions, ion-dipole interactions, hydrogen bonding, and π effects. We will also discuss the hydrophobic effect.

1.1.1. Ion Pairing Interactions

Electrostatic factors played dominant or important role in most non-covalent interactions. The definition of an electrostatic interaction discussed here is a strictly Coulombic attraction or repulsion between charges or partial charges that exists without change before or after the interaction.

Since the majority of reactions carried out by organic chemists occur in solution, selection of appropriate solvent(s) to assist reactions is essential. Chemists often examine the dielectric constant (ε) of a solvent to determine its polarity, the higher ε values the greater the polarity. It also gives information about how well the solvent screens electrostatic forces. Coulomb's law, which describes the electrostatic energies between full and partial charged molecules (solvent or solute), has ε in the denominator (Eq. 1.1).

$$E = \frac{q_1 q_2}{4\pi\varepsilon\varepsilon_0 r} \qquad \text{(Eq. 1.1)}$$

Where q_1 and q_2 are two charges, r is the distance between the two charges, E is the attractive or repulsive potential energy, ε_0 is electric constant. It demonstrated that many factors can influence the energy of attraction between an ion pair: the distance between an ion pair, the dielectric constant of the solvent, and the size and shape of the cations and anions. For instance, the decreasing of the energy of an ion pair is significant when moving the pair form gas phase (ε = 1) to an organic solvent (ε < 10), whereas in water (ε = 78) is substantially attenuated.

The ion pairing interaction is a particularly strong intermolecular interaction between a cation and an anion. In the gaseous phase the forces between an ion pair can be over 100 kcal mol^{-1}. An ion pair separated by a close distance can have an electrostatic attraction that is larger than the thermal energy available to separate them. In other words, the ions stays associated longer than the time required for Brownian motion to separate non-interacting species.[1] On example is that NaCl is fully dissociated in water. The Na^+ and Cl^- are far apart from each other and are also hydrated by water molecules with ion-dipole interactions (*vide infra*). In totality, ion pair formation can be viewed as a competition with ion solvation as a means to lower the Gibbs free energy of the solution.[1]

1.1.2. Ion-Dipole Interactions

The ion-dipole interaction is a type of intermolecular interaction that results from the electrostatic attraction between an ion and a neutral molecule that has a dipole. Coulomb's Law also can be applied to demonstrate the strength of this type of interactions (Eq. 1.2).

$$E = -\frac{Q\mu cos\theta}{4\pi\varepsilon\varepsilon_0 r^2} \qquad \text{(Eq. 1.2)}$$

where μ is the dipole moment, θ is the angle between the charge and dipole. Ion-dipole

interactions are commonly found in polar solutions of ionic compounds. When a charged solute is dissolved in a solvent with a dipole moment, the electric field associated with the charge exerts a force on the dipole, orienting the oppositely charged end of the dipole toward the charge. The attractive force can be quite large for a polar solvent molecule in direct contact with an ion. Also, important solvation trends are evident in considering the simple ions. A clear trend in hydration energies emerges, the smaller the ion, the greater the hydration energy. As considering these ions as spheres of charge, the smaller ion has the same total charge as a larger ion, but it is distributed over the surface of a smaller sphere. Thus, the charge per unit area is larger, and so Coulombic interactions are stronger.[1]

In aqueous solution, cations and anions can be solvated by water molecules that are organized in a different way than pure water. One common example of this ion-dipole interaction is the aqueous solution of NaCl (**1**) – the interaction between sodium ion and polar water molecule (Figure 1-1). The introduction of a NaCl into aqueous solution is accompanied by the creation of a cavity in order to accommodate the solute. The change in the average number of hydrogen bonds a water molecule participates in, ΔG_{HB}, due to the presence of an ion (or a solute) in solution is linearly related to the water structure breaking and making properties of ions such as alkali metal and halide ions.[2] Ions having $-0.024 \leq \Delta G_{HB} \leq 0.024$ (in cal mol^{-1}) are to be considered as neither significantly breaking nor making water structure, eg. Na^+, Ag^+, Et_4N^+, $H_2PO_4^-$. Ions having $\Delta G_{HB} \leq -0.024$ are considered water structure breakers. In general, the bulkier the ions (mostly are anions) the more negative the ΔG_{HB}. Ions having $\Delta G_{HB} \geq 0.024$ are water structure makers, such as ions having larger electrostatic field with high charge and small size (thus these have stronger Coulombic interactions). As an exception, the hydrophobic tetraalkyl ammonium and similar ions with alkyl chains or aryl rings behave differently, they induced a clathrate type of water structure around them rather than centrally oriented as for the other high-field ions.[3]

The structure of water is also affected by the nature of the present ion pairs. The process of solvating ions in water cannot be simply demonstrated as an entropically costly process. Krestov has addressed the structural entropy, called ΔS_{struc}, which is obtained by subtraction of the entropy contribution of the primary hydrating water around an ion from the total standard molar entropy of hydration.[2,4,5] Ions acting as water structure breakers have $\Delta S_{struc} > 0$ whereas water structure makers have $\Delta S_{struc} < 0$. The values of ΔS_{struc} highly correlate with temperature. With increasing the temperature, the value of ΔS_{struc} can diminish for certain ions. Some ions can even change the character from a water structure makers to structure breakers. For instance, Na^+ is a water structure maker at 25 °C while it becomes a water structure breaker at 20 °C. In contrast, K^+ or S^{2-} are water structure makers at 25 °C while they become water structure breakers at 70 °C.

Ion-dipole interactions also play an important role in supramolecular chemisty. For instance, the existence of the weak chemical bonds between alkali metal cations and ether oxygen atoms determined the binding of alkali metal cations inside crown ethers **2** (Figure 1-1). Ion-dipole interactions also include coordinative bonds between non-polarisable metal cations and hard bases.[6] Certain transition metal cations such as Cu(II) or Pd(II) can accept the electrons donated by polar ligands and result in the metal-ligand coordination which is extensively applied in supramolecular chemistry (*vide infra*).

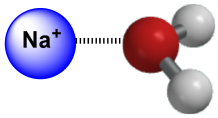

The Hydration of Na^+

1

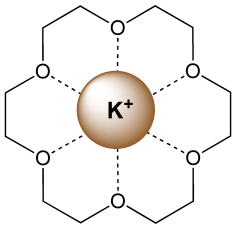

K^+ crown ether complex

2

Figure 1-1. Ion-dipole interactions between 1) Na^+ and water; 2) K^+ and crown ether.

1.1.3. Dipole-Dipole Interactions

The interaction between dipoles on solutes and solvents is analogous to the interaction between a dipole and a charge. It can be attractive or repulsive. The polarizing field of dipole-dipole interactions comes from a permanent dipole.[7] If a dipole μ is fixed in space and oriented at an angle θ to the line joining it to a polarizable molecule, the interaction energy falls off as a function of the inverse distance between the dipoles to the third power. In this case, the dipole-dipole interaction is very sensitive to the distance r between dipoles.[1] Eq. 1.3 gives the energy between two fixed dipoles that are in the same plane and parallel where μ_1 and μ_2 are the two dipole moments.

$$E = \frac{-\mu_1\mu_2(3cos^2\theta-1)}{4\pi\varepsilon\varepsilon_0 r^3} \qquad \text{(Eq. 1.3)}$$

1.1.4. π Effects

π effects are a type of non-covalent interactions that involves π systems. The strength of these interactions covers a wide range from extremely strong to very weak. Specific types of

π interactions include: the cation- π interaction, the polar- π interaction, and π donor-acceptor interactions.

The cation- π interaction is the non-covalent interaction between a cation and the face of a simple π system, such as benzene. Water molecules have a dipole moment in which we can describe an interaction between an ion and the electrostatic model of water as an ion-dipole interaction. In contrast π systems such as benzene and ethylene have no dipole moment but have a quadrupole moment. By viewing the electrostatic potential surfaces of these molecules with π systems, for benzene, the electrostatic potential surface is negative on the face of the aromatic ring and positive along the edges. It is evident therefore that cation should be attracted to the face.[1]

The strength of cation-π interactions can be linked to solvent effects. We would expect this interaction to be attenuated in water. This is true to some extent, but the weakening of the strength in water is much less than expected. In other words, water is much less effective at attenuating a cation-π interaction than an ion pair or a hydrogen bond. This probably can be viewed from two reasons. First, is the nature of molecules with π systems. Benzene is hydrophobic. Cation – π interactions allow one face of benzene to be covered by the cation rather than with water. The second reason concerns the long-range solvation of the counter anion by water. The solvation energy can be described as the Born equation (Eq. 1.4), which is a simple model involving the dielectric constant (ε), the ionic radius (a), and the charge of the ion. For the model of long range solvation we can consider the distance between ion and the effected water to be over two or three solvation shells, and this distance can be treated simple as the ion radius.

$$E_{sol} = -(1 - 1/\varepsilon)(q^2/8\pi\varepsilon_0\, a) \qquad \text{(Eq. 1.4)}$$

In the case of solvating a cation-π system, such as a cation bindibg to a benzene ring, the system remains full positively charged regardless of the separation between the interaction cations and benzene. This makes the application of full Born solvation possible.

A polar-π interaction occurs when a conventionally polar molecule interacts with the quadrupole moment of a π system. The aforementioned face of electrostatic surface of benzene ring tends to associate with any hydrogen bond donor with a favorable electrostatic interaction. For instance, the binding energy between water and benzene is 1.9 kcal mol^{-1} in the gas phase with the water hydrogen pointing to the face of the benzene ring. Although this type of interactions is weaker than the cation-π interaction, they also play essential role in the protein structures and solid state packing interactions.[1]

In general, the π···π interaction refers to aromatic-aromatic interactions, interactions that can be observed between simple aromatic rings. Like benzene, the face of an aromatic surface has negative electrostatic potential and positive electrostatic potential along the edges. This makes two benzene rings stack with an edge-to-face orientation (T-shape) or a displaced orientation (slip stacked) instead of face-to-face orientation (stacked form, Figure 1-3). The edge-to-face and displaced orientations are more energetically favored even in water, because of the hydrophobic effect (*vide infra*). In some complicated structures in water, if the edge-to-face orientation could be favored, a displaced orientation will be favored with positive electrostatic potential edges aligning with the negative electrostatic potential faces.

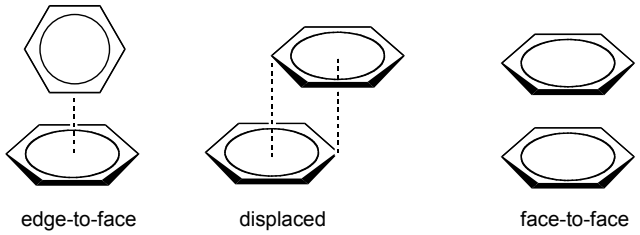

Figure 1-2. π···π interaction geometries.

1.1.5. van der Waals Interactions

van der Waals interactions include attraction between atoms, molecules, and surfaces. They are the sum of the attractive or repulsive forces between non-polar molecules. van der Waals interactions are a combination of three distinct types of forces: the induction force, the orientation force, and the dispersion force. Dispersion forces is a type of force acts between all atoms and molecules, even totally neutral ones.[7] They make up dominant contribution to the total van der Waals interactions between atoms and molecules. They are present in many important phenomena such as adhesion, surface tension, wetting, and physical adsorption.

The London theory has generally been applied in dispersion forces. However, two serious shortcomings have always been concerned. First, it assumes that atoms and molecules have only a signal ionization potential. Second, it cannot handle the interactions of molecules in a solvent.[7] A general theory of van der Waals interactions between molecules was present by McLachlan in 1963. This theory included the induction, orientation and dispersion force in one equation. Moreover, it could also be applied to interactions in a solvent medium and interactions of molecules or small particles in a medium.

Unlike the straightforward electrostatic interactions involving charged or dipolar

molecules, van der Waals forces are not generally pairwise additive, the force between any two molecules is affected by the presence of other molecules nearby.[7] Thus the total interaction energy cannot be simply obtained by adding all the pair potentials of a molecule to its net interaction energy with all the other molecules. This property is particularly important in the interactions between large particles and surfaces in a medium.

1.1.6. Hydrogen Bonding

Hydrogen bonding is another important non-covalent interaction. Weak and moderate hydrogen bonds can be describes as a Coulombic attraction between a polar donor bond ($D^{\delta-}$-$H^{\delta+}$) and an acceptor atom ($:A^{\delta-}$) (short-strong hydrogen bonds are not applicable in this model). There are many factors that can intensify the electrostatic attraction, such as solvent effect, electronegativity, resonance, and polarization. The strength of a hydrogen bond is strongly dependent on the nature of both the donor and the acceptor, and the microenvironment of the hydrogen bond. In general, we can divide the hydrogen bond strengths into three categories. The very strong hydrogen bonds bear the energy between 15 to 40 kcal mol^{-1}, the moderate hydrogen bonds are in the range of 5 to 14 kcal mol^{-1}, whereas the weak hydrogen bonds which are the most common have energy between 0 to 4 kcal mol^{-1}. According to Coulomb's Law, in the case of one or both of the partners is charged, the electrostatic attraction can increase substantially.

Another factor of considering the strength of hydrogen bonding is geometry. One of the most common examples of hydrogen bond is those formed in water. Water consists of one highly electronegative oxygen atom and two weakly electropositive hydrogen atoms. This structure allows water molecules to form a hydrogen bond between the partially positively charged hydrogen and the partially negatively charged oxygen of a neighboring water molecule.

This property of water allows significant H-bond between water molecules.

In the tetrahedral ice lattice structure (Figure 1-2), each water molecule is surrounded by four hydrogen-bonded neighbors, two as the H-bond donor and two as the H-bond acceptor. The water molecule at the centroid of the tetrahedral lattice has a distance of 2.75 Å to the water molecules that are located at the vertices of a tetrahedron. The distance between two vertices is ca. 4.5 Å and the H-O···O angle for the H atom on the vertex makes the smallest angle of 109.4° with O atom at the centroid. This H-bond angle is revealed to be very dependent on the structure of water.

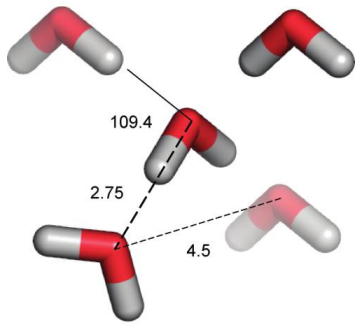

Figure 1-3. Tetrahedral arrangement and dimensions in the ice lattice structure.[8] (See copyright permission in appendix)

In the presence of solutes with different properties, water structure varies. Studies have showed that the changes of heat capacity (ΔC_p) correlate with the changes of this H-bond angle.[9] "Dissolving" apolar solutes increases the population of more linear water-water H-bonds with larger water-water interaction energy, thus the hydration heat capacity of solvating water increases. For polar solutes, they interact with water weakly with more bent water-water H-bonds. This produces lower water-water interaction energy, thus resulting in a decreased C_p. Also, the effects are largely dependent on the solvent accessible area of the solute.[8] For instance, a comparison of $\Delta_{hydr}C_p$ between inorganic ion, such as K^+, and tetramethylammonium

(TMA^+), a so-called hydrophobic ion, revealed the subtle solvation effects upon the changes of these water-water H-bond angles. Although TMA^+ is soluble in water, it increases the hydration heat capacity rather than decreases it ($\Delta_{hydr}C_p$ = 16 cal mol^{-1}), whereas K^+ decreases the heat capacity rather than increase it ($\Delta_{hydr}C_p$ = -16 cal mol^{-1}).[2] This behavior is seen from the angular structure that TMA^+ promotes more linear water-water H-bonds while K^+ promotes more bent H-bonds.[9,10] Also the effects of solutes are highly dependent on the first coordination shell of water. In other words, the effects of hydration C_p are proportional to polar and apolar solvent-accessible areas of solutes.[11]

1.2. The Hydrophobic Effect

Although the application of the Coulomb's Law can provide the electrostatic energy for non-covalent interactions involving electrostatic attractions as their origin, the hydrophobic effect is a deviation from this theme. It cannot be simply describe as one type of non-covalent interaction. It is a combination of dipole-dipole interactions, hydrogen bonds, and van der Waals interactions between water-water molecules. Polar water molecules can form an unusual large number of intermolecular hydrogen bonds that can lead to strong attractive forces between water molecules. The hydrophobic effect is a phenomenon of segregation between simple organics such as hydrocarbons and water. Hydrophobic effects are very important in membrane and micelle formation, protein folding, ligand-protein and protein-protein binding.[12] They also play key roles in the binding of organic guests by water-soluble hosts.

Although the basic principle of this ubiquitous phenomenon has been extensively studied, a complete understanding of this fundamental topic is still elusive. In order to understand the mechanism of how the hydrophobic effect occurs, extensive studies on the structure of water

molecules involving hydrophobic solutes have been accomplished. Fisicaro *et al*.[13] demonstrated that the solubilization process of noble gases or methane involves creating a cavity in the solvent by extruding water molecules. When dissolving a hydrophobic solute, three forms of water molecules were addressed in their study. Form I is bulk water that is held together by weak hydrogen bonds and form a structure of low density. Form II is water molecule with a cage-like structure around the solute. Water molecules with this form are held together by stronger hydrogen bonds and form a structure of high density. Type III water molecules are the isolated water and relaxed around the solute within the cage and surround the solute. Fisicaro *et al.* also addressed the process of solubilizing a hydrophobic solute is also associated to an entropy/enthalpy compensation linearly correlated with the temperature. Guillot and Giussani[14] applied molecular dynamics calculations of the solubility of small gases (noble gas and methane) in the evaluation of the temperature dependence of hydrophobic hydration. They found that in the absence of a hydrophobic solute, water molecules are able to exist as a distorted pentagonal dodecahedron structure whereas these structures collapse rapidly when the boiling point is reached.

Chandler[15] addressed different regimes and theories of the hydrophobic effect. Several factors are involved in the physical origin of this topic. First is the high surface tension of water. The very strong interaction between water-water molecules makes a significant penalty for creating a cavity in water. Although water has high surface tension, liquid water is dynamic and is not maximally hydrogen bonded. The rigid structure with four hydrogen bonds per water molecule is only seen in the solid structure. Water loses its favorable water-water contacts after dissolving organic molecules. In a system with small alkanes (particle radius ~ 0.4 nm, such as methane), water molecules create a cavity with the smallest excluded volume to accommodate this hydrophobic particle with each water molecule participating in four hydrogen bonds. In this case, a modest thermodynamic cost is enough to trigger the water reorganization. Instead of

breaking hydrogen bonds, this hydration of a small solute only re-orders hydrogen bonds. Thus this hydrophobic solute is coated by water molecules without creating an interface in which the solute is considered to be hydrated. With increasing the size of hydrophobic particle or cluster, the resulting large cavities are dehydrated because the cluster is sufficiently large and the hydrogen bonds cannot simply surround the hydrophobic cluster. The broken hydrogen bonds lead to the liquid moving away from the cavity and an interface between the solute and water is created. The second factor behinds the hydrophobic effect is van der Waals interactions between the non-polar hydrocarbons. Although van der Waals interactions are relatively weak (-0.024 to -0.24 kcal mol^{-1}), when dealing with contacted surfaces of macromolecules or proteins, several hundreds van der Waals interactions may be involved. van der Waals interactions of a correctly folded protein molecule could therefore sum to hundreds of kcal mol^{-1}. On the other hand, van der Waals interactions between water and non-polar solutes are weak attractive weak interactions, they are too weak to affect the existence of interfaces in water but they do affect the position of an interface.[15] Third, hydrocarbons are polarizable and water is not which makes water molecules tend to interact with each other.

In the regime of supramolecular chemisty, a few synthetic molecular and supramolecular hosts bear a hydrophobic cavity. Introducing a guest to the system tends to stabilize the water molecules by excluding the water molecule from the hydrophobic pocket to the bulk. Within the cavity, the water molecules do not interact strongly with the hydrophobic walls and are therefore of high energy.[16]

1.3. Water-soluble Molecular Hosts and Self-Assembled Supramolecular Hosts

The fundamental discovery of crown ethers by Pedersen in 1967[17] pioneered the extraordinarily rapid development of a new phase of chemistry – supramolecular chemistry. It

includes molecular self-assembly, folding, molecular recognition, mechanically interlocked molecular architectures, dynamic covalent chemistry, and host-guest chemistry. In the past forty years, extensive studies on the chemistry of synthetic hosts for the selective complexation of organic and inorganic guests have been reported with prominent implications. Without doubt, the design and synthesis of water-soluble molecular hosts is becoming a new stream in the development of supramolecular chemistry. The most well characterized water-soluble molecular and supramolecular hosts are cyclophanes, cyclodextrins, cucurbitrils, metal coordinate hosts, and cavitands. We summarize these below.

1.3.1 Cyclophanes

Cyclophanes consist of aromatic units linked together through suitable bridging and spacer groups.[18,19] Although Stetter and Roos[20] reported the first approach to the synthesis of systems with binding sites for apolar molecules and recognized the potential of cyclophanes of inclusion complexation, a later report by Koga provided direct evidence for inclusion.[21] Host **3b** was synthesized by Koga and co-workers using a two-step procedure.[22] *N, N'*-ditosyl-4,4'-diaminodiphenylmethane **4** and tetramethylene bromide were cyclized in DMF in the presence of potassium carbonate under high dilution condition to give **3a** in 25% yield (Scheme 1-1). Detosylation of **3a** gave **3b** in 67% yield. Host **3b** was soluble in water below pH = 2. In its acidic solution, **3b** and 1,8-ANS formed 1:1 complex with the association constant of K_a = 6.25 × 10^3 M^{-1}.

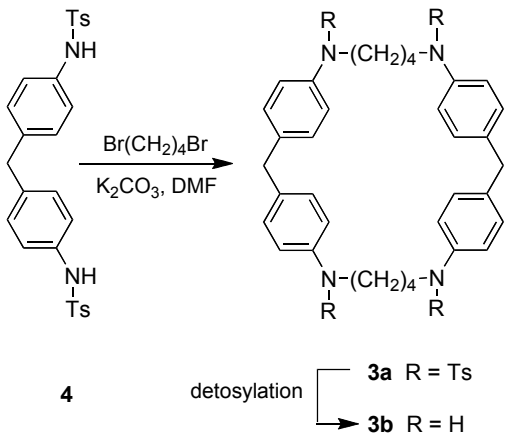

Scheme 1-1. Synthesis of water-soluble cyclophane **3b**.

Further modifications on the structure of cyclophanes expanded their applications to numerous areas. Varying the aromatic units, the bridging unit, or the spacer group, are other approaches to adjust the binding properties of these hosts. In the case of varying the aromatic units, Akkaya and co-workers synthesized calixpyridinium tetracation **5**, an cationic receptor, and observed very strong interactions between the positive charged host **5** and the fluorescent guest (HPTS). The binding of the guest induced the fluorescent quenching and their further studies showed the displacing HPTS by 5'-ATP turned the fluorsence "on" which indicated host **5** can selectively bind between these two guests (Scheme 1-2). [23]

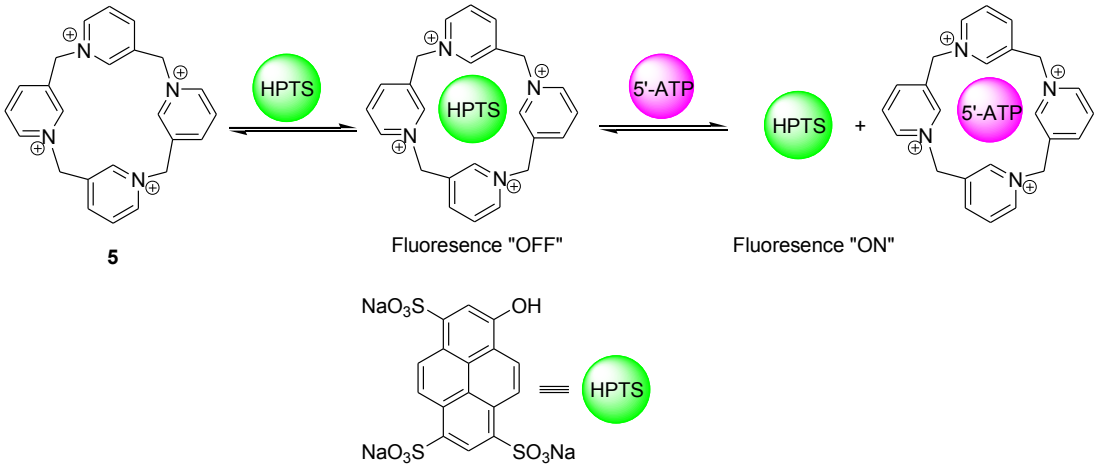

Scheme 1-2. 5'-ATP recognition by cyclophane **5**.

Also, adding metal centers to the system to create additional non-covalent interactions such as metal coordinations and cation-π interactions will greatly increase the binding association between the host and guest. One example, Fabbrizzi and co-workers[24] designed a dicopper cyclophane **6** (Figure 1-4). Introducing this metal ion binding core enhances the tendency of coordinating anionic guests. Host **6** is capable of binding polyatomic anions within its intermetallic cavity in an aqueous solution at pH of 8. They have previous demonstrated that the distance between two consecutive donor atoms, so-called "bite length", plays a crucial role in ion selectivity.[25] A survey of a variety of ambidentate anions such as NCS^-, NO_3^-, SO_4^{2-}, HPO_4^{2-}, $HCOO^-$, CH_3COO^-, N_3^-, NCO^-, HCO_3^- revealed that N_3^-, NCO^-, and HCO_3^- showed stronger affinity to the cavity than the other anions. This result is attributed to the appropriate bite length of the triangular HCO_3^- and linear triatomic ions N_3^- and NCO^-. In a later example, Fabbrizzi and co-worker reported an analogous cyclophane **7** (Figure 1-4), which successfully detected pyrophosphate (PPi) from phosphate and other small inorganic anions in neutral aqueous solution using an on/off fluorescent response.[26] In virtue of the potentiality of this type of cyclophane, Taglietti and co-workers designed a larger analogous cyclophane host **8** (Figure 1-4) which is able to distinguish micromolar concentrations of ATP from other millimolar

quantities of the other classical neurotransmitters at neutral pH water solution.[27]

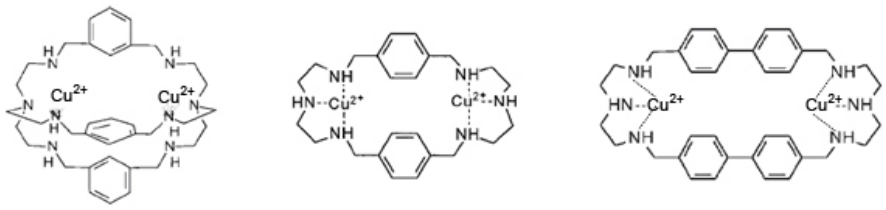

6 **7** **8**

Figure 1-4. Water-soluble cyclophanes **6**-**8** with copper (II) center.

1.3.2 Cyclodextrins

The host-guest chemistry of cyclodextrins (CDs) has developed steadily over the past century. CDs are a group of macrocyclic host molecules, the most common of which, having 6, 7, or 8 D-glucose convalently linked by α-1,4-glucose bounds, are so-named α-CD, β-CD, γ-CD, respectively (Figure 1-5).[28,29] CDs with fewer than six glucose residues are too strained to exist, whereas those with more than eight residues are very soluble, difficult to isolate, and hardly studied to date. α-CD, β-CD, and γ-CD are commonly referred to the native CDs.[30] They have an average structure of a truncated cone with hydrophobic cavity, while the rims formed by the primary and secondary OH groups possess a hydrophilic character. Because these water-soluble molecules have rigid and well-defined structure, they have been tremendously applied in molecular recognition of organic, inorganic, and metalloorganic compounds that may be neutral, cationic, anionic, or even radical.[31] Usually, smaller molecules can be trapped within their cavity forming host-guest complexes. This feature of CDs makes them excellent hosts for molecular recognition. For instance, γ-CD derivative has been used as a reversal agent (or antidote, antagonist) to a biologically active drug.[32]

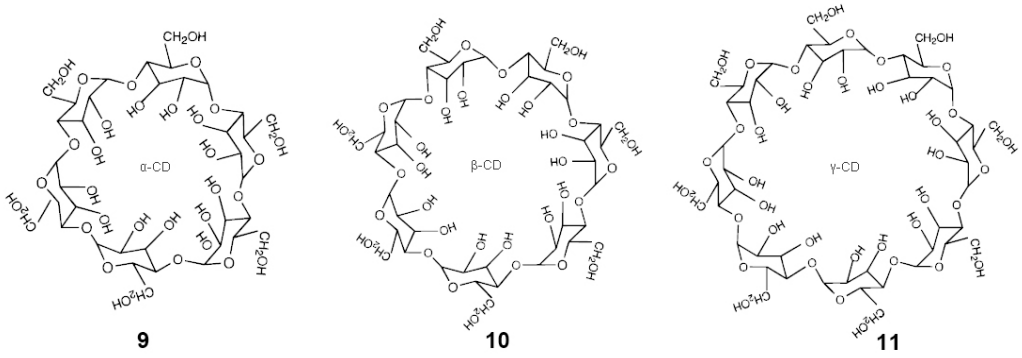

Figure 1-5. Structures of natural cyclodextrins **9** - **11**.[30]

All CDs are truncated cone-shaped molecules with two portals to the hydrophobic interior. The larger portal is ringed by secondary alcohol, named the secondary face, and the smaller portal is the primary face. All of the CDs are 780 pm in height. Their cavity diameter ranges between ca. 500 pm and ca. 800 pm (Figure 1-6).

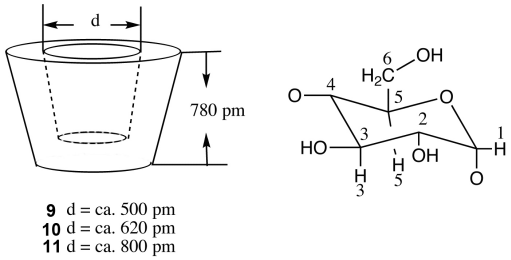

Figure 1-6. Dimensions of Cyclodextrins **9** – **11**.

The native CDs tend to weakly self-associate in aqueous solution. The solubility of β-CD (25 °C, 16.3 mM) is around 10 times less than α-CD and γ-CD (25°C, 121.1 mM and 168 mM respectively). According to Coleman *et al*.,[33] the low solubility is due to the interruption of the hydrogen-bond structure of water by aggregated β-CD with its 7-fold symmetry, whereas the even symmetries do not behave in this way. This explanation does not apply to the relatively

high solubility of δ-CD, which contains nine glucose units.[30,34] Szejtli[35] attributed its low solubility to the intramolecular hydrogen bonds of the β-CD rim. Further research, such as alkylation of β-CD hydroxyls, leads to increases in solubility and these attempts stimulate motivation for carrying out such chemical modifications.

Due to the structure of CDs, they have been widely applied in the studies of molecular recognition,[36-38] nanomaterials,[39,40], protein recognition,[41,42] and drug delivery and removal.[32,43-45] Water molecules that are included in the hydrophobic cavity of CDs cannot fully form hydrogen bonds with the hydrophobic wall of CDs and are energetically less stable than bulk water molecules. By introducing a guest molecule of suitable size, water molecules in the CD cavity will be replaced by the guest molecule. When a guest molecule is larger than the cavity space of CD, it will partially embed in the cavity. The release of the water molecules from the cavity to bulk water[46-48] and the conformational changes or strain release of the CD upon complexation are two main factors[38] that contribute to the complexation thermodynamics of CDs.

Complexation reactions involving CDs are extremely important for understanding general inclusion phenomena. Rekharsky *et al*.[38] reviewed several classes of compounds which can be included in natural CDs, and demonstrated the general trends of the thermodynamic quantities for these complexation reactions. For instance, in these systematic thermodynamic studies, thermodynamic quantities such as the standard Gibbs free energy change (ΔG^o), enthalpy (ΔH^o), and entropy (ΔS^o) are plotted against the number of aliphatic carbon atoms (N_C) in guest molecules (Figure 1-7 for β-CD). By examining the inclusion thermodynamics, interesting information can be obtained. For example, as Figure 1-7 shows ΔG^o and ΔH^o values become more negative with increasing N_c for all combinations of guests and β-CD. The slop of the plot in Figure 1-7, $d\Delta G^o/dN_C$, provides further insight of the stability of the host-guest complexes upon increasing N_C. Figure 1-7 shows that the slope remains

almost constant up to N_C = 10. This length of the guest exceeds the depth of β-CD (7.8 Å) and indicates that guests longer than the depth of β-CD only partially accommodate inside the hydrophobic cavity. Guests with amphiliphatic groups of $N_C \geq 7$ will have at least one methylene group protruding out of the hydrophobic cavity and exposing to the water. This results in the reduced van der Waals interactions between the guests and the inner wall of cyclodextrin. The idea of "expanded hydrophobic cavity" is also used to describe this behavior. In the study of complexation thermodynamics of β-cyclodextrins, adding a methylene group to the guest molecules leads to the average of ΔG^o increment of -2.8 kcal mol^{-1}. This energy difference indicates that the difference in the binding affinities between two host-guest pairs is greater than 100. In other words, this difference of the binding energy is sufficient to switch the complexation from one to the next guest in the homologous series with a selectivity greater than 95%.

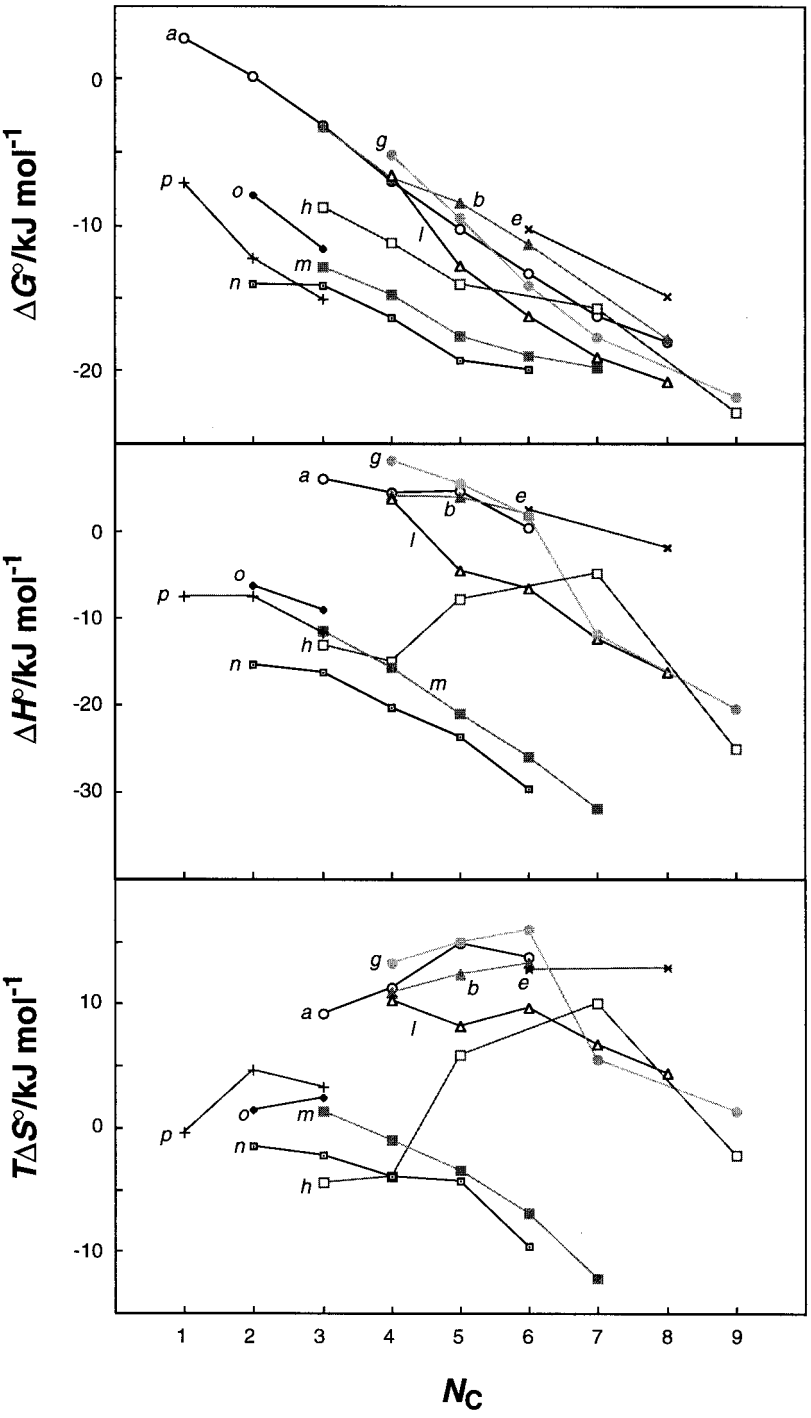

Figure 1-7. Thermodynamic quantities (ΔG^{o}, ΔH^{o}, and $T\Delta S^{o}$ at 298 K) for the complexation of various classes of guests with β-CD as a function of the number of methylenes (N_c) in guest molecules, the carboxyl carbons being not counted. (a) 1-alkanol (O), (b) *sec*-alkanol (▲), (e) alkylammonium (X), (g) alkanoate (●), (h) alkanoic acid (□), (l) cycloalkanol (Δ), (m) alkylbarbituric acid (■), (n) alkylthiobarbituric acid (⊡), (o) ω-phenlyalkylamine (◆), and (p) ω-phenylalkanoate (+). Permission License No. 2633161300884.

1.3.3. Cucurbiturils

Cucurbiturils (CBs), whose shape resembles a pumpkin, are a family of macrocyclic compounds obtained from a condensation of glycoluril (acetyleneurea) and formaldehyde in concentrated HCl. Although the synthesis is first reported in 1905 by Behrend *et. al*,[49] the study of these substances developed slowly due to its extremely poor solubility in most common solvents (the exception being strongly acidic aqueous solution. Furthermore, no method to introduce any functional groups to the molecule was known.[50] Until 1981, the first full characterization of the structure and chemical nature was reported by Mock and co-workers[51] who disclosed the remarkable macrocyclic structure comprising six glycoluril units and twelve methylene bridges (Scheme 1-3).

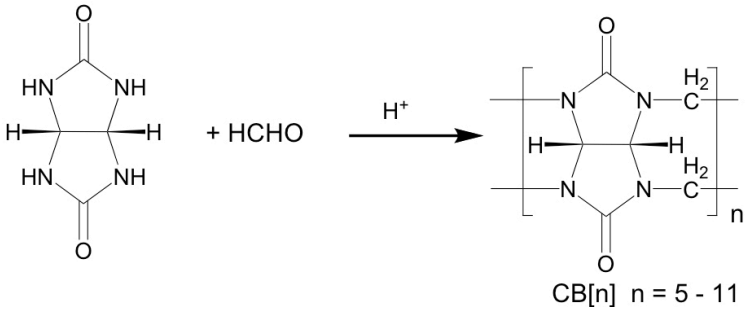

Scheme 1-3. Synthesis of CB[n] under acidic conditions.

From CB[5] to CB[10], the height of the cavity is 9.0 Á, with the mean diameter of the internal cavity increases progressively from ~4.4 to ~8.8 Á. The average diameter of the portal increases from ~2.4 Á to ~ 6.9 Á (Figure 1-8).[52] In term of cavity size, CB[6], CB[7], and CB[8] are analogous to α-, β-, and γ-CD, respectively. When the reaction was conducted under mild condition, Day and co-workers also isolated CB[5]@CB[10]. Isaacs and co-workers successfully isolated free CB[10] from this complex by replacing the guest CB[5] with melamine diamine followed by removal of the new guest through acylation and excessive washing.[53]

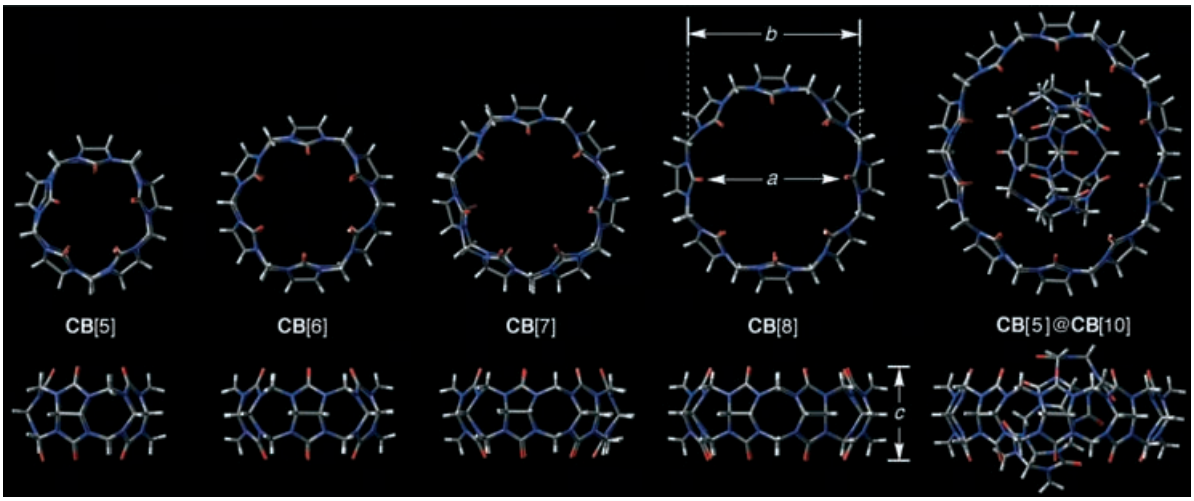

Figure 1-8. Top and side views of the X-ray crystal structures of CB[5], CB[6], CB[7], CB[8], and CB[5]@CB[10].[54] The various compounds are drawn to scale. (Permission License No: 2627791097898, 2642181099119)

The ion-dipole interactions of the portals with their rich hydrogen-bonding ability, and the covalent rigidity of the hydrophobic cavity of the host, contribute to the essential molecular recognition properties of CBs. Investigation of the binding properties involving neutral organic guests, charged organic guests, and metal ions with CB[6] is well studied. The binding ability of CB[6] generally equals or exceeds those of other well-known host molecules such as cyclodextrins and crown ethers. For instance, in the study of binding affinities between alcohols with CB[6] and α-CD, CB[6] forms stronger interactions with the guests (except hexanol) (Table 1-1).

Table 1-1. Calorimetrically determined log *K* values for the complexation of alcohols with CB[6] in HCO_2H/H_2O (1:1) at 25 °C and with α-CD in H_2O at 25 °C .[55,56]

	CH_3CH_2OH	$CH_3(CH_2)_2OH$	$CH_3(CH_2)_3OH$	$CH_3(CH_2)_4OH$	$CH_3(CH_2)_5OH$
CB[6]	2.64	2.61	2.53	2.73	2.71
α-CD	0.99	1.46	1.91	2.51	2.90

CB[6] possesses high binding selectivity due to its rigid structure and two binding regions that favor positively charged groups and hydrophobic residues. For instance, a series of stable host-guest complexes formed between CB[6] and alkyl amines of different chain length yield binding affinities with significant differences. Plotting the logK_a value against the chain length of the guests, Figure 1-9 shows that butylamine has 8-fold stronger binding affinity than propylamine and 4-fold stronger than pentylamine. While for a series of α,ω-alkyl diammonium ions, CB[6] prefers pentanediamine and hexanediamine relative to butanediamine and heptanediamine. Mock interpret this result as length-dependent selectivity of CB[6].[52] The property of high selectivity (guest size, shape, and polarity) of CB[6] has also been applied in molecular logic gate[57] and constructing molecular switches.[58]

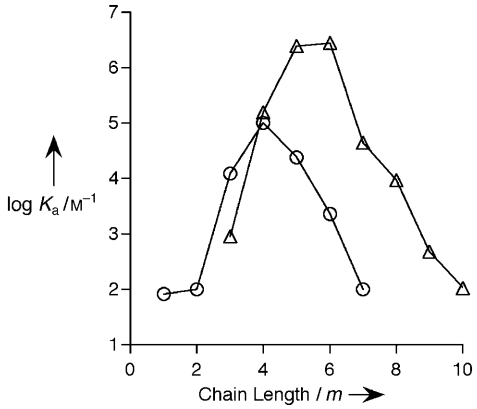

Figure 1-9. Relationship between the binding constant (log K_a) versus chain length m for $H(CH_2)_mNH_3^+$(O) and $^+H_3N(CH_2)_mNH_3^+$(Δ).[52]

Comparing the electrostatic potential of CB[7] with β-CD (Figure 1-10), CB[7] exhibits a preference to interact with cationic guests whereas β-CD prefers to bind to neutral or anionic guests.[50] The hydrophobic cavity of CB[7] is slightly more voluminous than that of β-CD, with its portals surrounded by polar carbonyl groups. These features lead to remarkable molecular

recognition properties. CB[7] can bind a wider range of guests than CB[6] and CB[5], and also it binds a variety of positively charged compounds such as adamantanes, bicyclooctanes, and ferrocene derivatives.

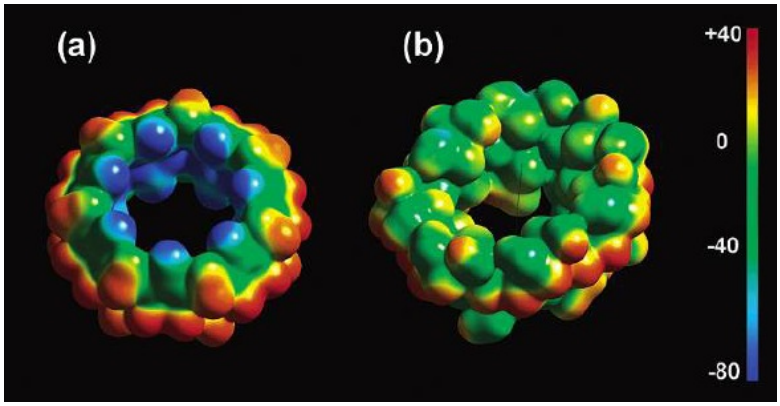

Figure 1-10. Electrostatic potential maps for a) CB[7] and b) β-CD. The red to blue color range spans -80 to 40 kcal mol^{-1}.[50] (Permission License No: 2643240970294)

CB[7] also retains the high selectivity as CB[6]. Kaifer and co-workers have demonstrated that CB[7] can reside in different locations along guests **12a** through **12i** which contain multiple binding sites (Figure 1-11).[59,60] The viologen nucleus of derivatives that contain shorter or hydrophilic groups enhanced the stability of these host-guest complexes whereas in the presence of guest **12c** and **12d**, the host prefers to reside on the longer butyl and hexyl chains and afford more stable complexes.

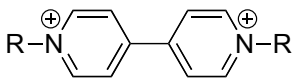

12a R = CH_3
12b R = nPr
12c R = nBu
12d R = n-C_6H_{13}
12e R = C_5H_6OH
12f R = $C_3H_6NH_2$
12g R = $C_{12}H_{25}$
12h R = $C_{16}H_{33}$

12i R =

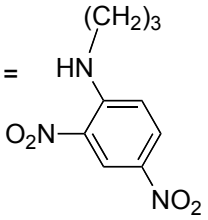

Figure 1-11. Guests containing multiple binding sites for CB[7] binding study.

Geckeler *et. al*. reported the formation of a weak 1:2 exclusion complex with C_{60} by high-speed vibration milling.[61] CB[7] has been used as an additive to separate positional isomers by capillary electrophoresis.[62] It also has been investigated in reducing toxicity in cancer treatment.[50,63-65]

1.3.4. Self-Assembled Metal Coordinated Hosts

Molecular containers such as cyclophanes, cyclodextrins, and cucurbiturils are molecular hosts constructed by covalent bonds. As an alternative strategy, reversible metal coordinative bond has played an important role in a variety of self-assembled supramolecular systems. As a pioneer of the research on the metal coordination hosts, Fujita has focused on the use of palladium or platinium ions, and principle ancillary ligands such as ethylenediamine derivatives. One of the best characterized supramolecular clusters is the M_6L_4 octahedral assembly cage **13** which is first reported in 1995.[66] This highly charged nanocage (overall charge +12) self-assembles from six Pd(II) complexes and four 2,4,6-tri-4-pyridinyl-1,3,5-triazine tridentate ligands (Scheme 1-4) and provides a hollow, hydrophobic cavity which is capable of binding

neutral organic molecules inside. These self-assembled hosts can function as molecular flasks and thus provide a hydrophobic reaction environment in aqueous solution for encapsulating reaction substances and bringing about novel reactions.

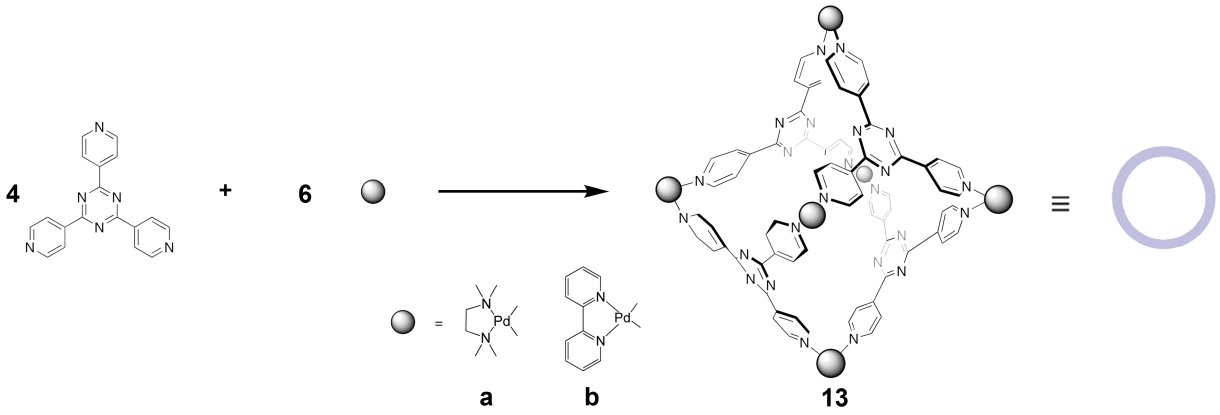

Scheme 1-4. Self-assembled coordination cage **13**.[67]

A recent successful application of nanocage **13a** is to bringing about an unusual regioselectivity in the Diels-Alder coupling of anthrancene and *N*-cyclohexylmaleimide in aqueous solution (Scheme 1-5).[68,69] In the absence of cage **13a**, the Diels-Alders reaction of anthracence generally yields an adduct bridging the center ring (9,10-position) of the anthracene framework[70-72] and results in the formation of high localization of π-electron density at that site.[73] However, in the presence of cage **13a**, two factors play essential roles in changing the course of this reaction: first, the increase in the effective molarity induced an increased rate of reaction; second, the steric constriction of the molecular flask force the reaction substrates into orientations that favor specific reaction at one of the terminal rather than central anthracene ring. The steric bulk of *N*-alkyl substituent such as *N*-cyclohexyl and *N*-cycloheptylmaleimide on the maleimide is essential to both the pair-selective recognition and 1,4-regioselectivity, while the less bulky *N*-propylmaleimide gives the 9,10 adduct.

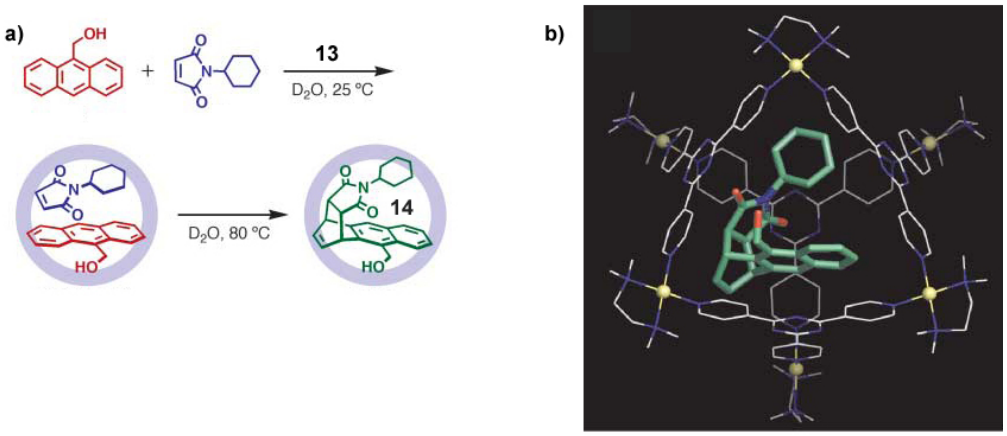

Scheme 1-5. a) Unusual regioselectivity of the Diels-Alder reaction of anthrancenes and *N*-cyclohexylmaleimide within **13a** in water and b) the X-ray crystal structure of **14@13a** (R=CH_2OH); guest: green C, blue N, red O; host; gray C, blue N, orange Pd.[68] (Permission License No: 2643280065525)

Utilization of cage **13** in photochemical reactions also has been investigated by the Fujita group.[74] Encapsulation of photochemical inert alkanes such as adamantanes and photoexcitation of the resulting complex under aerobic conditions, afforded a mixture of 1-adamantylhydroperoxide and 1-adamantanol in 24% yield.[74] Quickly quenched by O_2 and/or H_2O, the reactive radical species gave oxidation products **15** encapsulated within the hydrophobic cage **13** (Scheme 1-6).

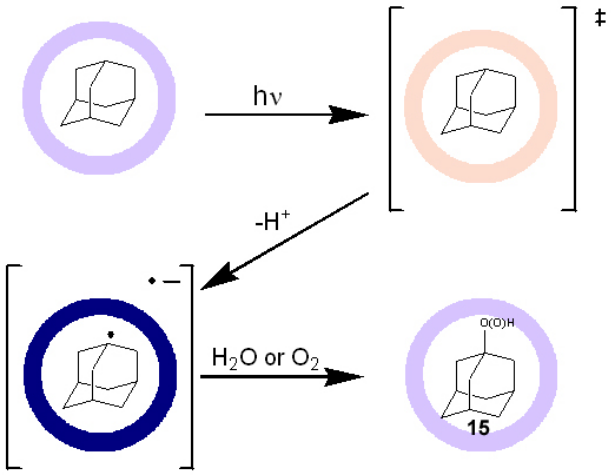

Scheme 1-6. Photo-induced oxidation of adamantane within **13** in water. Initial photoexcitation of the cage framework is followed by electron transfer from the adamantane to form the adamantly radical which is subsequently trapped by water or oxygen.[69]

The aforementioned studies all involve organic compounds as guests. In the absence of guest molecules, a T_d-symmetric adamantanoid $(H_2O)_{10}$ cluster termed "molecular ice" is formed within the hydrophobic cavity of **13**.[75] An X-ray structure analysis and neutron diffraction study show that instead of being sustained by any metal or anion coordination, the molecular ice is non-covalently accommodated in the hydrophobic cage with close contacts of 3.06 and 3.09 Å. The observed molecular ice bears similar structural parameters as I_c-type ice.[76-79] The molecular ice has average adjacent O···O distances 2.84 Å which is close to 2.74 Å in I_c-type ice. The O···O···O angles at the bridgehead (108.8 ~ 122.3º) are slightly larger than the ideal 109.47º, whereas those at the corners (96.7 ~ 104.1º) are slightly smaller than the ideal (Figure 1-12). Single-crystal neutron diffraction study reveals that the molecular ice accommodated inside the cage with a compressed conformation and it is formed not by a simple void-filling effect but by D_2O···π interactions. In this case, instead of following the rule that aromatic-systems donate electrons to the electron-deficient or cationic species, the molecular ice donates lone pair electrons to form a D_2O···π interaction with the ligands which, became of the electron withdrawing metal centers, are electron deficient. These highly organized water clusters are stable without "melting" at room temperature. With the introduction of guest molecules into the cavity, "melting" of the molecular ice gives free water molecules to the bulk. Fujita and co-workers suggested that the binding of guest molecules into the cavity is therefore entropy-driven.[80-82]

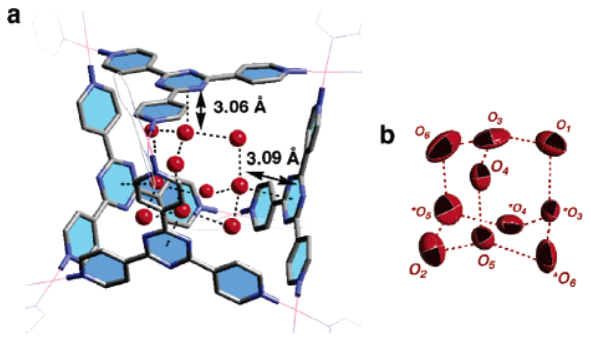

Figure 1-12. a) X-ray crystal structure of **13b** along with oxygen atoms (water molecules) around the cage. b) ORTEP drawing (50% probability ellipsoids) of 10 oxygen atoms (molecular ice) within **13b**. Interatomic distances (Å): O1-O3) 2.87, O2-O5) 2.78, O3-O4) 2.93, O3-O6) 2.72, O4-O5) 2.85, O5-O6) 2.92. (Permission License Number：2643411278484)

Another family of aqueous based metal coordinated supramolecular hosts is the tetrahedral M_4L_6 (M = Al^{3+}, Ga^{3+}, In^{3+}, Ti^{4+}, Ge^{4+} or Fe^{3+}, L = *N,N'*-bis(2,3-dihydroxybenzoyl)-1,5-diaminonaphthalene) assembly **16** studied by the Raymond group.[83] For trivalent metal vertices, the assemblies **16** have a charge total of -12 and the six naphthalene-based ligands coordinate to the four metal atoms to construct a supramolecular architecture with a cavity favorable of trapping small guest molecules (Figure 1-13). The volumes of the hydrophobic cavity range from 0.35 to 0.5 nm^3.[84-87] The affinity of the bound guests depends on their size, hydrophobicity, enthalpy of desolvation, and charge. Although each component of the assembly is achiral, the overall structure is intrinsically chiral. For example, a simple $[GaL_3]^{3-}$ catecholate complex exists in solution as two slow interconverting enantiomers (Δ and Λ) at temperature ranging between 273K to 340 K,[88] while in the case of the host $[Ga_4L_6]^{12-}$, the bis-bidentate catechol amide ligands coordinate the tridentate metal center by following the Bailar-twist mechanism that force the assemblies to be a racemic mixture of homochiral clusters with either the ΔΔΔΔ- or ΛΛΛΛ-configuration. With the encapsulation of a designed chiral guest, *N*-methylnicotinium cation (Nic), a complete resolve can be accomplished. Thus the enantiopure chiral clusters with ΔΔΔΔ-form precipitate out from methanol solution, while adding excess acetone to the remaining concentrated methanolic solution yields quantitative ΛΛΛΛ-form. Interestingly, introducing

NEt_4^+ ion to displace the chiral guests yields enantiopure ΔΔΔΔ and ΛΛΛΛ clusters with complete retention of chirality of the metal center.[89,90]

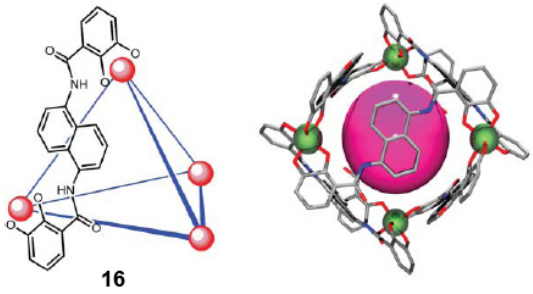

16

Figure 1-13. Left: M_4L_6 host **16** with six bisbidentate catechol amide ligands. Right: A generic spherical guest in an assembled tetrahedron host. (*Reproduced by permission of The Royal Society of Chemistry* http://dx.doi.org/10.1039/b603168b)

Although some water-reactive species, such as tripylium,[91] cationic phosphine-acetone adducts,[92] and iminium ions[93] are commonly stable in organic or acidic solution, Raymond's tetrahedral host can encapsulate these species in their protonated forms to yield stable host-guest complexes in neutral or basic aqueous solution. Guests such as small amines and phosphines bind with **16** in a 1:1 manner which is confirmed by NMR spectroscopy.[94] For guest amines, monoprotonation is confirmed by the pH dependence of encapsulation, whereas the monoprotonation of phosphines was determined by ^{31}P NMR by comparison of the *J* coupling constants in both water and deuterium water.

A variety of protonated amine guests were surveyed in order to obtain further information of the encapsulation of protonated guests in **16**. Small tertiary diamines with a methylene backbone from 1 ~ 6 can be encapsulated in the cavity, while primary diamines do not bind because: 1) they are more greatly solvated in the free solution; 2) in order to be encapsulated in the cavity, large associate enthalpy loss of desolvation is required.[95] Secondary and tertiary monoamines both are encapsulated.[94] Substituted pyridines do not bind due to their low basicity.[96]

This highly charged, water-soluble, metal-ligand assembly also mimics enzymes in promoting chemical reactions (Scheme 1-7). The hydrophobic cavity accelerates up to 890-fold the acid hydrolysis of orthoformates in basic solution. The mechanism parallels enzymatic pathways that obey Michaelis-Menten kinetics. Raymond and co-workers interpret the mechanism as occurring in three steps: first, the interior cavity of the assembly is protonated, then the substrate enter the preprotonated cavity and undergoes the protonation step by deprotonation of water, two successive hydrolysis steps follow in the cavity and yield the corresponding alcohol. Last, the protonated ester is released from the cavity and undergoes further hydrolyzed in the basic solution.[97]

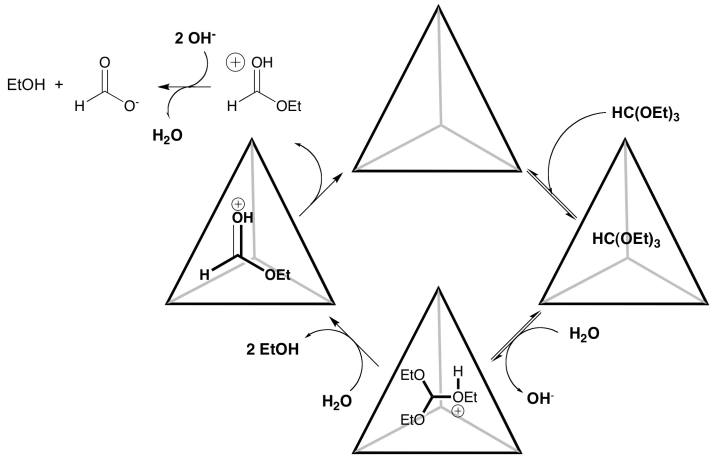

Scheme 1-7. The catalytic cycle for orthoformate ester hydrolysis within host **16**.

Intrigued by these results, the Raymond group also investigated the binding preferences of a wide range of saturated neutral guest molecules including *n*-alkanes, cyclic alkanes, polycyclics,[98] and enantiopure diterpenoids.[99] Addition of *n*-alkanes to the basic solution of **16** led to the formation of kinetic stable 1:1 host-guest complexes. Guests *n*- pentane through *n*-nonane are suitably sized to be trapped inside the cavity while guest decane is too large to fit. In the presence of smaller guests, such as *n*-pentane through *n*-heptane, relatively broad bound

guest signals are observed due to an intermediate exchange rate between free and bound states while the host region gave sharp, well-defined signals. With increasing the length of the alkyl chain to *n*-octane and *n*-nonane, the bound guest region gave sharp signals while the host region showed broad signals. Within the cavity, larger alkanes are relatively static and induce higher degree of asymmetry in the host ligand protons. The gradual downfield shift signals of the bound guest methyl groups indicate that the terminal of the guests move towards the center of the cavity and the alkyl chains accommodate a coiled conformation inside the cavity.[100] This binding event is driven by the hydrophobic effect: the nonpolar solute enters the hydrophobic cavity and displace the highly organized water molecules into the bulk soultion.

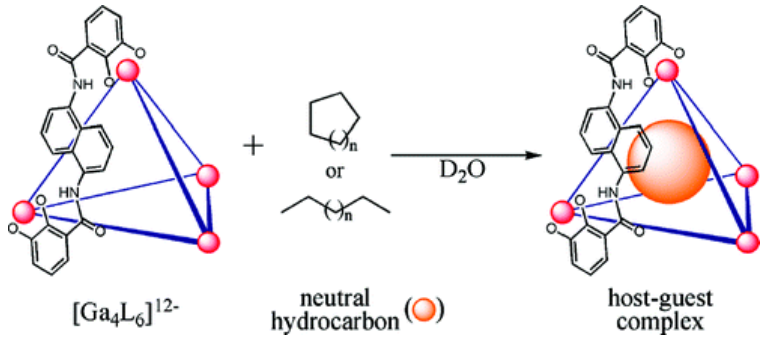

Scheme 1-8. Hydrocarbons binding inside a tetrahydral $[G_a4L_6]^{12-}$ host **16.** Permission License Number: 26431041719

The hydrophobic effect also triggered the encapsulation of a series of cyclic alkanes in host **16**. The bound cyclopentane and cyclohexane give one broad signal while the larger cycloheptane, cyclooctane, and cyclodecane are represented by one sharp peak. Although *n*-decane is too big to be trapped inside the cavity, the less flexible cyclodecane can be encapsulated in the cavity to form a 1:1 host-guest complex.[98]

1.3.5. Cavitands

The resorcin[4]arene-based cavitands and capsules have been widely exploited by supramolecular chemists during the past three decades. These host molecules offer a significant interior cancave surface available for contact with convex guests. The initial structures were quite flexible which formed short-lived complexes with weak binding affinity. By introducing more recognition features to these flexible structures, the modified cavitands present stronger binding affinity with slower dissociation rate as well as increased binding selectivity. The earliest simple cavitands resorcin[4]arenes **19**, which are synthesized from the condensation of resorcinol **17** with a series of aldehydes **18** (Scheme 1-9), were reported in the 1880's without full characterization.[101-107] A tertrameric structure was determined by Niederl and Vogel[108] in 1940, and Högberg[109-111] developed the efficient synthesis of the cyclic tetramer in the 1980's, a procedure that is still popular today. A stable, shallow-bowl shaped, host was obtained by exposing the simple resorcin[4]arene **19a** to excess NaOH and deprotonating one hydroxyl group on each aromatic ring.[112] This tetraanionic structure is capable of binding tetramethylammonium ion and acetylcholine chloride with association constants between 10^4 and 10^5 M^{-1}. No binding was observed between this host and neutral guest such as *tert*-butyl alcohol thus the electrostatic interactions between host and guest contributed to the strong binding affinity.

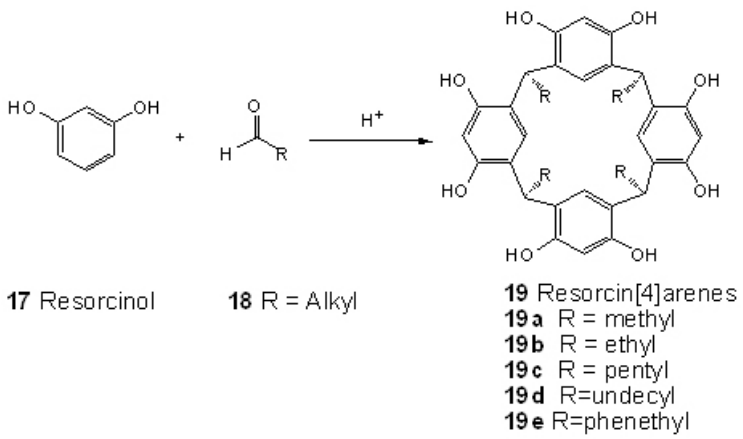

Scheme 1-9. Synthesis of resorcin[4]arenes bearing a variety of pendant R groups.

Bridging the hydroxyl groups in those bowl-shaped resorcin[4]arenes **20** with four equivalents of bromochloromethane produced hosts with slightly larger, less flexible cavities (Figure 1-14 (a)). Solubilizing groups can be introduced on either the upper or lower rim. The simplest cavitands, **22** and **23** have the same water-solubilizing groups on their upper rim which lead to only the binding of caesium cations due to their limited cavity volume and functionality. Addition of one methylene group between the aromatic rings and the hydroxyl groups, lead to **24**, which is insoluble in water even at pH > 12.[113] Hong and co-workers[114] produced cavitand **25** through alkylation of these hydroxymethyl groups with isophthalates. It deprotonated under basic condition and gave an octa-anoinic cavitand. This negative charged cavitand has a preference of binding cationic guests such as *N*-methylpyridinium, acetylcholine, and *N,N,N,N*-tetramethylbenzenaminium forming 1:1 host-guest complexes with association constants ranging from 10 to 10^3 M^{-1}, while no binding of anionic sodium 4-methylbenzoate was observed. This indicated that the electrostatic interactions are playing the essential role in these binding events. Tetracationic hosts **26-28** presenting sp^2 hybridized ammonium centers were all soluble in water; **26** is less aggregrated in water than **27** and **28**.[115] Electrostatic interactions also drive the formation of host-guest complexes. For instance, encapsulation of the guests *p*-cresol and *p*-toluenesulfonate in derivative **26** (with pendant methyl groups) afforded 1:1 complexes with

binding constants of 1.1×10^2 and 5.2×10^2 M^{-1}.[116] Another example of electrostatic interactions driving the host-guest complexes formation is the extensive binding studies between the tetra-hexamethylenetetramine cavitand **29** and both cationic and anionic guests. The corresponding results reveal that only anionic guests appear binding affinities with the cavitand whereas cationic guests do not. Binding affinity is two magnitudes stronger while introducing a second anionic center to the guests than that with mono-anionic guests (Figure 1-14 (b)).[117]

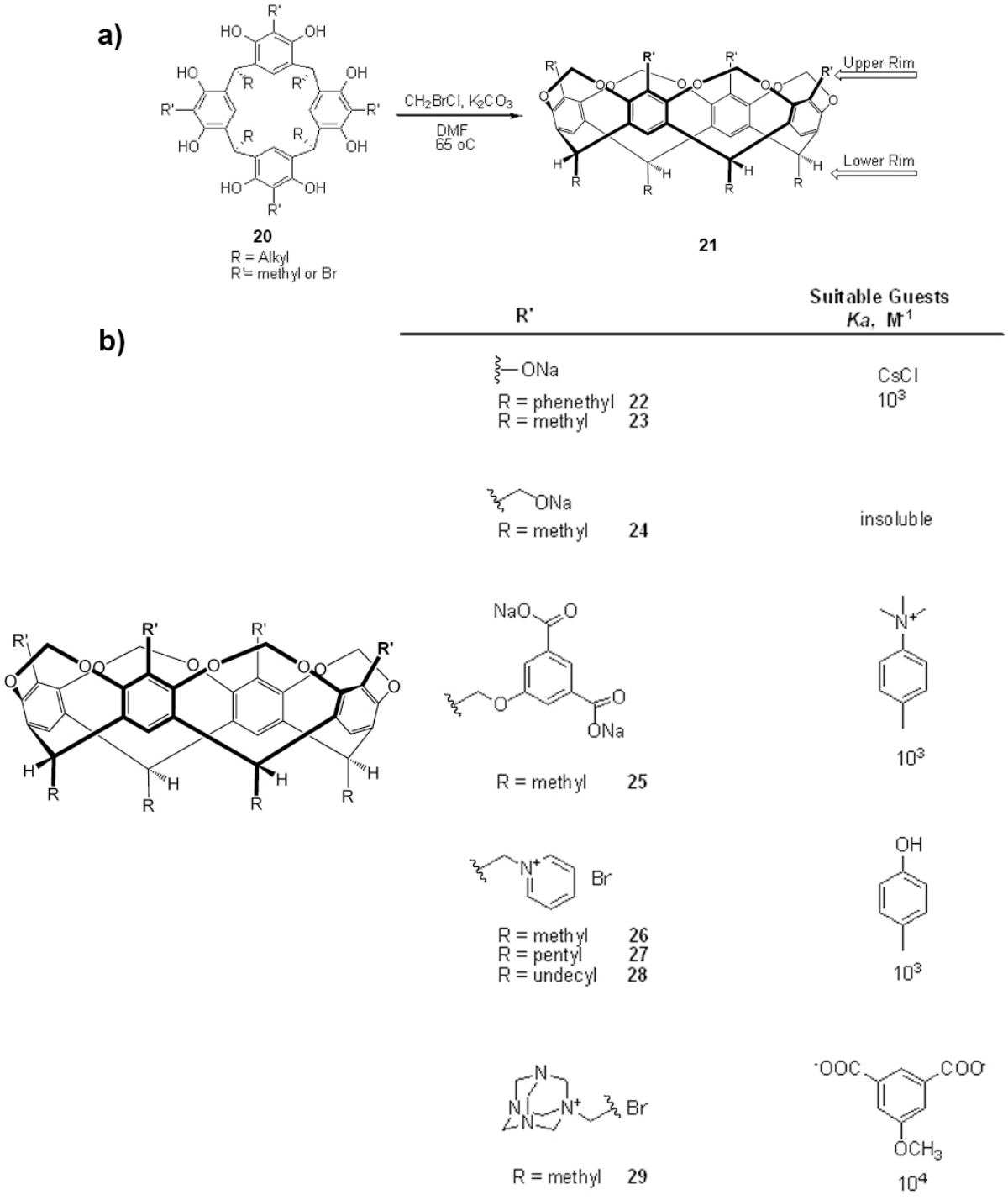

Figure 1-14. a) Methylene bridged cavitand **21**. b) Solubilizing groups attached to the upper rim of simple cavitands and examples of a suitable guest.

Introducting solubilizing groups on the lower rim ("feet") is an alternative strategy to construct water-soluble cavitands. Sebo and Diederich[118] prepared an ethylene bridged cavitand presenting four amidinium groups on their upper rim and four polyethyleneglycol chains on the lower rim which assist the cavitand **30** to achieve water-solubility (Figure 1-15). With a more expanded cavity volume than the aforementioned cavitands, in D_2O host **30** can accommodate two copies of a guest molecule, such as 5-methoxyisophthalate and 5-nitroisophthalate with association constants of ~10^4 M^{-1} (K_{a1}) and ~10^3 M^{-1} (K_{a2}), respectively. In 5 mM sodium tetraborate solution, the formation of 1:1 host-guest complexes was observed; the borate ions interact strongly with the ammonium groups at the portal of the cavitand and blocked the binding site for the second guest.[116] Under other conditions, 1:2 ratios were observed. For instance, one isophthalate guest occupied the hydrophobic cavity while the second guest is present outside the cavity and is associated by electrostatic and/or non-specific hydrophobic contacts. The Rebek group created larger and deeper cavity cavitands **31**[119] and **32**[120] which are synthesized from condensation resorcin[4]arenes with electron-poor aromatic rings. They all have an octa-amide upper rim and four ammonium centers on the pendant alkyl chains (Figure 1-16). In order to reduce the exposure of lipophilic surfaces to aqueous solution,[119,120] these structures accommodate the kite conformation as D_{2d} velcraplex dimers in water.[121] With adding guests into the solution, the cavitands rearranged to the C_{4v} vase conformation and formed kinetic stable complexes with exchange rates slow on the NMR time scale.

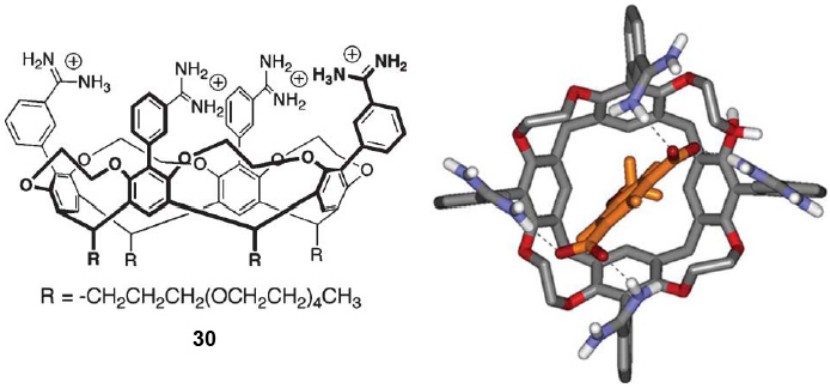

Figure 1-15. Left: Structure of Diederich's ethylene bridged cavitand **30** bearing PEG groups on the lower rim; Right: top view of energy-minimized model of cavitand **30**–methoxyisophthalate complex showing hydrogen bonds between host and guest (dashed lines, some protons and the pendant (chains have been omitted for clarity). (*Reproduced by permission of The Royal Society of Chemistry* http://dx.doi.org/10.1039/B508530F)

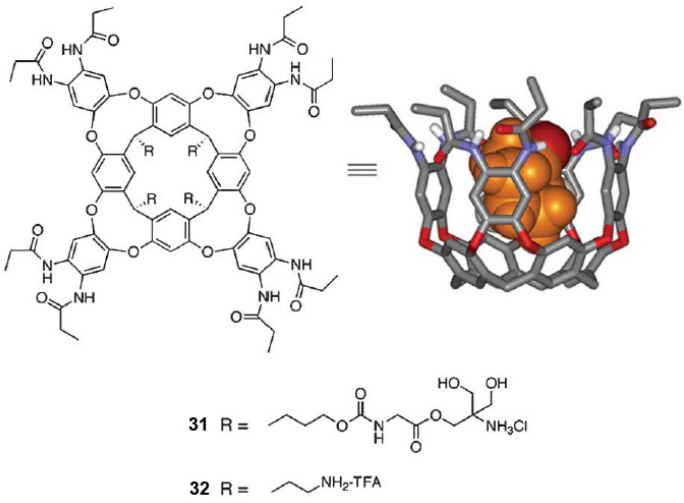

Figure 1-16. Left: Structure of water-soluble, octaamide cavitands **31** and **32**; Right: energy-minimized structure of a deep cavitand with bound cyclohexanone (some protons and the pendant alkyl groups have been omitted for clarity). (*Reproduced by permission of The Royal Society of Chemistry* http://dx.doi.org/10.1039/B508530F)

The best characterized water-soluble Rebek cavitand is cavitand **33**. Modification of the intermediate octa-amine cavitand with four carboxylate-substituted benzimidazoles gave this third water-soluble cavitand bearing a C_{4v} symmetry at its free state in aqueous solution at neutral pH (Figure 1-17).[122] Two factors have been attributed to the stability of the cavity of **33**:

first, hydrogen bonds on the rim formed between four solvent water molecules and the nitrogen atoms of the benzimidazole rings; second, a THF molecule, from the final NaOH hydrolysis step in the preparation of **33,** reside in the cavity thus enhancing the stability of the cavity. A tetracationic derivative **34** was also synthesized (Figure. 1-17). It is soluble in acidic water solution and bears a C_{2v} kite symmetry without a cavity at this pH.

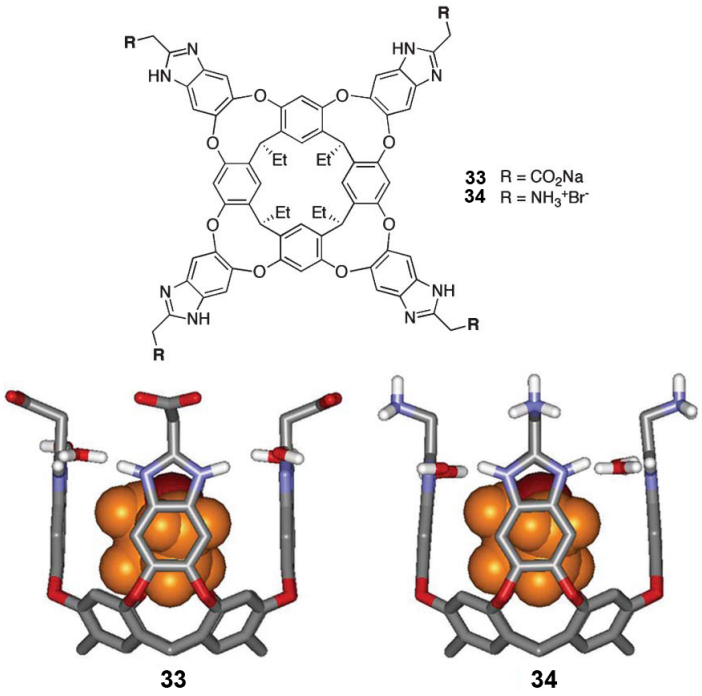

Figure 1-17. Structure of deep, tetraanionic cavitands **33** and **34** binding one molecule of THF. (*Reproduced by permission of The Royal Society of Chemistry* http://dx.doi.org/10.1039/B508530F)

Without expectation, the Rebek group obtained surprising results in the study of cavitand **33** in the presence of solutions containing sub-micellar concentrations of sodium dodecylsulfate **35** (SDS) and dodecyl phosphatidylcholine **36** (DPC).[123] Both guests form 1:1 complexes with the hydrophilic group pointing outwards from the cavity and the hydrophobic alkyl chains coiled into a helix inside the cavity. In order to minimize steric interactions and maximize surface area, alkanes (such as ethane and butane) generally favor *anti* conformations in solution whereas their eclipsed conformations necessary for a helical conformation are at higher energy. Folded

conformations can reduce the amount of hydrophobic surface exposed to solvent but induce sterically unfavorable gauche interactions. Upon complexation, water molecules inside the cavity were replaced by alkanes and released to its bulk solvent. This process is entropically favorable which contribute the formation of the complexes. Also, the alkanes accommodate a helix conformation in order to increase the contacts with a large fraction of the π surfaces offered by the aromatic rings that line the cavity (Figure 1-18). This coiled helix conformation was confirmed by a NOESY experiment at low temperature which demonstrated NOEs between the terminal methyl group and the methylene at C4. This hydrophobic effect driving the formation of host-guest complexes also has been observed in the binding of long alkyltrimethylammonium salt such as **37** in cavitand **33**. In a previous study, choline was shown to bind with an affinity of > 10^4 M^{-1} in **33** in D_2O.[124] Thus guest **37** bears two binding sites, the long alkyl chain and a trimethylammonium "knob" afforded a similar binding constant as choline. Again, the hydrophobic effect induces the alkane chain to accommodate a coiled helix conformation in the cavity to create the maximum CH-π interactions with the cavity wall, and also the electrostatic interactions between the tetracarboxylate upper rim and the tetraalkylammonium center provide supplementary attraction.

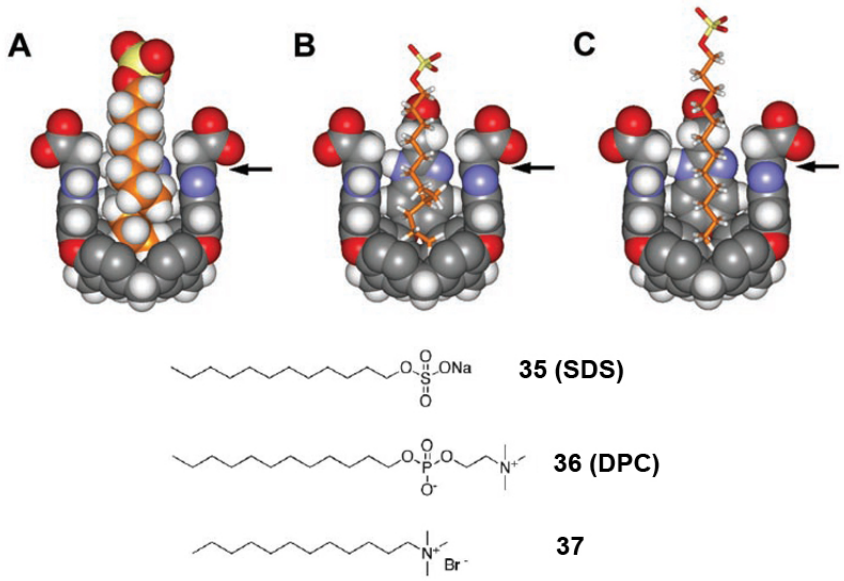

Figure 1-18. Energy-minimized structures of the complexes; one wall of the receptor has been removed for viewing clarity. (A) Space-filling model of partially coiled SDS showing C-H/π contacts. (B) Polytube model showing the accommodation of eight carbons with five gauche conformations within the cavity. (C) Extended conformation of SDS in the cavity. The arrows indicate the highest aromatic atom on the rim of the cavity. Included atoms above this level are not expected to show strong upfield shifts in their NMR signals.[123] Permission License No.: 2643750132214

The Rebek group has also synthesized a fifth water-soluble deep cavitand **38** by appending four benzoate groups on the upper rim (Figure 1-19).[125] Instead of binding a series of straight-chain alkanes, this restricted cavitand is more size dependent in the binding of alkanes – it can only bind small size alkanes such as pentane through octane, guest larger than octane do not bind inside the cavity.[116] The benzoate groups function as a "resolving door" on the portal of the cavity which results in restrict guest entry and release. For instance, THF bounded in **33** gave broad NMR signals while in **38** sharp signals were observed.

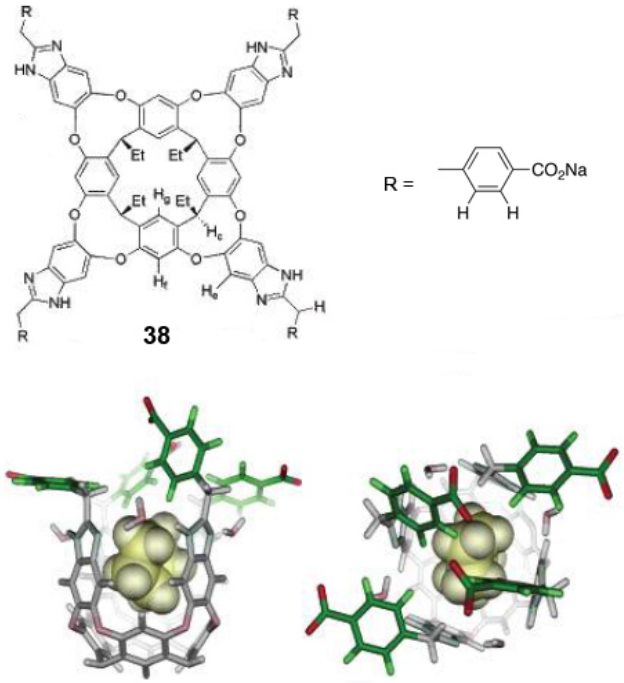

Figure 1-19. Top: Chemical structure of tetrabenzoate cavitand **38**. Bottom: Depiction of the **38**–cyclopentane complex featuring aromatic ‘‘revolving doors’’. On average, two doors are suspended above the open end of the cavity at any time. (See appendix from copyright permission)

The Reinhoudt group has synthesized a series of calix[4]arene based water-soluble cavitand with either amidinium, sulfonate or carboxylate groups on the upper rims (Figure 1-20). Although the monomers were soluble in water, their dimeric assemblies precipitate out from aqueous solution.[126] Further modification of these cavitands improved this limitation. Thus, increasing the length of the ethylene glycol feet of monomer **39** and replacing the sulfonates of **40** by carboxylates greatly improved water solubility. In basic water buffer, deprotonation of **42** gives a negative charged cavitand, while **41** is cationic. The electrostatic interactions between these two cavitands yield a hetero-dimeric capsule **41•42**.[127] The propyl amidinium chains are included inside the cavity of the capsule which results in the corresponding protons of the propyl amidinium chains of **41** showing upfield shifts because of the shielding provided by the aromatic rings of the calix[4]arenes. Also, the hindered rotation around the propyl C-N bond is attributed

to the broad propyl signals.[126] Studies with isothermal titration calorimetry (ITC) determined the binding constant K_a of 3.3×10^4 M^{-1} and a ΔH^o of -3.3 kcal mol^{-1}.[127]

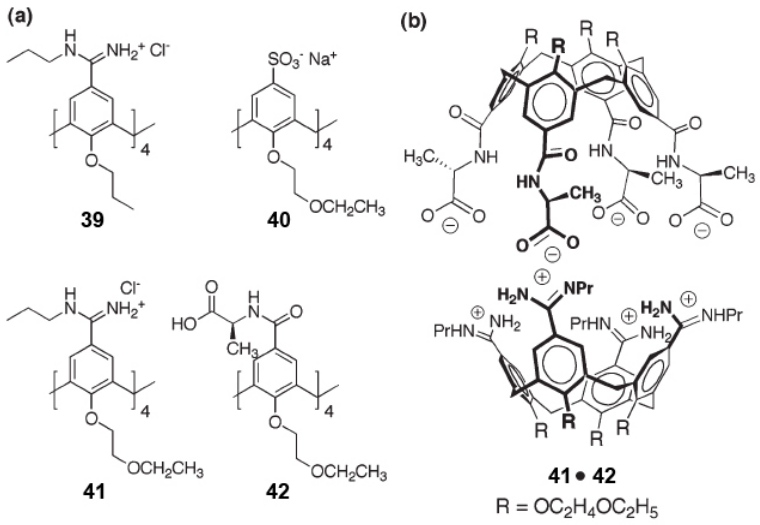

Figure 1-20. Structure of (a) tetra-substituted calix[4]arene monomers; (b) depiction of a water-soluble dimeric capsule assembled through electrostatic interactions.[126,127] Permission License No: 2643760581673.

A family of water-soluble deep-cavity cavitands reported by Gibb and co-workers relies on hydrophobic, CH···π, and π···π interactions to form self-assembling dimeric capsules. These deep-cavity cavitands are resorcin[4]arene-based molecular hosts and have three rows of aromatic rings in their structures which build up the host's cavity.[128-133] In particular, one container within the family (host **43**) is "coated" with eight water-solubilizing carboxylic acid groups and also bears a large hydrophobic cancave pocket (Figure 1-21).[134] Although it has limited solubility in aqueous solution at neutral pH due to the eight carboxylic acid groups, it has considerable water-solubility at pH 8.9. By increasing the concentrations of host, broad ^{1}H NMR signals were observed which demonstrate that the hosts aggregate at higher concentration, presumably due to the hydrophobic rim that promotes these kinetically unstable assemblies.[135]

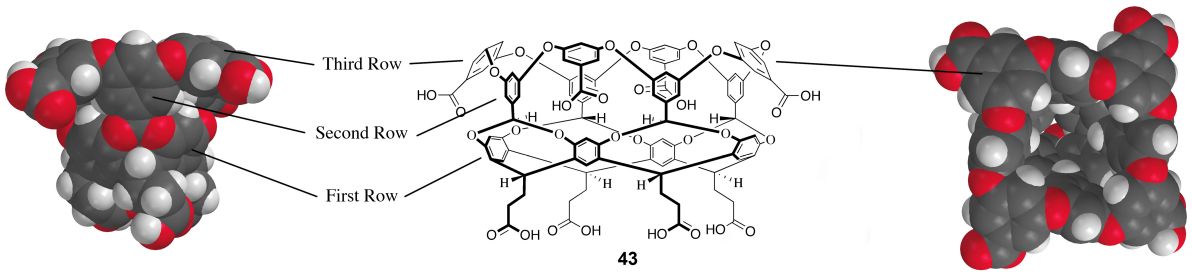

Figure 1-21. Different perspectives of deep-cavity cavitand **43**. Left to right respectively: 'side" view of space-filling model; similar side view of chemical structure; and "Plan" view of space-filling model looking down into the binding site.

Investigations of the binding various guest molecules inside **43** (Figure 1-22) have been carried out by the Gibb group. The addition of guests of suitable size triggers the dimerization of the host and encapsulation of the guests. The assembly occurs for various sizes of guests such as small guest propane[136] and large guest steroids.[134] Guests with polar groups, such as triethylene glycol derivatives,[137] and flexible structures, such as straight-chain alkanes,[138] are also sufficient to template the assembly formation. Amphiphilic Guests with a hydrophilic group tend to form a 1:1 monomeric complex with the hydrophilic group pointing outward from the cavity (Figure 1-22).[139]

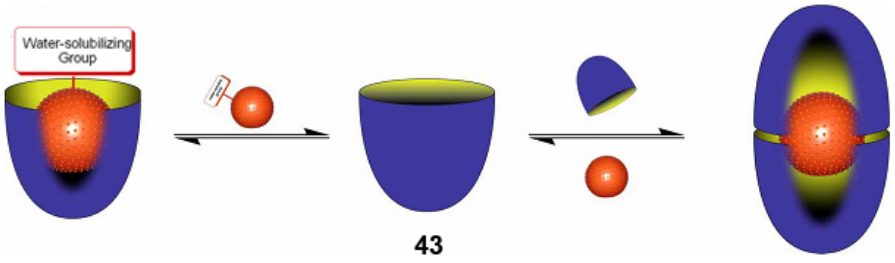

Figure 1-22. Schematic of the formation of 1:1 complexes or 2:1 assemblies using cavitand **43**.

Two recent studies revealed that flexible *n*-alkanes propane to heptadecane are able to template the dimerization of cavitand **43** to form a nano-capsule in water.[136,138] This

homologous series of guests demonstrates that the combination of the hydrophobic effect[140,141] and a suitably predisposed subunit[142] are powerful inducers of assembly. In aqueous solution, host **43** can sequester hydrocarbon gases (propane and butane) directly from their gaseous phase and form kinetically stable quaternary complexes. Binding competition experiments revealed that although propane forms a kinetically stable capsule within **43**, it binds one order of magnitude weaker than butane. This fact can be applied in the separating the two gases from the gas phase.[136] The smaller gas ethane forms a 1:1 complex in the absence of salt, (which is known to increase the hydrophobic effect). Guest *n*-pentane through *n*-heptane formed 2:2 dimeric assembly while guest larger than octane formed distinct 2:1 dimeric assemblies. The stoichiometry of each complex was confirmed by integration of the bound host and guest while the formation of dimeric assembly was confirmed by plus-gradient stimulated spin-echo (PGSE) NMR experiments. The most interesting guest octane formed a mixture of both 2:2 and 2:1 capsule. The bound octane signals were broad and were also temperature dependent. First, the NMR spetra showed that the separate signals of methylene of the hydrocarbon straight chain and terminal methyls appear between 0 to -3.5 ppm. The second evidence involved the host atoms, the *endo* protons which are located on the third row of the cavitand and point into the cavity are most influenced by complexation. They found themselves going from a water-exposed environment in the host monomer to a dry[143] aromatic solvent-like environment in the nanocapsule. In these entities, the methyl ^{1}H NMR signal of the guest was the most upfield shifted. This indicated that each terminal of the straight-chain alkanes “anchored” down to the polar bottom of each hemisphere. Guest larger than *n*-dodecane cannot adopt a fully extended conformation which is proved by NOESY and COSY NMR experiments.

In order to understand how the guest polarity affected the ability of assembly and formation of a supramolecular capsule, a series of approximately isosteric guests (**44** – **49**) was investigated (Figure 1-23). In this series, guest **48** proved to signify the boundary between

assembly to form 2:1 complexes and simple 1:1 complexation. Thus, guests **44**-**47** formed kinetically stable capsules, with increasing the hydrophilic properties of guest molecules guest **48** formed a capsule that was unstable on the NMR timescale, and guest **49** which is the most hydrophilic guest in this series formed a simple 1:1 complex with the binding constant of 2.5 × 10^3 M^{-1}, suggesting perhaps that it is more appropriate to discuss polyethylene glycol derivatives as hydrophobic rather than hydrophilic.[137]

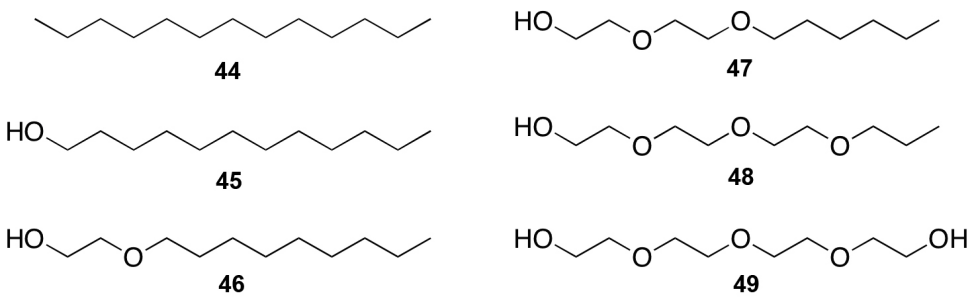

Figure 1-23. Isosteric Guests **44** – **49**.

Inspired from the study of controlling photochemistry inside this nano-capsule,[143-146] a most recent report demonstrated the nano-capsule formed by the dimerization of water-soluble cavitands **43** can function as a yocto-litre reaction flask to control the kinetic resolution of constitutional isomers.[147] The hydrolysis of two families of esters was examined. In free solution these esters hydrolyzed at similar rates due to the similarity of their chemical structures and it was not possible to obtain selective reaction within a two-component mixture. However, the addition of the nano-capsule $\mathbf{43}_2$ led to a competitive binding equilibrium in which the stronger binder primarily resided inside the host, whilst the weaker binder resided in the bulk hydrolytic medium. The quality of the kinetic resolution highly correlates with the difference of the binding constants of the isomers. The greater difference in binding constants led to a better

kinetic resolution. The resulting kinetic resolutions were highest within the optimally fitting smaller esters (Scheme 1-10).

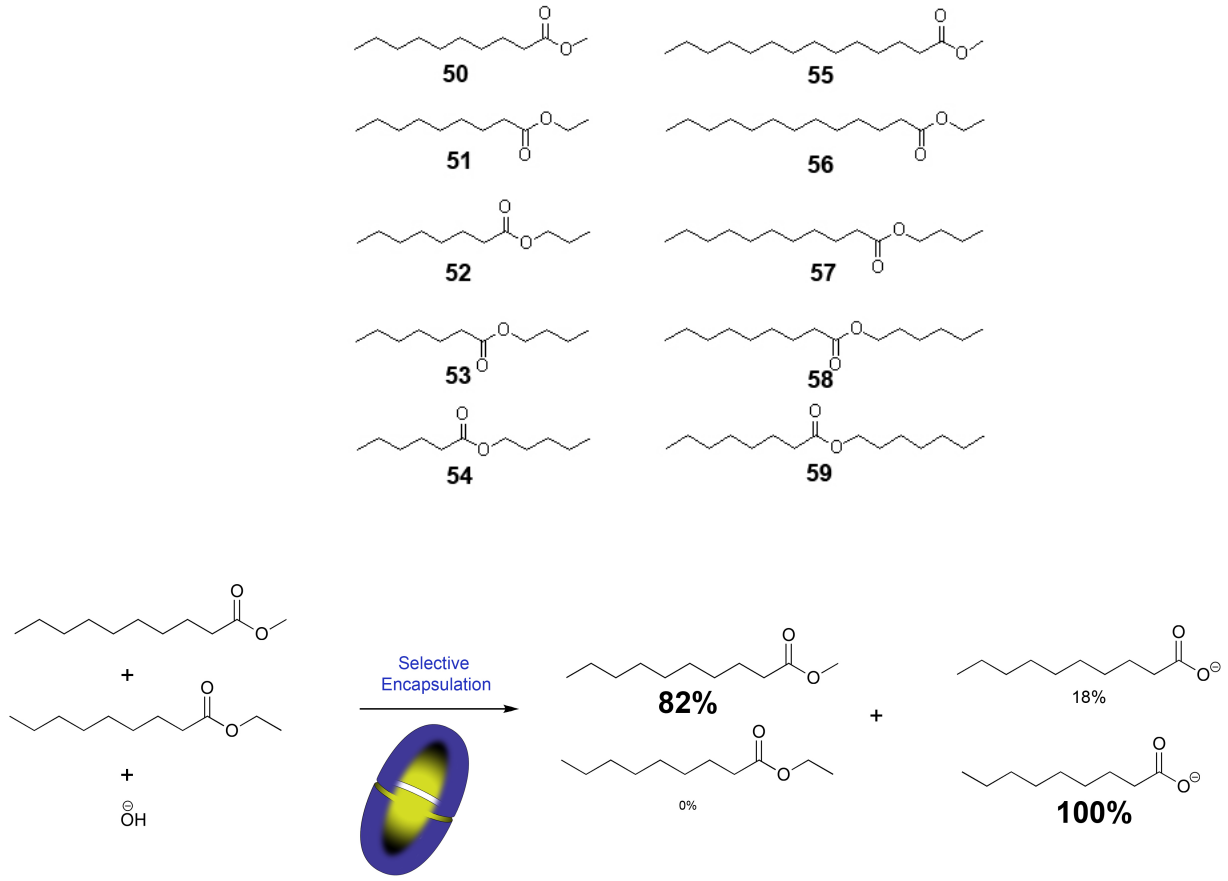

Scheme 1-10 Water-soluble capsule $\mathbf{43}_2$ led to kinetic resolution of constitutional isomers.

The relatively easy synthesis of OA **43** allows other research group to explore its assembly properties further.[148-164] Gibb and Grayson[165] have reported another water soluble deep-cavity cavitand **60** which was the first neutral, self assembling host (Figure 1-24). Attaching hydroxyl-terminated aliphatic polyester dendrons onto the cavitand core improved both pH-dependent water solubility and high biocompatibility. G-1 cavitand was sparingly soluble in methanol, G-2 was soluble in 80% (v/v) water and methanol solution, and G-3 cavitand was freely soluble in pure water. The binding properties of the dendritic host are

qualitatively very similar to the aforementioned cavitand **43** except that self-inclusion of the long coating chains into the cavity can compete with guest binding.

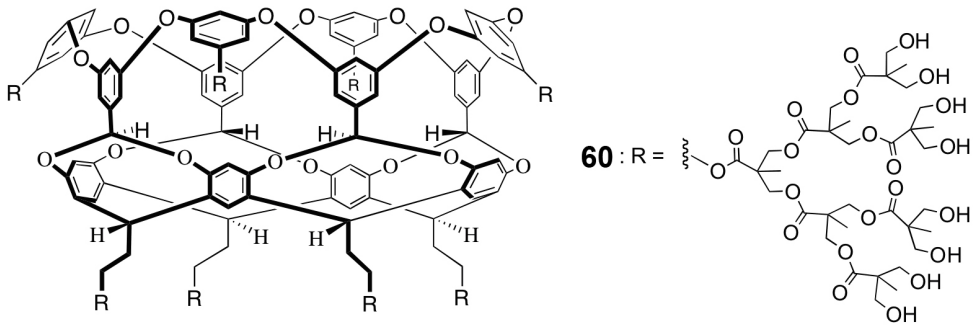

Figure 1-24. Dendronized water-soluble deep-cavity cavitand **60**.

II. Non-monotonic Assembly of a Novel Deep-Cavity Cavitand (TEMOA) License No.: 2643820276311

Understanding the assembly behavior of proteins is essential if the full repertoire of switching processes in biological networks is to be appreciated. The ultimate goal of systems biology is being able to predict, control, and eventually design biological systems. However, our understanding of biological networks is still at the fundamental level.[166] In general, a node is any molecule and an edge can be any covalent or non-covalent interactions. Specifically, network in biological systems, signals are inputs to the network, genes are nodes, and transcriptional regulation of one gene to another are edges (Figure 2-1).

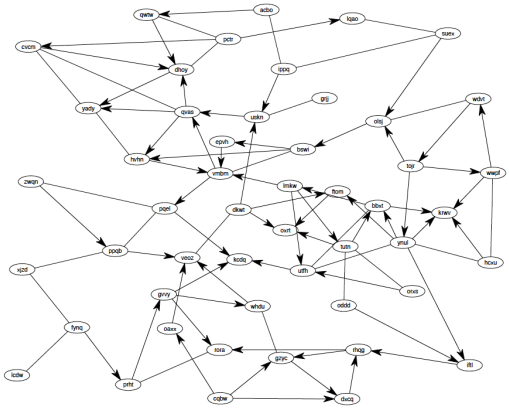

Figure 2-1. An example of a biological network

As an assist method, chemistry is beginning to build an understanding of the different components of chemical systems. With this in mind, monotonic switching behaviors are commonly observed in natural and synthetic systems. In Boolean algebra, a monotonic function is one such that for every combination of inputs (external signals) switches one of the inputs from on (1) to off (0), and can only cause the outputs from on (1) to off (0) or off (0) to on (1) with a strict increase or decrease. With appreciation of devices and machines at the molecular

level, chemists have began to establish a variety of means by which external stimuli can switch nodes between one states and another (on and off).[167,168] For example, in synthetic assemblies it is commonly observed that guests of increasing size induce a gradual increasing tendency to trigger assembly, such as the aforementioned linear relationship between the energy changes and the size of guests in the binding study of β-CD (Figure 1-7).[38] In contrast, novel water-soluble deep-cavity cavitand **61** possesses an unusual non-monotonic assembly profile. For a homologous series of alkanes, the host can form different types of isoenergetic supramolecular species (1:1, 2:1 and 2:2 complexes). Simple alkanes are useful probes for examining these types of complexes because: an extended homologous series is available; their hydrophobicity promotes complexation; and their simple structure leads to more easily interpretable NMR spectra. Here we identify **61** that functions as an unusual node. An examination of the binding of a homologous series of *n*-alkanes (C_1-C_{14}) reveals three possible supramolecular entities: 1:1, 2:1 and 2:2 host-guest complexes. The relatively small energy differences between many of the different supramolecular complexes leads to a 'confluence' at the node, and an unexpected, non-monotonic, assembly profile.

2.1. Synthesis and Characterization of a Novel Deep-Cavity Cavitand TEMOA 61

Deep-cavity cavitand **61** (Scheme 2-1) was formed by an analogous procedure to that used in the synthesis of the cavitand **43** (octa-acid).[134,169] Known cavitand **62** was 'woven' with 3,5-dihydroxy-4-methylbenzyl alcohol through an eight-fold Ullmann ether reaction using pyridine, K_2CO_3, and CuO nanopowder to yield octol **63**. Each of the eight ether bonds is formed with greater than 70% efficiency. Oxidation by potassium permanganate then gave the crude product **61**. No chromatography is involved in these two steps due to the high polarity of the compounds **63** and crude **61**. A traditional step of using HCl saturated EtOH gives the

esterification product, which contains the major product octa-ester **64**. Purification of octa-ester **64** is the only step in the synthesis requiring chromatography and ensured the removal of impurities arising from both the weaving step and the oxidation of octol **63**. Pure octa-ester **64** was hydrolyzed under basic condition yields the desired pure product **61**.

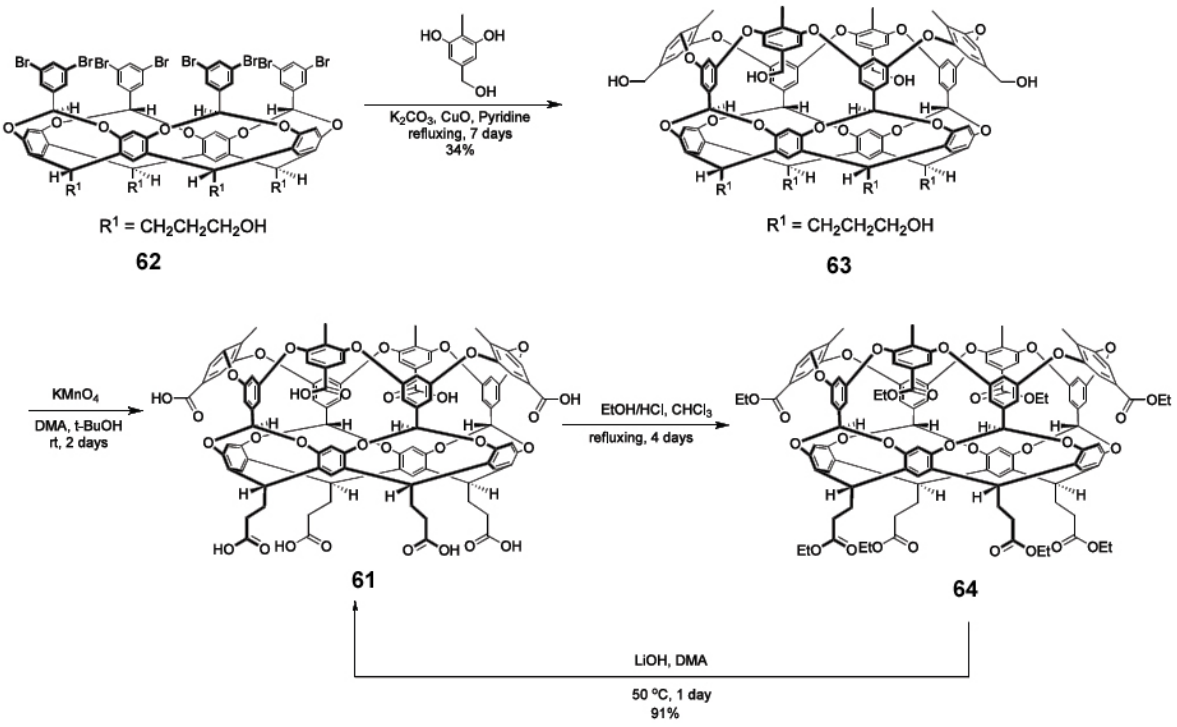

Scheme 2-1. Synthesis of deep-cavity cavitand **61**.

In the structure of OA **43**, there are four protons at the rim of the cavity pointing toward its center, the so called *endo* protons. Replacing those four *endo* protons by methyl groups gives, tetra *endo* Me Octa-Acid **61** (TEMOA), whereas posseses different binding and assembly properties compared to OA **43**. Although cavitand **61** has a slightly narrower portal (0.8 nm) than OA **43** (1 nm), the *endo* methyls also deepen the cavity which result in the similar cavity volume (Figure 2-2).

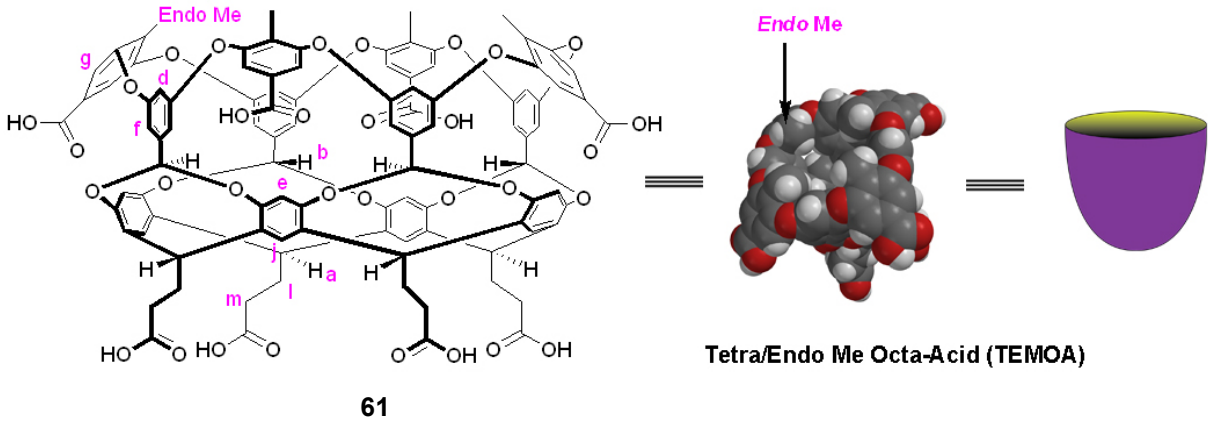

Figure 2-2. Space filling model of deep-cavity cavitand **61**.

These subtle features result in a reduced predisposition of TEMOA **61** to dimerize relative to OA **43**. This was first apparent in the ^{1}H NMR spectrum of **61** that showed sharp signals over the concentration range of 1-3 mM (in D_2O buffered with 10-30 mM $Na_2B_4O_7$). In contrast, **43** showed broad signals at concentrations above 2 mM (20 mM $Na_2B_4O_7$) indicative of partial assembly. The second line of evidence is that ^{1}H NMR spectrum of **61** showed sharp signals over the pH range 7.4 to 11.9 while **43** underwent aggregation at neutral pH (Figure 2-3).

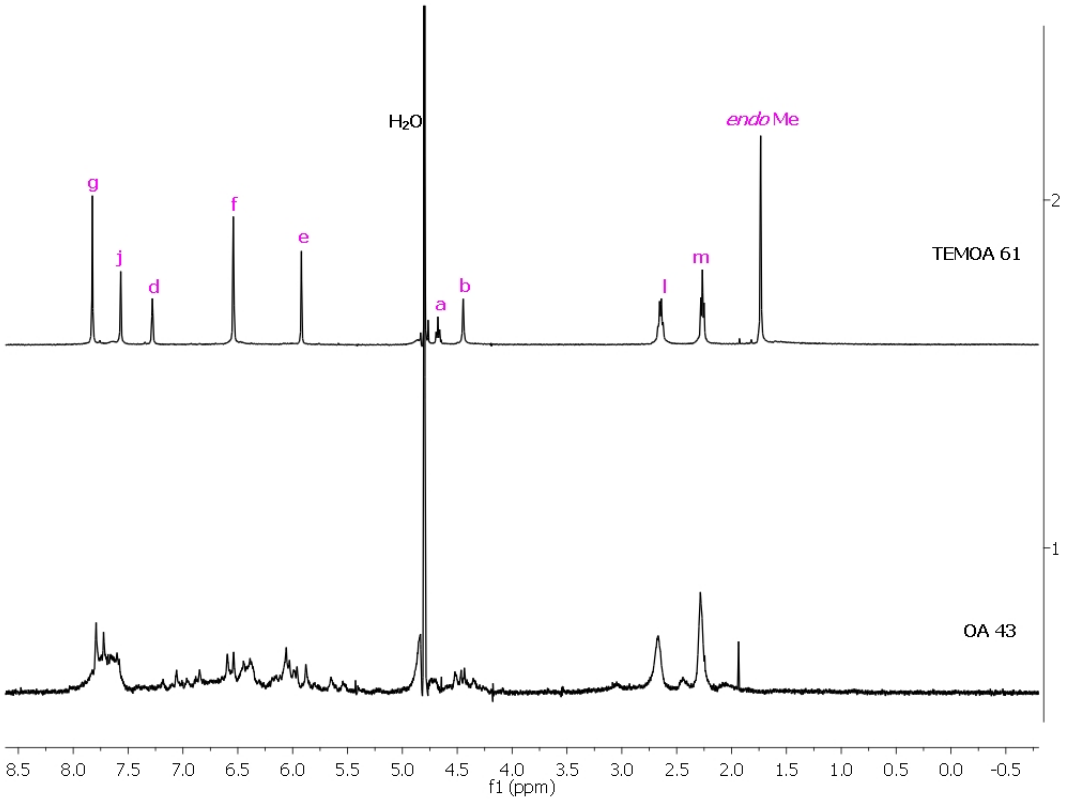

Figure 2-3. [1]H NMR spectra of the cavitand 1) 0.3 mM OA **43**; 2) 0.45 mM TEMOA **61** in 10 mM, pH = 7.46 phosphate solution.

In order to determine the effective size and shape of a molecular species, Pulse-gradient stimulated spin echo (PGSE) NMR spectroscopy is a method of choice for simultaneously measuring diffusion coefficients (*D*) for a entire set of signals in a high-resolution spectrum with high sensitivity and accuracy. Diffusion coefficients are sensitive to structural properties of the observed molecular species such as weight, size, and shape, as well as binding phenomena, aggregation, and molecular interactions.[170] In supramolecular chemistry, PGSE NMR experiments can be applied to determine the binding and association constants, and complement [1]H NMR to determine assembled states.[170] For instance, in the case of a spherical particle in a continuouse medium of viscosity η, the hydrodynamic radius R_H can be obtained by Stokes –Einstein equation (Eq. 2.1)

$$R_H = \frac{k_B T}{6\pi\eta D} \qquad \text{(Eq. 2.1)}$$

where k_B is the Boltzmann constant. In our study, we assume the particles we examined have spherical shape thus the corresponding hydrodynamic volume (HV) can be extracted from equation (Eq. 2.2).

$$V = \frac{4}{3}\pi R_H^3 \qquad \text{(Eq. 2.2)}$$

TEMOA **61** is monomeric over the 1-3 mM concentration range was confirmed by PGSE NMR experiments[170] which reveal a diffusion rate of D = 1.79-1.90 × 10^{-6} cm^2 s^{-1}, corresponding to a HV of between 6.3-7.6nm^3 (Figure 2-4).

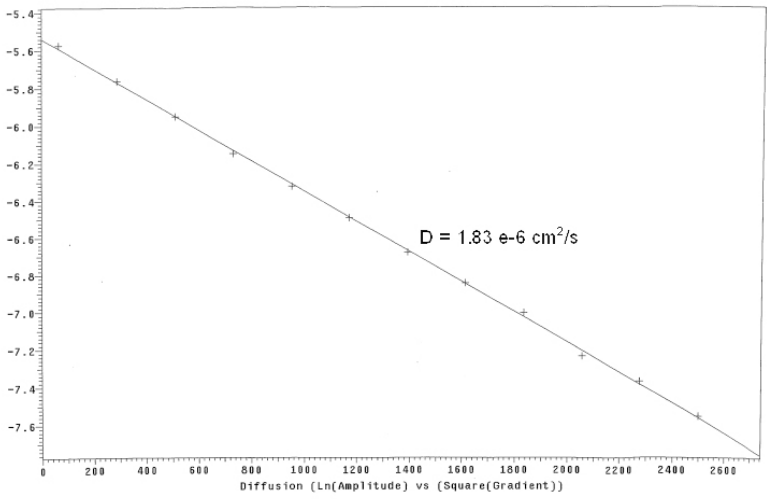

(a)

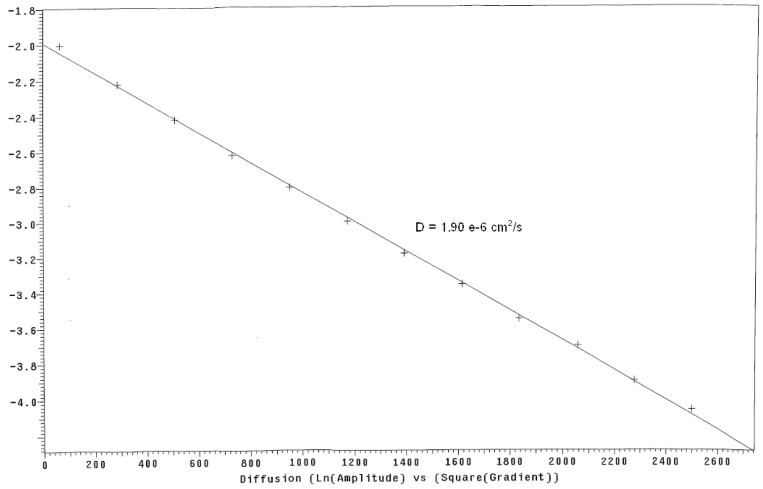

(b)

Figure 2-4. Plot of the ln(amplitude)versus the square of gradient strength applied that was obtained in the case of cavitand a) OA **43**, b) TEMOA **61**.

2.2. NMR Binding Studies of TEMOA 61

The binding of the homologous series of the *n*-alkanes methane (C1) through *n*-tetradecane (C14) to TEMOA **61** was examined using a combination of ^{1}H and PGSE NMR experiments. ^{1}H NMR confirmed guest binding or encapsulation as evidenced by high-field

signals for the bound guest between 0 and -3.5 ppm (Figure 2-5). These experiments also confirmed the number of species formed by each guest, and the ratio of the host and guest in the different complexes. The PGSE NMR experiments were used to determine the stoichiometry of the complexes formed and hence the extent of assembly.

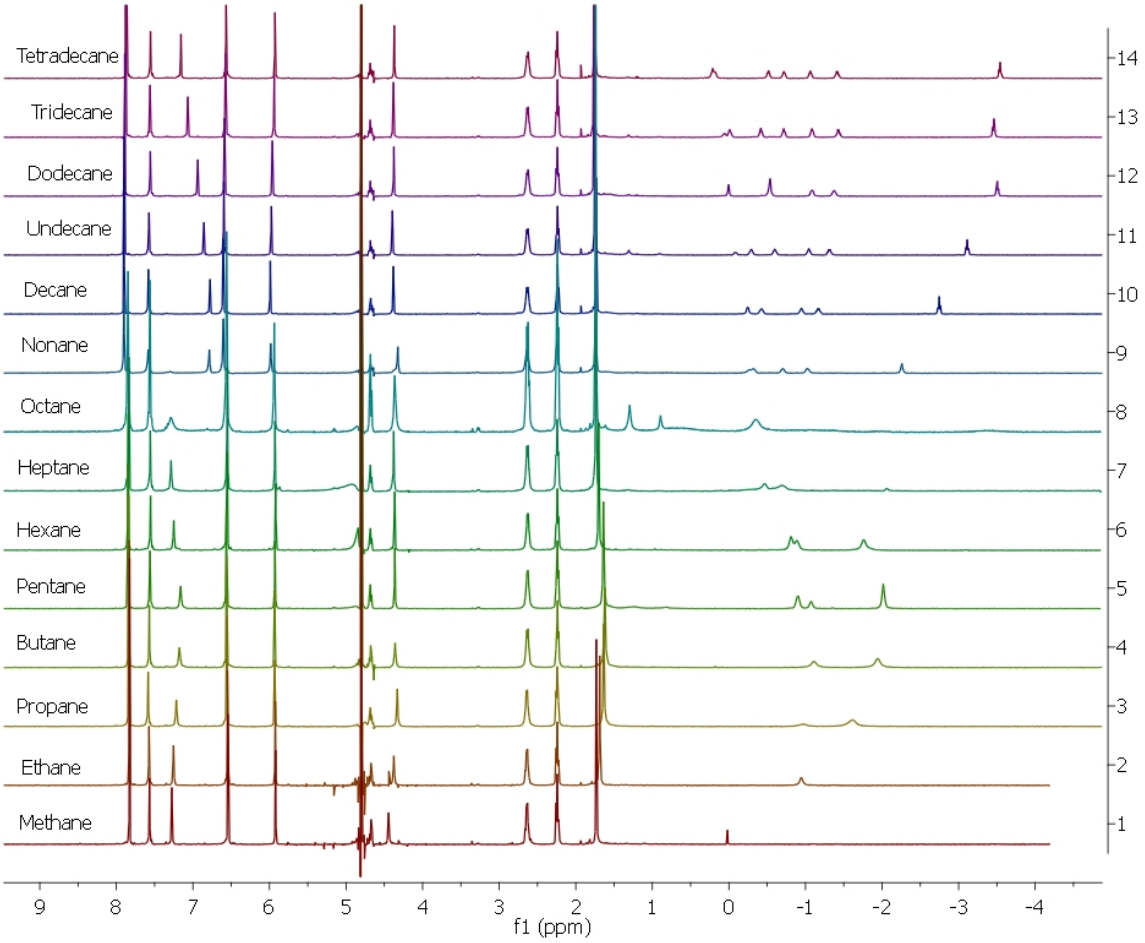

Figure 2-5. ^{1}H NMR spectra of the complexes of **61** and hydrocarbons methane through *n*-tetradecane.

The first line of evidence of the binding between TEMOA **61** and straight-chain alkanes was revealed by ^{1}H NMR binding studies. The smallest guest, methane, can be weakly trapped inside the cavity to form a monomeric complex which **43** does not. The distinctive bound, but fast exchanging, methane signal was observed at -0.02 ppm (c.f. 0.2 ppm for free methane). The stronger binding of methane to **61** is attributed to the four methyl groups at the rim

narrowed the portal to the pocket and increased the kinetic stability of the 1:1 complex. Following the monotonic trend, the signals of bound guest ethane, propane, *n*-butane appeared at -0.95, -1.62, and -1.95 ppm respectively. The broader bound host and bound guest signals indicated that the formed complexes were exchanging slower on the (500 MHz) NMR timescale than fast binding methane, while their exchanging rates were close to the (500 MHz) NMR time scale. The kinetics of complexation from the gas phase also revealed the different binding properties between **43** and **61**. Injection of 20 equiv. of appropriate gases (methane through butane for **61**, propane and butane for **43**) into the headspace resulted (without agitation) in the binding of the gases over a period of 18 h. (Figure 2-6). In the case of cavitand **43**, a fast binding complex with broad bound guest signals was observed for ethane, while propane and *n*-butane formed slow exchange complexes with the observation of both bound and free host signals. While in the case of cavitand **61**, chemical shifts were observed for the bound benzal protons which are located at the bottom of the cavitand inner wall. These formed complexes exchanged faster on the NMR timescale than the slow binding propane and butane to cavitand **43**. In addition, a competition experiment between methane and ethane revealed a K_{rel} for the latter of 3 which corresponds to a 25:75 selectivity. The competition experiment between propane and *n*-butane revealed a K_{rel} for the latter of 20 which indicated the efficient separation between these two guests from their gas phase.[136]

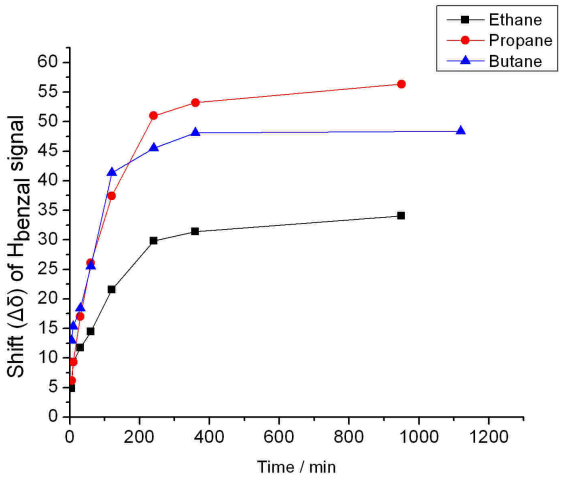

Figure 2-6. Kinetic Formation of **61** in the presence of light hydrocarbon ethane, propane, and *n*-butane.

The guest *n*-pentane continued this monotonic trend with a methyl signal at -2.02 ppm, but showed sharper guest signals suggesting a kinetically more stable complex. Unexpectedly, a break in the monotonicity of the extent of assembly was observed with guests *n*-hexane through *n*-octane. All guest signals, and many of the host signals were again broad indicating intermediate exchange rates. Guest *n*-nonane behaved very differently than *n*-octane, with the NMR experiments demonstrating that this guest is an efficient template for the formation of a slow exchanging 2:1 host-guest complex. Finally, for the larger guests *n*-decane through *n*-tetradecane, within experimental error there were monotonic shifts in both the bound guest methyl signals (Figure 2-7). This non-monotonic switching behavior was not observed in the binding studies of cavitand **43**.

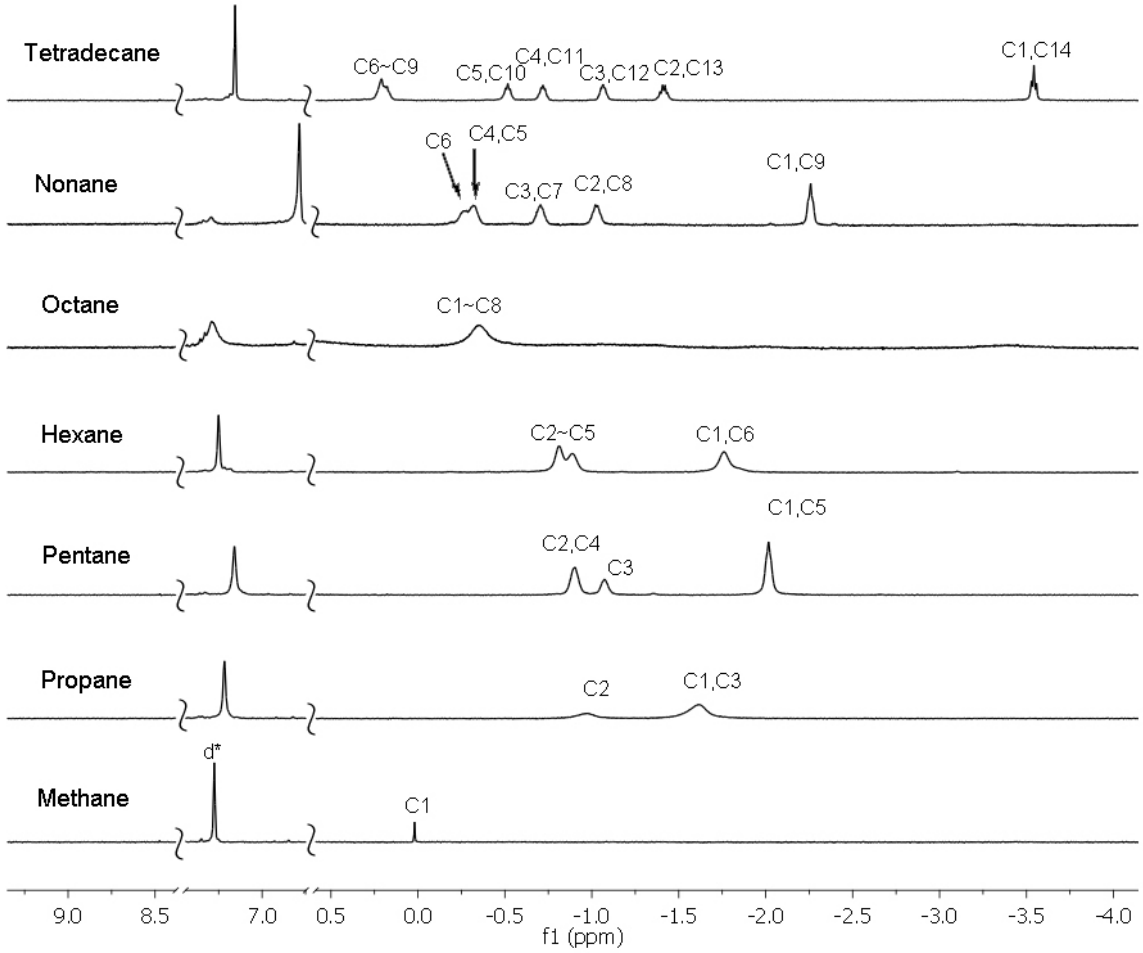

Figure 2-7. ^{1}H NMR spectra of the complexes formed between host **61** and: a) methane; b) propane; c) *n*-pentane; d) *n*-hexane; e) *n*-octane; f) *n*-nonane; g) *n*-tetradecane. Shown is the guest binding region (0.50 to -4.00 ppm) and the signal from the H atoms para to the acetal group in the host (ca. 7.20 ppm). All solutions were 1 mM complex in D_2O, 10 mM $Na_2B_4O_7$ buffer.

The second line of evidence of this non-monotonic switching behavior is confirmed by PGSE NMR experiments. The methane complex possesses the same hydrodynamic volume (HV) as the free host (6.3 nm^3, Figure 2-8). The diffusion constants obtained from both host and guest signals showed that while the ethane complex was essentially monomeric (HV = 7.6 nm^3), propane and *n*-butane led to a mixture of 1:1 and 2:2 complexes (HV = 10.3 nm^3 and 10.6 nm^3 respectively), while *n*-pentane led to mostly 2:2 complex (HV = 12.6 nm^3). The unexpectedly diffusion constants which broke the monotonic trend were observed in the case of *n*-hexane, *n*-

heptane, and *n*-octane. The measured HV value for *n*-hexane complex was 10.1 nm^3 (Figure 2-8) confirmed that these were the 1:1 and 2:2 host guest complexes. With increasing the size of the guests to *n*-heptane and *n*-octane, the measured HV values for these complexes were essentially the same as that obtained for ethane (Figure 2-8). This indicated that *n*-heptane and *n*-octane form 1:1 complexes with host **61**. Guest *n*-nonane switched this assembly trend for a second time with a HV value of 13.2 nm^3, as it forms a 2:1 capsular complex. This is consistent with the aforementioned ^{1}H NMR result which showed a kinetically stable 2:1 complex. Finally, for the larger guests *n*-decane (C10) through *n*-tetradecane (C14), within experimental error there were monotonic shifts in both the bound guest methyl signals and the HV values. Respectively, these leveled off at δ = -3.54 ppm and HV = 14.8 nm^3 in the case of the largest guests examined (Figures 2-7 and 2-8).

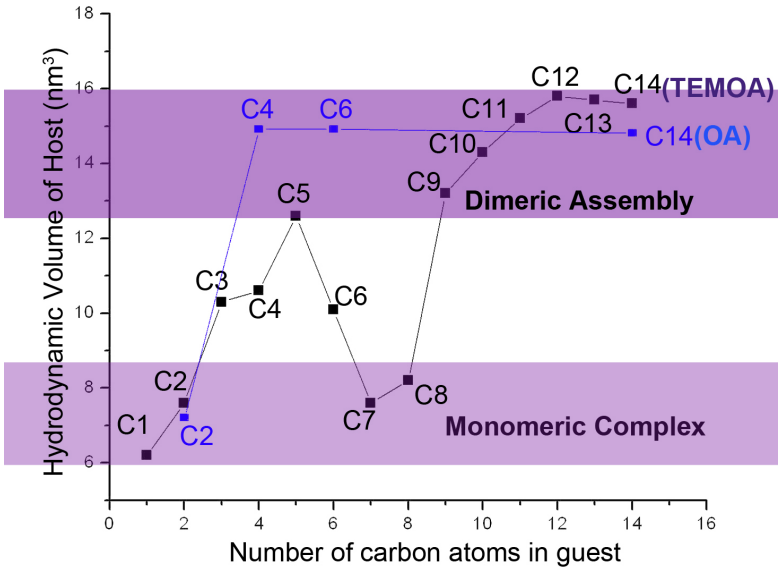

Figure 2-8. Graph of the hydrodynamic volume (HV) of the complexes formed between host **61**/**43** and alkanes guests, against the number of carbon atoms in each guest. Data shown in black corresponds to host **61**. Data shown in blue corresponds to host **43**.

With the evidence from the combination of ^{1}H NMR and PGSE NMR and the aid of CPK models, this non-monotonic switching behavior can be interpreted as follow. Guests methane

through butane bind to the host, but are small enough and not efficient to template the formation of dimeric assemblies. Those small guests accommodated inside the cavity and the upper region of the cavity remained hydrated which resulted in the inhibition of dimerization. Alternatively, these guests are too small to accommodate in a 2:2 dimeric assembly manner, which contain too much void space inside the capsule and lead to less stable assembly formation and a preference for the 1:1 complexes. In contrast to these results, cavitand **43,** which is devoid of methyl groups at it rim, forms thermodynamically and kinetically stable 2:2 complexes in the presence of propane and butane (butane data shown in Figure 2-8). Its hydrophobic rim comprised primarily of aromatic rings that can *π*-stack in the capsular form. While in the case of cavitand **61**, the four methyl groups at the rim reduced these π-stack interactions and therefore the predisposition of dimer assembly formation. On the other hand, the sufficient size of *n*-pentane leads to a relatively hydrophobic portal region with little void space in the 1:1 complex and dimerization to form a 2:2 complex subsequently occurs. However, the guests *n*-hexane through *n*-octane are too large to form 2:2 complexes and too small to template 2:1 complexes. As a result, *n*-hexane forms a mixture of 2:2 and 1:1 complexes, while the 1:1 complex is energetically preferred in the case of *n*-heptane and *n*-octane. In contrast, the still larger guests are of sufficient size to template stable 2:1 host-guest complex but no 1:1 complexes were observed because a significant portion of the guest would remain hydrated in free solution.

Although guest larger than *n*-nonane can efficiently template capsule formation, the slightly narrowed portal of the cavity reduced the predisposition of cavitand **61** to dimerize. This unusual switching trend of the ethane through *n*-octane complexes reveals that the formation of these complexes are approximately isoenergetic. For instance, the selectivity of 1:1 and 2:2 complexes of *n*-hexane is ca. 30:70 corresponding to the 0.5 kcal mol^{-1} difference of the binding

energy ($\Delta\Delta G^{\circ}$). Houk, *et al.* highlights an easy way to predict rough association constants of the binding affinity and thermodynamics of guests and many types of hosts.[171] In order to produce a 95:5 selectivity of better guest at room temperature among those host-guest pairs, the difference of the binding energy of the target molecule and the next best binder is only 1.7 kcal mol^{-1}.[38,171] This energy difference can significantly switch a monomeric complex to a dimeric complex. In addition, competition experiments involving guest binding in simple 1:1 host-guest systems frequently reveal $\Delta\Delta G^{\circ}$ values of 2-3 kcal mol^{-1} for guests differing only in a methylene group.[38] Hence for the guests ethane through *n*-octane, many of the 1:1, 2:1 and 2:2 complexes and assemblies observed here likely lie within 0-1.0 kcal mol^{-1} of each other, a range that is hard to engineer in a simple host guests system.

The non-monotonic trend of switching between monomeric and assembled state of **61** for the guests methane through *n*-nonane can be envisioned in terms of Boolean logic. For example, a pair of selected guests (A and B) can be considered as inputs, whilst the output of the logic gate is either 0 (no assembly) or 1 (assembly into a 2:1 or 2:2 complex).[172] In this regard, both hosts **43** and **61** function as B gates (true whenever B is true), when A inputs correspond to those guests that do not induce assembly (methane to *n*-butane and *n*-hexane to *n*-octane in the case of **61**, and methane and ethane in the case of **43**), and B-guests (*n*-pentane and *n*-nonane or larger in the case of **61,** propane or larger in the case of **43**) are those that do. Defining these systems as two-input, one-output gates does however fail to illustrate an important difference between host **43** and **61**; that is that when considering adjacent pairs in the homologous series **43** is only capable of differentiating between ethane and propane, whereas **61** can differentiate between *n*-butane and *n*-pentane, *n*-pentane and *n*-hexane, and *n*-octane and *n*-nonane. Hence, it is perhaps more appropriate to consider the nine guests methane through *n*-nonane as unique inputs and treat the system as a nine-input, one-output gate (Table 2-1).

Table 2-1. Abbreviated truth table for Host **61** as a nine-input, two-output switch.

Input				Output
Methane-Butane	**Pentane**	**Hexane-**	**Nonane**	
0	0	0	0	0
1	0	0	0	0
0	1	0	0	1
0	0	1	0	0
0	0	0	1	1
1	1	0	0	1
1	0	1	0	0
1	0	0	1	1
0	1	1	0	1
0	1	0	1	1
0	0	1	1	1
1	1	1	0	1
1	0	1	1	1
1	1	0	1	1
0	1	1	1	1
1	1	1	1	1

In conclusion, monotonic switching behaviors are commonly observed in natural and synthetic systems. In synthetic assemblies it is commonly observed that guests of increasing size induce a gradual increasing tendency to trigger assembly. In contrast, the water-soluble deep-cavity cavitand **61** performs an unusual non-monotonic assembly profile. For a homologous series of alkanes, the host can form different types of isoenergetic supramolecular species (1:1, 2:1 and 2:2 complexes). As a result, no or limited assembly is observed with small guests such as methane through butane, *n*-pentane triggers assembly, hexane through *n*-octane again do not induce assembly, whereas *n*-nonane and larger guest again induce assembly.

III. Guest-controlled Self-Sorting in Assemblies driven by the Hydrophobic Effect

In small molecule systems, molecules tend to aggregate with molecules bearing the same shape, functioning groups, or properties. This so-called self-sorting describes the ability to differentiate between self and nonself.[173-175] In the study of supramolecular chemistry, non-covalent interactions such as hydrogen bonding, metal-ligand interactions, and ion-dipole interactions are well-known as driving forces in the process of self-sorting. For instance, hydrogen bonding has been applied in driving the formation of self-assembly of micelles and vesicles, fibers,[176-178] gels,[179] and surfaces.[180] Studies of self-sorting within synthetic systems is revealing new phenomena that shed light on self-assembly and self-organization in biological systems. In addition self-sorting is beginning to generate intricate and complex self-assembling systems.[181-185] Such advances notwithstanding, much is still to be learned regarding the governing rules and limitations of self-sorting.

Deep cavity cavitands **43** and **61** both bear a large hydrophobic interior and eight water-solublizing carboxylic acid groups on their exterior. The hydrophobic effect drives capsule formation of $\mathbf{43}_2$ and $\mathbf{61}_2$ in the presence of suitable guests such as straight-chain alkanes. As discussed in the last chapter, although **43** and **61** both form 2:2 capsules in the presence of small guest such as *n*-pentane and 2:1 capsules in the presence of larger guests such as *n*-nonane through *n*-hexadecane, they have very different assembly properties. Considering these two very different assembly profiles, it was of interest to determine the extent of self-sorting in mixtures of these cavitands; and indeed whether the hydrophobic effect and the subtle differences between the dimerization interfaces of the $\mathbf{43}_2$, $\mathbf{61}_2$ and **43•61** capsules were sufficient to induce non-statistical assembly mixtures. As is discussed (Scheme 3-1), non-statistical assembly is observed in this system, with the precise outcome finely tuned by the

nature of the internalized guest or guests (Scheme 3-1).

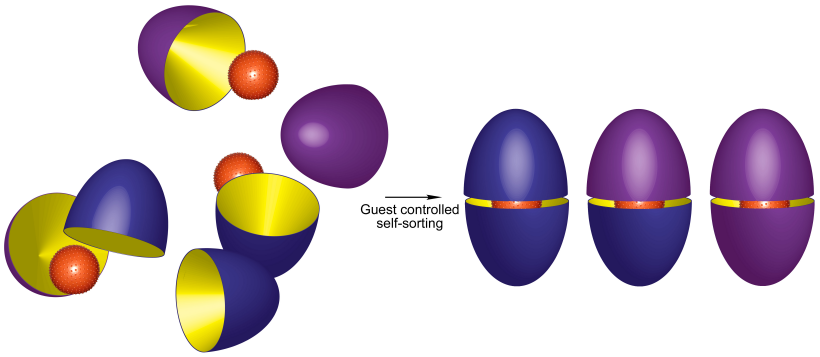

Scheme 3-1. Guest-controlled self-sorting in assemblies. Only 2:1 complexes are shown. 2:2 complexes are formed for the guest pentane.

3.1. Comparison of the Binding Properties of Two Water-soluble Hosts (OA 43 and TEMOA 61) involving Straight-Chain Alkanes

Water-soluble deep-cavity cavitands **43** and **61** both bear a large hydrophobic cavity and can accommodate suitable sized guests inside. **61** has a slightly narrower portal than **43** whereas its cavity is deeper because the four *endo* Me groups on the top rim extended the hydrophobic cavity. They both bear similar cavity interior volume, ca. 320 nm^3. The idea of self-sorting prompted us to ask whether the homo-complex could dominate in the simply mixed solution of these two hosts.

We investigated homo-capsular complex formation of $\mathbf{43}_2$ and $\mathbf{61}_2$ in the presence of a series of straight-chain alkanes. The first comparison to make in these different complexes is among the terminal methyl-H shifts of the alkanes (Table 3-1, Figure 3-1). In the case of $\mathbf{43}_2$, the bound methyl-H atoms of *n*-dodecane (C12) are shifted upfield the greatest amount ($\Delta\delta$ =

4.1 ppm), while smaller upfield shifts were observed in the presence of guests larger than C12 (Table 3-1). Rebek *et al.*[186] have observed this similar non-monotonic trend in the study of alkanes in a self-assembled cyclindrical capsule. They attribute this non-monotonic tend to the change of guest binding conformation within the capsule. Smaller guests adopt extended conformation while larger guests with maximum packing coeffience accommodate helical conformation to achieve a stable capsule formation.[186] In our study, CPK models suggest that guest C12 is an optimized size to be accommodated within capsule $\mathbf{43}_2$ with its terminal methyl groups anchor to the bottom of each hydrophobic pocket. Guests larger than C12 must adopt a slight 'compressed' conformation inside the capsule, the result of which is to move the terminal methyl groups away from the bottom of the pocket and less upfield shift comparing to guest C12 in $\mathbf{43}_2$.[138] Interestingly, $\mathbf{61}_2$ did not follow this non-monotonic trend. A maximum of 4.4 ppm upfield shift of the terminal methyl-H signals was observed for guest *n*-tetradecane (C14) and no significant decreasing of this upfield shift for larger guests was observed. This indicates that larger guests may adopt different conformations inside $\mathbf{61}_2$ than $\mathbf{43}_2$. Although a previous report of **43**,[138] and others,[123,186] have demonstrated examples of alkane guests adopting well-defined helical conformations within capsular assemblies, in this particular case NOESY NMR did not indicate any well defined conformation for the homo-complexes. Consequently, with guests longer than C8 being too long to adopt a fully extended conformation within the cavity, we assume that the intervening chain adopts a multitude of 'compressed' conformations. The data we described may suggest that instead of bearing a helical conformation, in the capsule formation the four *endo* methyl groups on the rim of **61** reduced the π-π stacking of the two hemispheres. Larger guests may accommodate a less 'compressed' conformation inside $\mathbf{61}_2$ thus result in the methyl groups of guests anchored to the bottom of the hydrophobic pocket.

Table 3-1. ^{1}H NMR chemical shifts (δ_{Methyl}) and changes in chemical shifts ($\Delta\delta_{Methyl}$) of the methyl-H atoms of encapsulated guest *n*-pentane through *n*-hexadecane (C16) internalized within capsules **43**$_2$ and **61**$_2$.

Guest No.of Carbons	OA **43** complex		TEMOA **61** comples	
	δ_{Methyl} (ppm)	$\Delta\delta$ (ppm)	δ_{Methyl} (ppm)	$\Delta\delta$ (ppm)
5	-1.59	-2.49	-2.02	-2.92
6	-1.65	-2.55	-1.78	-2.68
7	-1.73	-2.63	*	*
8	-1.82	-2.72	*	*
9	-2.17	-3.07	-2.26	-3.16
10	-2.73	-3.63	-2.75	-3.65
11	-2.89	-3.76	-3.11	-4.01
12	-3.18	-4.09	-3.51	-4.41
13	-3.11	-4.01	-3.46	-4.36
14	-3.05	-3.94	-3.54	-4.44
15	-2.54	-3.42	-3.48	-4.38
16	-2.27	-3.16	-3.45	-4.35

*denotes formation of 1:1 monomeric complexes.

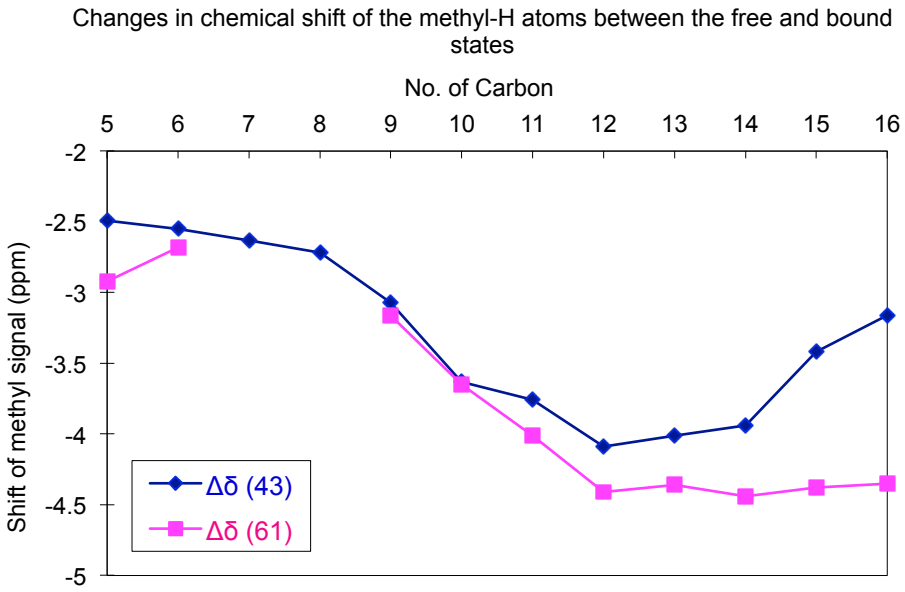

Figure 3-1. Changes in chemical shifts ($\Delta\delta_{Methyl}$) of the methyl-H atoms of encapsulated guest *n*-pentane through *n*-hexadecane (C16) internalized within capsules **43**$_2$ and **61**$_2$.

In addition, we reviewed the shift of the signals of the guest central protons of the two capsules to provide further insight of guests binding conformation. In the presence of C12, the central protons have shifted upfield of 1.21 ppm and 1.32 ppm in homo-capsular complexes $\mathbf{43}_2$ and $\mathbf{61}_2$ respectively. In these two capsules, the guest central protons are located close to the equator of the capsule and have less shielding effect from the aromatic walls of the hosts than terminal methyl-H protons. This leads to much smaller upfield shifts. In both cases of homo-capsule $\mathbf{43}_2$ and $\mathbf{61}_2$, there is enough void space in these 2:1 capsules and it leads to kinetically stable capsules with a complete dehydration of the hydrophobic surfaces of host and guest. However, the guest central protons of larger guest C16 have a 1.32 ppm upfield shift in $\mathbf{43}_2$ while only 0.42 ppm upfield shift in $\mathbf{61}_2$, an indication that capsule $\mathbf{43}_2$ has a larger shielding effect on the guest central protons than $\mathbf{61}_2$ (Table 3-2, Figure 3-2). This result can be explained by appreciating that the four *endo* methyl groups prevent the guest chain from closely approaching the wall of the host. These results also agree with the monotontic trend of **61** for the movement of terminal methyl groups of guests with increasing the size of guests. In other words, larger guests accommodated inside capsule $\mathbf{43}_2$ with their center carbons completely dehydrated by the hydrophobic cavity, whilst the four methyl groups at the rim of TEMOA **61** reduced the π···π interaction between each hemisphere which results in the less shielding effect from the cavitand walls.

Table 3-2. Change in ^{1}H NMR chemical shifts (Δδ) of methyl and methylene protons of guests C12 and C16 in the presence of host **43** and **61**, unit is in ppm.

Proton Position		1	2	3	4	5	6	7	8
Host + C12 complex	**43**+C12	-4.1	-2.6	-2.31	-1.68	-1.54	-1.21		
	61+C12	-4.43	-2.7	-2.41	-1.83	-1.83	-1.32		
Host + C16 complex	**43**+C16	-3.18	-2.15	-2.08	-2.01	-1.87	-1.62	-1.42	-1.32
	61+C16	-4.37	-2.72	-2.43	-1.89	-1.63	-0.75	-0.52	-0.42

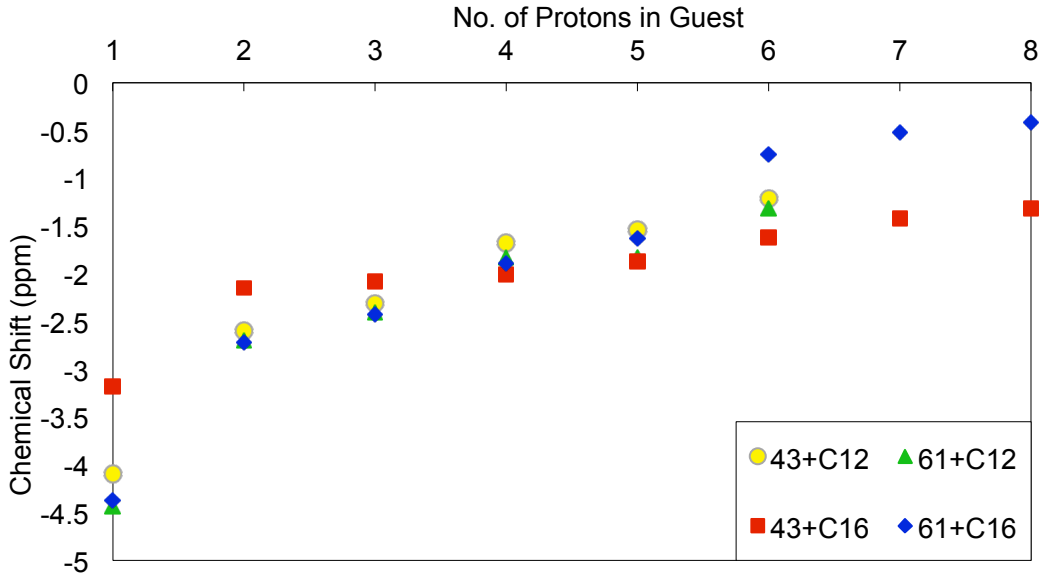

Figure 3-2. Change in ^{1}H NMR chemical shifts (Δδ) of methyl and methylene protons of guests C12 and C16 in the presence of host **43** and **61**.

3.2 Formation of Hetero-complexes

We examined the self-sorting of **43** and **61** in the presence of a series of the alkanes C5 through C16. The general experimental procedure was to add excess of guest to either 1 mM solutions of **43**, **61**, or a 1:1 mixture of the two hosts (10 mM sodium tetraborate). The use of excess guest ensured that all host molecules were in the bound state, even in the situation when both capsular and 1:1 complex were formed. The assembly state of the products was confirmed with PGSE diffusion NMR, with hydrodynamic volumes of 8.0 nm^3 for 1:1 complexes and 15.2 nm^3 for capsular complexes typically being observed (Figure 3-3). In all complexes, the bound terminal methyl-H and the methylene signals followed the same trend as the previous ^{1}H NMR study of home-capsule formation. The most upfield-shifted signal was for the terminal methyl-H atoms and the methylene signals of the chain spread over a ca. 1.25 ppm wide

window (Figure 3-3). COSY NMR experiments confirmed progressive upfield shifting of the signals from the central methylene(s) to the pair of C-2 methylene groups.

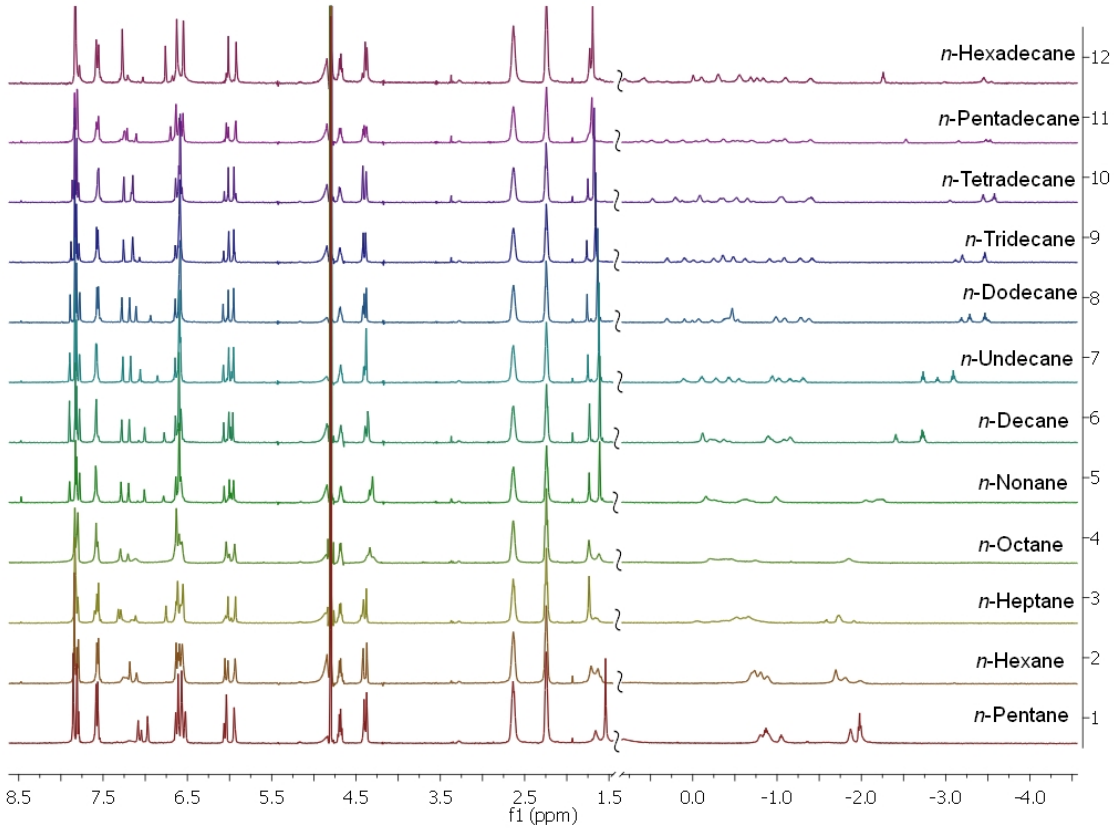

Figure 3-3. Partial ^{1}H NMR spectra of the **43•61** hetero-capsular and 1:1 complexes and hydrocarbons pentane through *n*-hexadecane.

Using the ^{1}H NMR spectra of the homo-capsular complexes as references, it was possible to assign most of the signals in the spectrum obtained from the mixture of hosts. In the cases where assignment was problematic using ^{1}H NMR data alone, COSY NMR experiments were also utilized (Figure 3-4). The spectra for the homo- and hetero-complexes formed between **43**, **61** and C11 show typical ^{1}H NMR data (Figure 3-5). The two homo-capsule complexes (Figure 3-5 a and b) showed gross overall similarity, but their combination reveals subtle differences between them, as well as differences with the corresponding hetero-complex

(Figure 3-5 c and d). The signals for the bound guests in the highfield region, as well as the signals at ca. 7.00 ppm from the "d" protons (see structures **43** and **61**) at the rim of the hosts, were the most chemically distinct, however this was also the case with many of the host signals between 6-8 ppm, as well as the *endo*-methyl groups of host **61** (1.50-1.70 ppm).

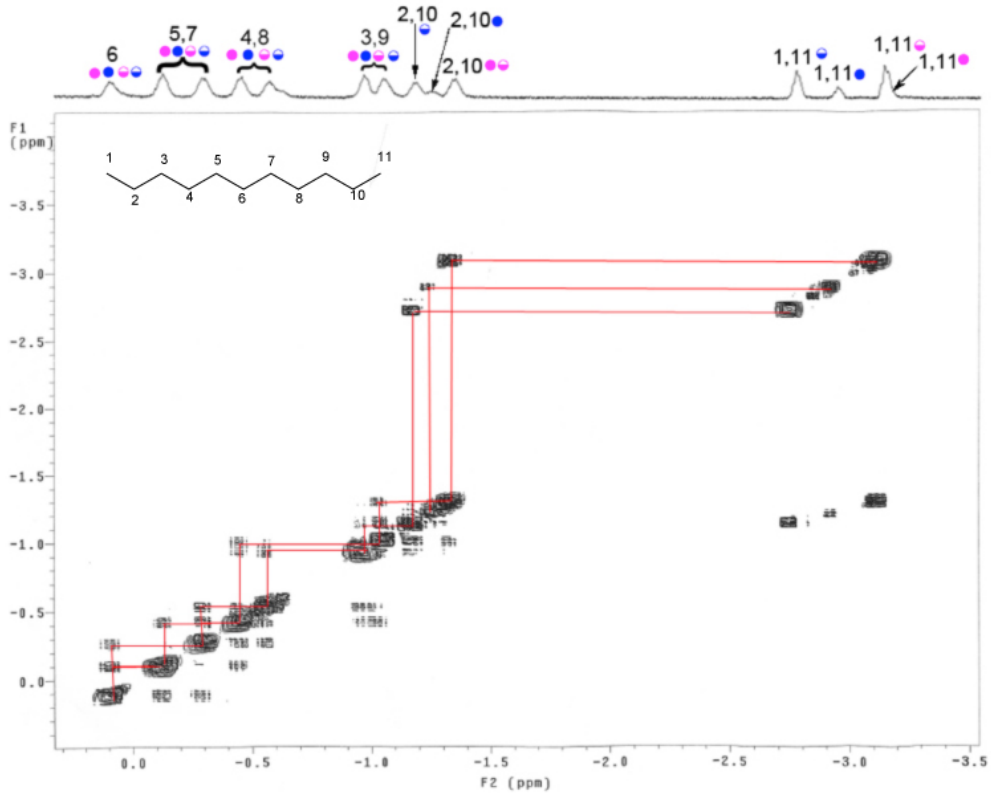

Figure 3-4. Bound guest region of the COSY NMR spectra of the mixture of OA **43** and TEMOA **61** in the presence of *n*-undecane (C11). Designations are: **1**.**1** homo-capsule (●), **2**.**2** homo-capsule (●), host **1** of hetero-capsule (◒), host **2** of hetero-capsule (◒). In each spectrum the total host concentration is 1 mM, each guest was added to the solution as an excess, and the buffer was 10 mM $Na_2B_4O_7$.

In the homo-complexes with *n*-undecane the bound guest methyl signals occur at δ = -2.89 and δ = -3.11 for the capsules involving **43** and **61** respectively (Figure 3-5 a and b). The combination of the two hosts and C11 lead to three, rather than four, signals for the bound methyl groups (Figure 3-5 c and d). Evidence was a small peak for the methyl signal from the $\mathbf{43}_2$ capsular complex, as well as two signals at -2.69 and -3.06 ppm. The first of these was

assigned to the methyl group located in cavitand **43** of the **43•61** complex, whilst the latter was assigned to the methyl located in cavitand **61** of the **43•61** complex, as well as the methyl groups in the $\mathbf{61}_2$ capsule. Integration of the three signals in the mixture of **43**, **61** and *n*-undecane respectively suggested a 31:69 ratio of the homo- and hetero-complexes. This ratio was confirmed by examining the "d" signal region of the NMR spectrum that showed four baseline-resolved signals for the homo and hetero-complexes (Figure 3-5 c and d): 6.89 and 7.09 ppm for the homo-capsule complexes $\mathbf{61}_2$ and $\mathbf{43}_2$, and two "d' signals in the hetero-complex appeared at 7.20 (hemisphere comprised of **61**) and 7.29 ppm (hemisphere comprised of **43**). For this particular guest, the ratio of the complexes could be further confirmed by the two distinct signals for the *endo*-methyl groups (Figure 3-5 c). Integration of these peaks readily established that the signal at 1.65 ppm arising from the **43•61** hetero-complex, whilst the signal at 1.78 ppm corresponds to the $\mathbf{61}_2$ homo-complex.

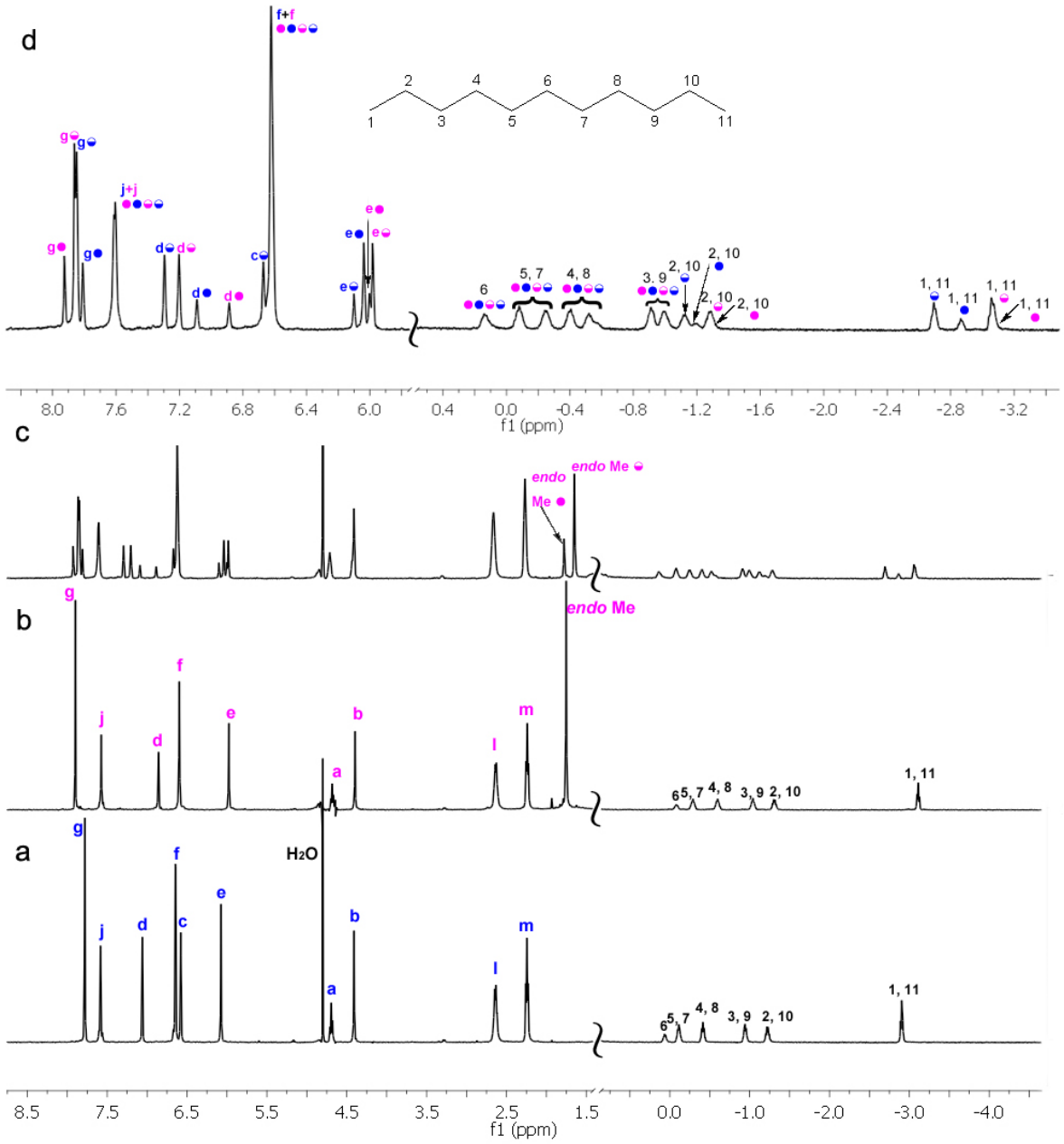

Figure 3-5. Partial ^{1}H NMR spectra of the 2:1 complexes formed between: a) **1** and *n*-undecane (see structure for atom designations); b) **2** and *n*-undecane; c) **1** and **2** and *n*-undecane; d) Expansion and assignments of signals in spectrum c). Designations are: **1**.**1** homo-capsule (●), **2**.**2** homo-capsule (●), host **1** of hetero-capsule (◒), host **2** of hetero-capsule (◒). In each spectrum the total host concentration is 1 mM, each guest was added to the solution as an excess, and the buffer was 10 mM $Na_2B_4O_7$.

An inspection of the ^{1}H NMR spectra of the complexes for C5 through C16 reveals an 'island' of kinetic instability for the complexes formed by guests C6 though C9. Thus, whereas

the signals in the complexes of *n*-pentane and C12 through C16 were sharp, this was not the case for the signals for the complexes of C6 though C9. Three representative examples, the ^{1}H NMR spectra of the complexes formed by C5, C8, C10, are shown in Figure 3-6. As expected, for the relatively unstable hetero-capsular complexes formed by C8 signal broadening was particularly evident for the guest signals that undergo the largest chemical shift upon complex formation ($k_{coal} = 2.22\Delta\delta$). However, broadening was also evident with the "d" and *endo* methyl signals of the host. A variable temperature ^{1}H NMR experiment down to 5 °C reduced the signal broadening of the C8 complex somewhat, but did not fully sharpen the signals. Regardless, even at room temperature the sharp(er) host signals in the less stable complexes allowed the determination of the nature and the ratio of the different complexes formed, and hence it was possible to determine the extent of self-sorting in all of the systems studied.

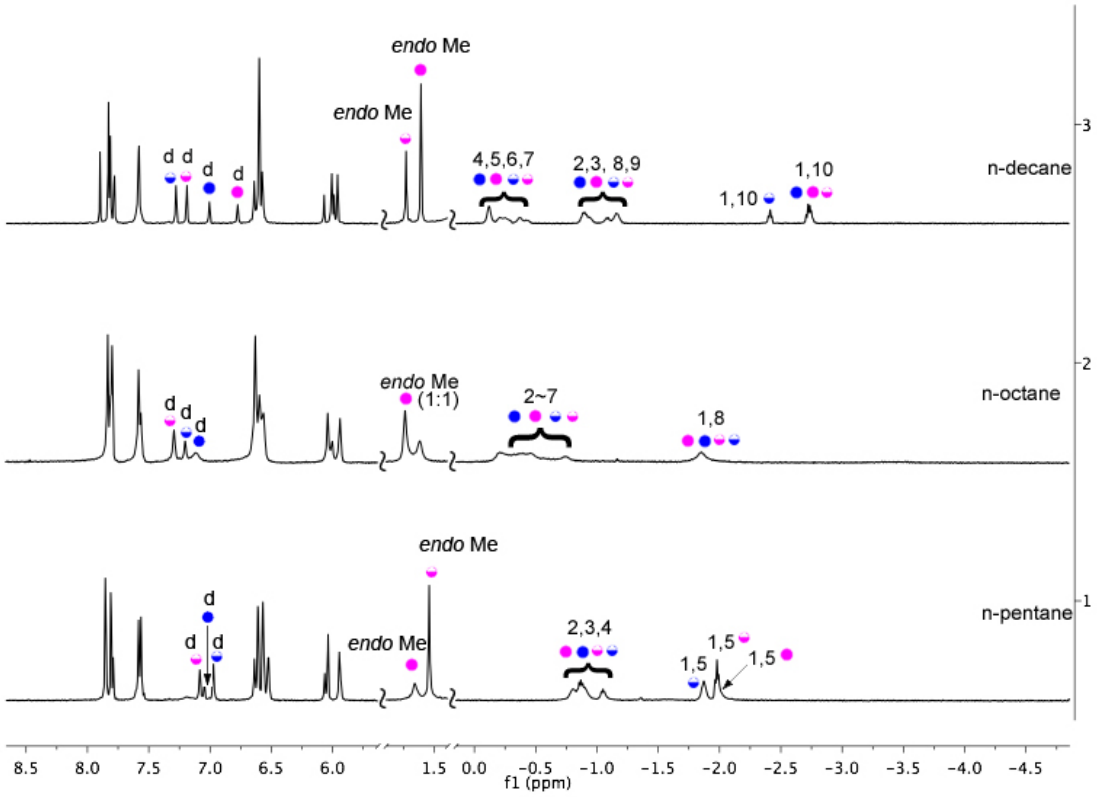

Figure 3-6. Partial ^{1}H NMR spectra of the complexes formed between hosts **43** and **61** and: a) *n*-pentane; b) *n*-octane; c) *n*-decane. Designations are: **43**$_2$ homo-capsule (●), **61**$_2$ homo-capsule (●), host **43** of hetero-capsule (◒), host **61** of hetero-capsule (◒). In each spectrum the total host concentration is 1 mM, each guest was added to the solution as an excess, and the buffer was 10 mM sodium tetraborate.

The formation of hetero-capsule of C5 was also investigated at a different host concentration and different temperature. At a low concentration (0.5 mM of each host) a broad peak at -1.59 ppm corresponds to the bound methyl signals of the C5 in its homo-capsule **43**$_2$ was evident, which indicates that exchanging rate between the free and bound states is close to the (500 MHz) NMR timescale. A sharp bound guest methyl atom signal of homo-capsule **43**$_2$ appeared with increasing the concentration of each host to 1 mM in their mixed solution. However, the mixture of the two hosts solution at higher concentration resulted in the aggregation of host **43** (Figure 3-7). The sharpening of the guest methyl signal may be due to the resulting faster exchange assembly with increasing the host concentrations. In addition, two new bound methyl groups appeared at -1.87 ppm and -1.98 ppm which correspond to the guest

encapsulated inside a capsule with two different hemispheres **43** and **61** respectively. A bound methyl group at -2.02 ppm corresponds to the *n*-pentane in the homo-capsule $\mathbf{61}_2$.

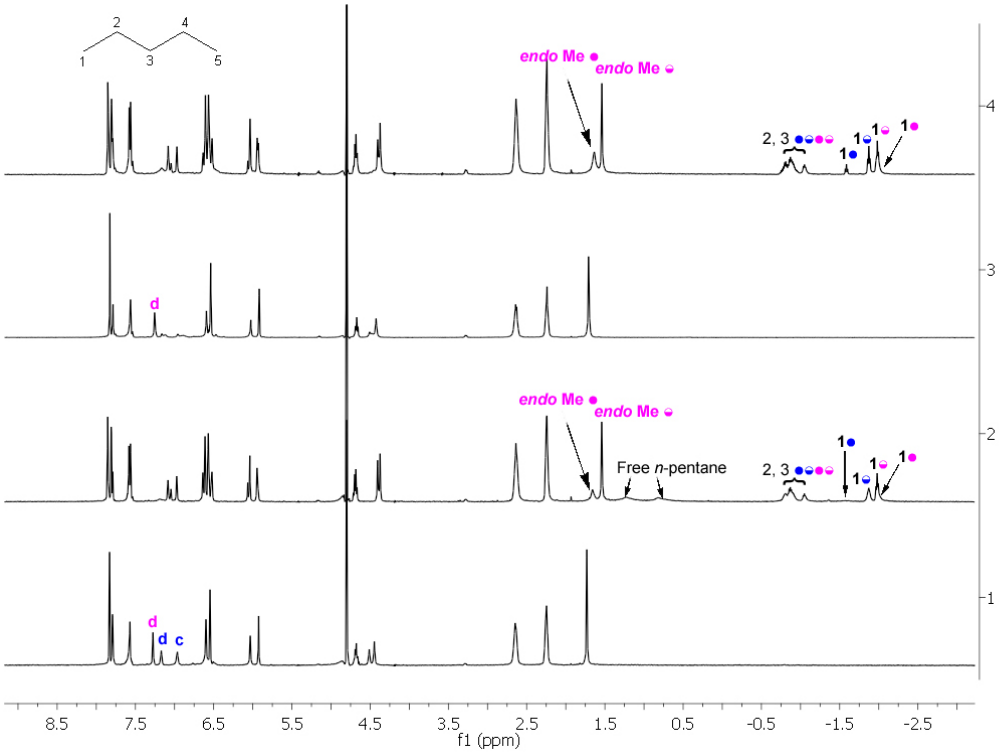

Figure 3-7. The mixture of host **43** and **61** at 1) 0.5 mM in 10 mM $Na_2B_4O_7$; 2) 0.5 mM in 10 mM $Na_2B_4O_7$ in the presence of *n*-pentane; 3) 1 mM in 20 mM $Na_2B_4O_7$; 4) 1 mM in 20 mM $Na_2B_4O_7$ in the presence of *n*-pentane.

We also examined the change in chemical shift data between methyl groups binding in the home and hetero capsules for a number of guests. Specifically the guest C5, C9 ~ C16 were examined (Figure 3-8). The bound methyl signals were overlapped in the case of C6 through C12 which prevented further analysis. In the case of host **61**, the chemical shifts Δδ (hetero **61** – homo **61**) changed steadily with slight downfield shifting in the presence of large guests. In contrast, in the case of host **43**, the methyl signals of guest in heteo **43** shifted upfield compared to its homo-capsule $\mathbf{43}_2$ in the case of C5. Unexpectedly, the signal moved downfield with Δδ (hetero **43** – homo **43**) of 0.17 ppm in the presence of C11 while switching to an upfield shift with Δδ up to 0.73 ppm in the presence of the largest guest C16. This result is

attributed to the four *endo* methyl groups at the rim of **61** which reduced the void space in the hetero-capsular complex comparing to its homo-capsule $\mathbf{43}_2$. Larger guests accommodate a less 'compressed' conformation in their hetero-capsules which resulted in the methyl-H atoms of the guests moving further to the bottom of the hydrophobic pocket comparing to their packing in homo-capsule $\mathbf{43}_2$. Neglecting guest C5, the changes in chemical shift data between methyl groups binding in the home and hetero capsules for guest C11 to C16 follow a monotonic trend. The chemical shifts of terminal methyl-H in homo-capsule $\mathbf{61}_2$ are similar as in hetero **61** (Figure 3-8, purple line), whereas greater changes in the case of **43** (Figure 3-8, blue line). We attribute this results to the guest binding in both homo-capsule $\mathbf{61}_2$ and hetero-capsule **43•61** accommodate similar less compressed conformation, which results in a similar chemical shift of the terminal methyl-H atoms. However, in the case of homo-capsule $\mathbf{43}_2$, the compressed conformation dominates which results in greater difference between the homo and hetero **43**.

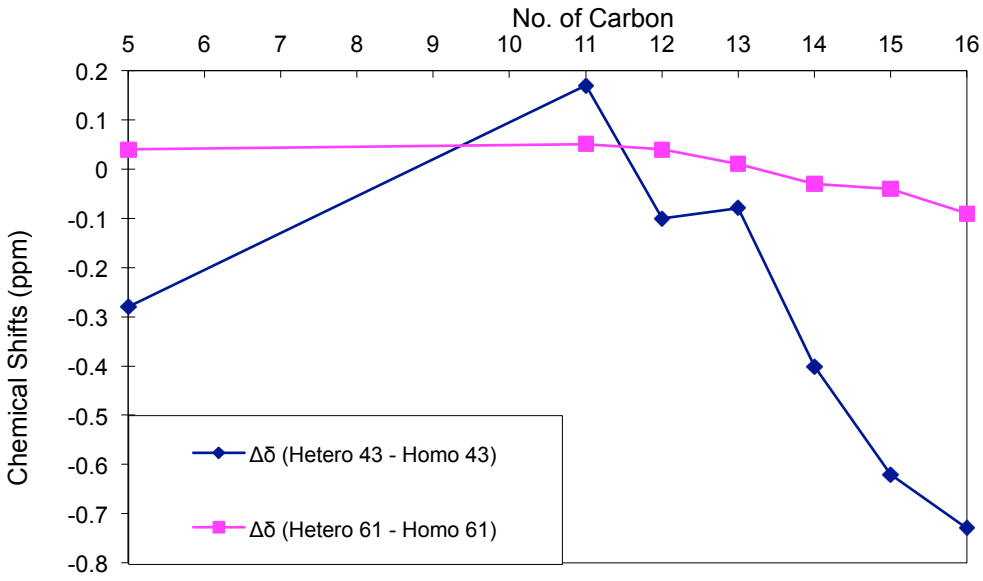

Figure 3-8. Changes in ^{1}H NMR chemical shifts (Δδ) of methyl-H of guests between hetero- and homo-capsular complexes versus the number of carbons in guests.

Figure 3-9 shows the percentage of hetero-capsular complex formed as a function of the size of the internalized guest. The percent hetero-complex ranges from 24% in the case of C7 to 74% in the case of C13. Also apparent is a non-monotonic trend in percent hetero-complex as a function of guest size; with there being an increase in the amount of self-sorting between the guests *n*-pentane and *n*-heptane, a decrease in the amount of self-sorting between C7 and C14, and then again an increase in self-sorting for C15 and C16.

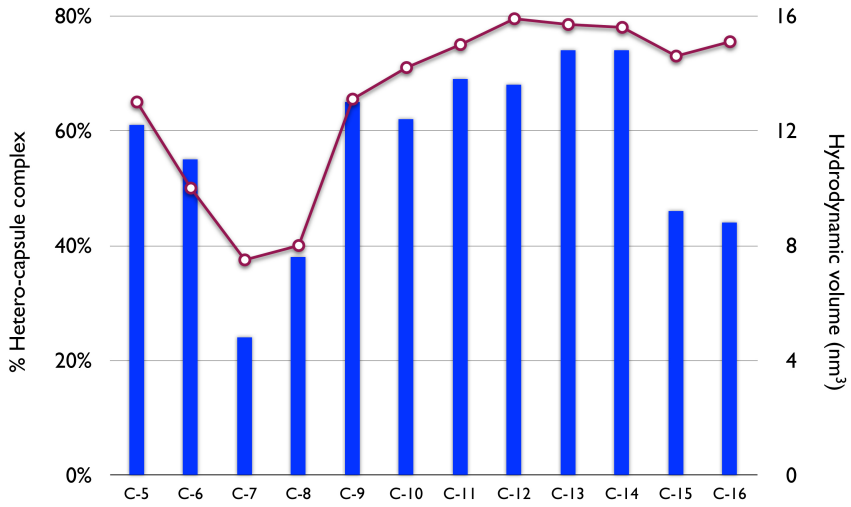

Figure 3-9. Bar graph showing the relationship between the extent of hetero-capsule (**43•61**) formation and the size of the encapsulated guest(s). Also shown (red line) is the relationship between the hydrodynamic volume for the complexes formed between pure **61** and the different guests.[187]

An appreciation of the assembly profiles for each individual host allows us to understand the fundamentals behind the variation in self-sorting as a function of guest for the mixture of hosts. As we have pointed out, cavitand **43** possesses the expected assembly profile as a function of guest size[136,138] with ethane forming a 1:1 host-guest complex whereas guests propane and larger induce dimerization to form supramolecular capsules. NMR shift data suggests that the stability of these complexes increases as guest size increases up to C12, and beyond this size the stability of the complex decreases as the cavity of the capsule becomes increasingly packed.[138] In contrast, the assembly profile of **61** – represented in Figure 3-9 as the plot of the average hydrodynamic volume of the host-guest complex(es) formed by the

different guests – is more complicated.[187] For the series of guests *n*-pentane to *n*-octane, host **61** forms an increasingly unstable homo-capsular complex because crowding of the two guests within the capsule increases, and energetically, encapsulation of only one guest is not an option. The net effect of this and the steric interaction induced by the four *endo*-methyl groups projecting into the dimerization surface is a decreasing predisposition to assemble. As a result mostly 1:1 complex is formed with *n*-heptane and *n*-octane. In contrast, with the guests *n*-nonane and larger only one guest is bound within the capsule. In these cases guest-guest 'clashes' are not an issue and the capsular complexes are more stable.

In the system comprised of both hosts, there are four possible complexes: a simple 1:1 host-guest complex (host **61** only), two homo-capsular complexes $\mathbf{43}_2$ and $\mathbf{61}_2$, and the hetero-capsule **43•61**. Cavity volumes were measured in quadruplicate by measuring the water-holding capacity of CPK models lined with polyethylene films. All of the capsular complexes are measured to have approximately the same volume (ca. 650 $Å^3$). Thus, although the methyl groups of **2** project into the binding pocket of the host, the fact that they also project 'upwards' deepens the cavity somewhat and compensates for the narrowing of the cavity lip.

Although all of the capsules formed are of approximately the same volume, they are not of the same stability. No direct comparison is possible because the very low solubility of the guests precludes titration experiments, and because formation of hetero-complexes prevents competition experiments between the two homo-capsules. However, the comparison of the methyl-H shift in both homo-capsules, the chemical shifts of central guest protons in both homo-capsules, and the methyl-H shift in the hetero-capsules combined with consideration of the relative predispositions of each host to assemble, it is evident that the capsular complexes formed from **43** are of greater stability than those formed by **61**. Furthermore, with half the

number of destabilizing methyl groups the hetero-capsule **43•61** is likely to be of intermediate stability.

For the guests C5 and C6, 61% and 55% of the cavitands form hetero-capsular complexes, which is close to the 1:2:1 statistic ratio between homo- and hetero-complexes. This indicates that no preference of the formation of either the homo- or hetero-capsular complexes in the presence of these two guests. These guests are small enough to form relatively stable 2:2 homo-capsular complexes with pure **61**, and in the mixture of the hosts the hetero-capsule offers a more stable alternative to homo capsule formation.

Guests C7 and C8 form the least amount of hetero-capsular complex (24% and 38% respectively). An examination of the NMR spectra of the host mixture involving these guests (C8 is shown in Figure 3-7) reveals both form substantial amounts of 1:1 complex with **61**. Both guests are poor templates for the homo assembly of $\mathbf{61}_2$, so much so that in these cases any energetic benefit in forming the hetero-complex rather than the homo-capsule with **61** is itself limited. As a result, both guest systems self-sort into stable $\mathbf{43}_2$, leaving host **61** to form 1:1 complexes in preference to any of the corresponding homo-capsule. In other words, the combination of the stable capsular complexes formed by **43**, and the unstable homo-capsule formed by **61**, results in very little hetero-complex formation.

Figure 3-9 shows that for larger guests there is another swing in the date, with guests *n*-nonane through *n*-tetradecane forming between 62% and 74% of the **43•61** hetero-complex. The principle difference between these complexes and those involving smaller guests is that the efficient packing of the capsule requires only one guest. This biases each system towards hetero-capsule formation. However, it is unclear as to whether the shift in the equilibrium

towards the hetero-capsules and away from the homo-capsules is enthalpically or entropically based.

Finally, for the largest guests examined, C15 and C16, there is a relative drop in the amount of hetero-complex formed to approximately statistical levels. Why this occurs is unclear although these molecules are close to the maximum guest size for the different capsules. If this is an important factor, then the shift towards increased self-sorting indicates that one of the homo-capsules is better suited for binding the larger guest than is the hetero-capsule.

3.3. Isothermal Titration Calorimetry (ITC) Binding Studies of Water-soluble Complementary Guests

In terms of relative capsule stability, no direct comparison is possible because the low solubility of the guests precludes titration studies, and because formation of hetero-complexes prevents competition experiments. However, considering the relative predispositions of each host to assemble, it is evident that the order of stability is $\mathbf{43}_2$ > **43•61** > $\mathbf{61}_2$. As an alternative strategy, we applied Isothermal Titration calorimetry (ITC) experiments in the investigation of two water-soluble guests tri(ethylene glycol) dimethyl ether **65** (TriEGdiMe) and tetra(ethylene glycol) dimethyl ether **66** (TetraEGdiMe) binding with host **43** and **61**. The selection of these two water-soluble guests is on the basis of their similar size as C12 and C15, respectively. Guest TriEGdiMe **65** has twelve non-hydrogen atoms which bears a length of 12.596 Å, which compares to 13.835 Å for C12. ITC experiments revealed that the binding constants of host **43** and **61** in the presence of this water-soluble guest are 8.38×10^4 M^{-1} and 1.04×10^5 M^{-1}, respectively. Likewise, guest **66** with fifteen non-hydrogen atoms bears a length of 16.019 Å, which compares to 17.570 Å for C15. Interestingly, the binding constant of host **43** involving **66**

is 1.26 × 10^5 M^{-1} while the binding curve failed to fit for host **61** which indicates the weaker binding constants at the same condition of ITC experiments (Figure 3-10).[188,189] These parallel experiments revealed that larger guests tend to form a weaker capsule within $\mathbf{61}_2$ than $\mathbf{43}_2$. This may due to the four *endo* methyl groups at the rim reduced the predisposition of dimerization of **61**.

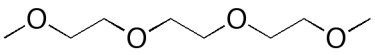

65

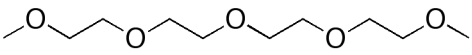

66

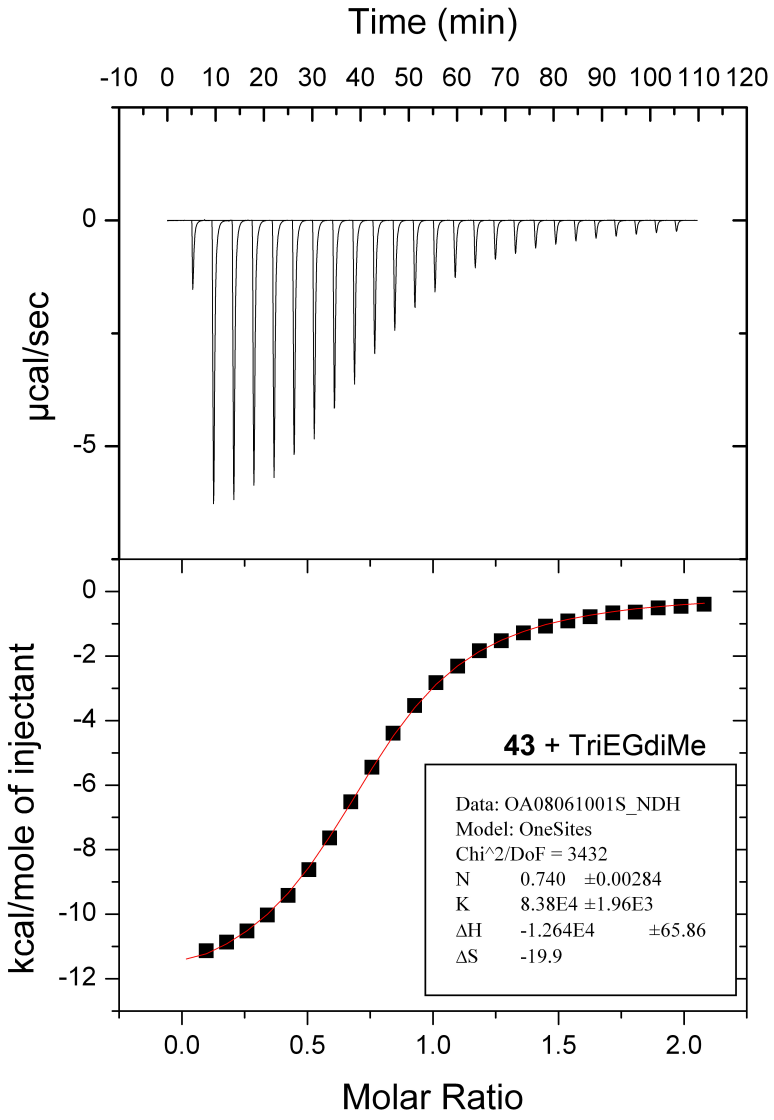
Time (min)
-10 0 10 20 30 40 50 60 70 80 90 100 110 120
µcal/sec
0
-5
kcal/mole of injectant
0
-2
-4
-6
-8
-10
-12
0.0 0.5 1.0 1.5 2.0
Molar Ratio
43 + TriEGdiMe
Data: OA08061001S_NDH
Model: OneSites
Chi^2/DoF = 3432
N 0.740 ±0.00284
K 8.38E4 ±1.96E3
ΔH -1.264E4 ±65.86
ΔS -19.9

(1)

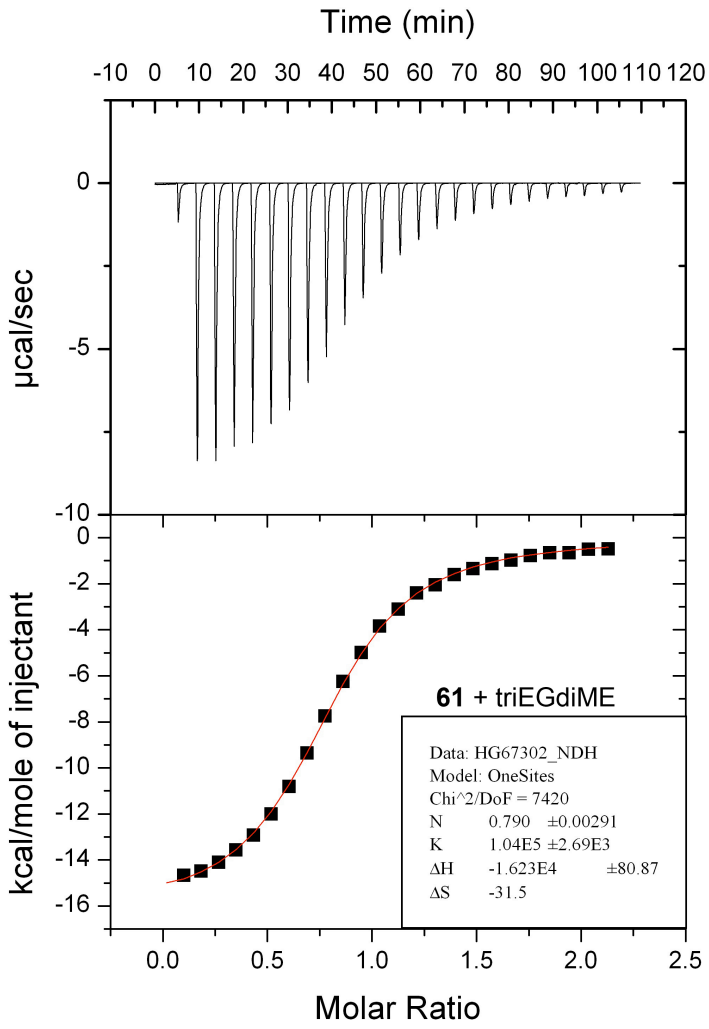
Time (min)
-10 0 10 20 30 40 50 60 70 80 90 100 110 120
µcal/sec
0
-5
-10
kcal/mole of injectant
0
-2
-4
-6
-8
-10
-12
-14
-16
61 + triEGdiME
Data: HG67302_NDH
Model: OneSites
Chi^2/DoF = 7420
N 0.790 ±0.00291
K 1.04E5 ±2.69E3
ΔH -1.623E4 ±80.87
ΔS -31.5
0.0 0.5 1.0 1.5 2.0 2.5
Molar Ratio

(2)

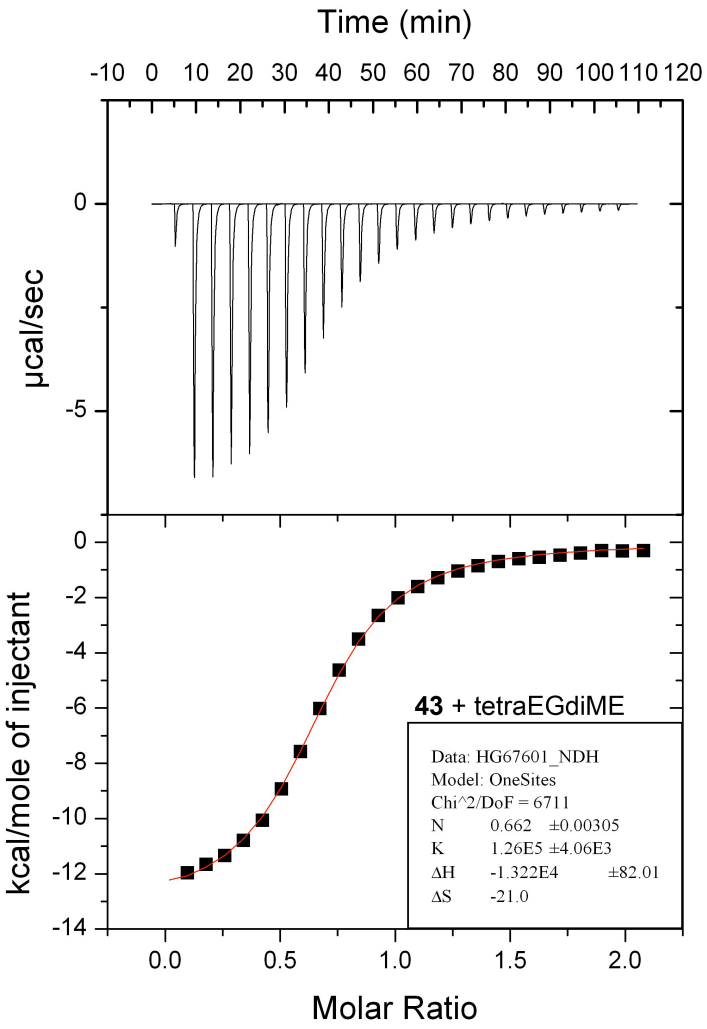
Time (min)
-10 0 10 20 30 40 50 60 70 80 90 100 110 120
µcal/sec
0
-5
kcal/mole of injectant
0
-2
-4
-6
-8
-10
-12
-14
0.0 0.5 1.0 1.5 2.0
Molar Ratio
43 + tetraEGdiME
Data: HG67601_NDH
Model: OneSites
Chi^2/DoF = 6711
N 0.662 ±0.00305
K 1.26E5 ±4.06E3
ΔH -1.322E4 ±82.01
ΔS -21.0

(3)

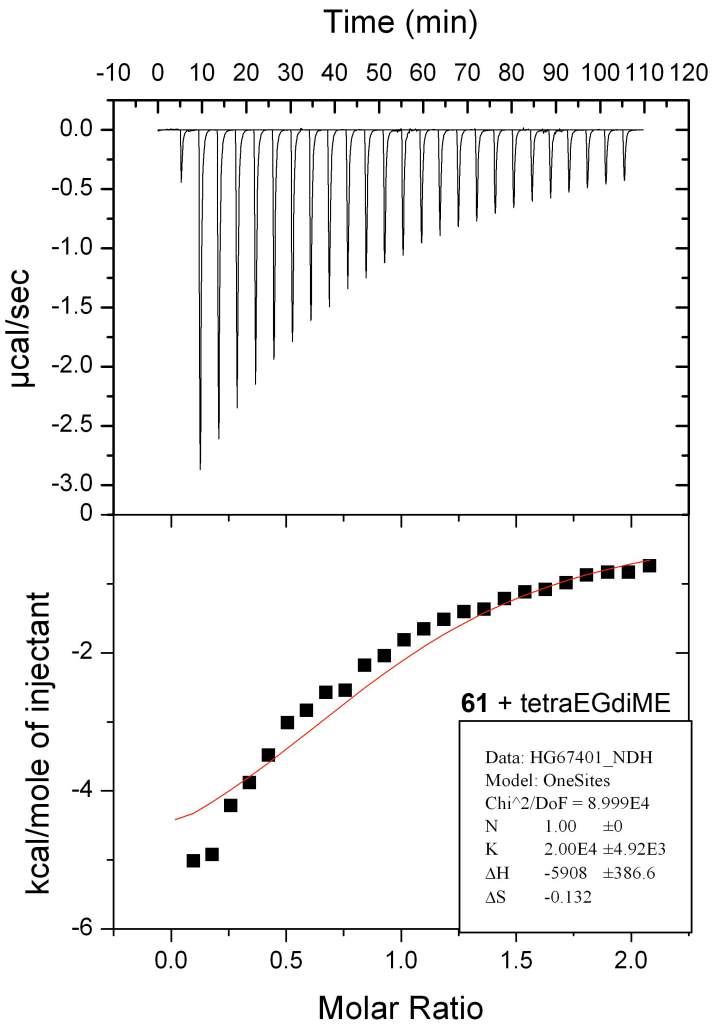

(4)

Figure 3-10. ITC experiments of 1) Host **43** in the presence of tri(ethylene glycol) dimethyl ether **65**; 2) Host **61** in the presence of tri(ethylene glycol) dimethyl ether **65**; 3) Host **43** in the presence of tetra(ethylene glycol) dimethyl ether **66**; 4) Host **61** in the presence of tetra(ethylene glycol) dimethyl ether **66**.

In summary, guest-sized induced self-sorting between two water-soluble hosts **43** and **61** were investigated. The degree of self-sorting in this two-hosts system is highly dependent on the size of the guest. Furthermore, for guests smaller than *n*-tetradecane the parallels between the propensity of **61** to assemble and the extent of hetero-complex formation suggest that the low stability of homo-capsules formed between **61** and smaller guests plays an

important role in the mixed system. This emphasizes that very subtle and intricate relationships between self-sorting and guest could be constructed by the judicious choice of (host) components, which correspondingly suggests avenues to the formation of switches with complicated response patterns. More generally, the results here demonstrate that the structural information contained within hydrophobic assembly surfaces can be sufficient to engender unusual supramolecular phenomena; highly directional non-covalent interactions such as hydrogen bonding and metal coordination between molecular partners are not a prerequisite.

IV. Guest-size Mediated Switching between Assembled States

The study of container molecules of nanoscale dimensions is relatively rare. One well-known high stoichiometry assembly is Atwood's hexameric assembly, cube **67** (Figure 4-1),[190] in which six resorcin[4]arene units are held together by 60 hydrogen bonds. As with most assemblies, **67** forms in organic solvents. This large assembly affords a ca. 1375 $Å^3$ internal volume and can thus provide sufficient space to encapsulate larger guests, or carry out reactions inside the cavity where a large space is a prerequisite.

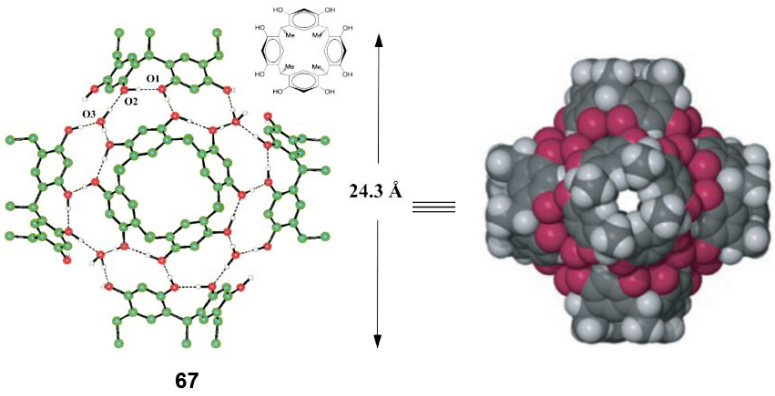

67

Figure 4-1. The structure of **67**: Left, cross-sectional view; Right, space-filling views along the crystallographic four-fold rotation axis. Permission License: 2781680243388.

Formation of this type of large assembly in water is elusive. Water is a polar solvent and has strong hydrogen bonds. These properties of water impose a considerable handicap on hydrogen bonding as an assembly strategy. Only a limited examples in the literature applied hydrogen bonding in the formation of 1:1 monomeric complex in water, such as the aforementioned Rebek cavitand **38** (Figure 1-19), whereas no formation of higher stoichiometry assemblies have been reported in literatures. Another commonly utilized approach in constructing assemblies in water is metal-ligand coordination bond. Appropriate metals and ligands can build large assemblies with large hydrophobic interior, such as the aforementioned

Fujita's octahedral nanocage **13** (Scheme 1-4) and Raymond's tetrahedral host **16** (Figure 1-13).

However, we are more interested in the formation of self-assembled host-guest systems driven by the hydrophobic effect. The Gibb group pioneered hydrophobic effect driven self-assemblies.[134] Hydrophobic guests with suitable size can template the formation of dimerization and gave mono-dispersed 2:1 stoichiometry assemblies in water. Recently, the Shionoya group reported the first higher stoichiometry assemblies formed in water.[191] To our knowledge, the reported tetrameric and hexameric assemblies made up of gear shaped molecules **68** are the only other examples utilizing the hydrophobic effect as a driving force (Figure 4-2).[191] These higher stoichiometry assemblies have relative small internal volume, for example two copies of 2,4,6-tribromomesitylene (24 non-hydrogen atoms) in the hexameric assembly, which may limit their application.

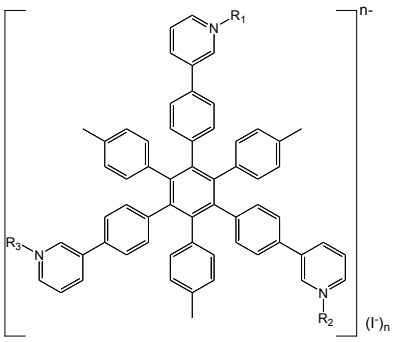

68

Figure 4-2. Gear-shaped amphiphiles **68** from the Shionoya group.

Our understanding of the binding and self-assembly properties of container molecules of lower stoichiometry assembled states (dimer) assists us to understand the new and unique properties in more complexed self-assembled states. Previous studies revealed that OA **43** is highly predisposed to dimerize in the presence of hydrophobic guests, whereas TEMOA **61**, with a different assembly profile, is less predisposed to dimerize. TEMOA **61** has an apparent

narrower energy difference between the monomeric and the dimeric states. This limited ability of forming dimeric assemblies led us to investigate whether the hydrophobic effect can drive TEMOA **61** to form mono-dispersed higher stoichiometry assemblies in water. This study involves TEMOA **61** and a series of larger straight-chain alkanes C14 through C26. The simple concept behind this strategy is that with an increase in the size of guests, packing inside the dimeric assembly would not be possible. In other words, due to space limitations larger guests would induce higher stoichiometry assemblies. Here we demonstrate that utilizing the hydrophobic effect, two truly water-soluble, mono-dispersed high stoichiometry assemblies are achieved. Their vast internal volume will provide an unprecedented opportunity in drug delivery, novel separations, and nanoscale reactor development.

4.1. Formation of Higher Stoichiometry Assemblies

We examined the encapsulation of the homologous series of the *n*-alkanes tetradecane (C14) through hexacosane (C26) involving TEMOA **61** using a combination of ^{1}H NMR (Figue 4-3) and PGSE NMR experiments. The general experimental procedure was to add excess of guest to 1~3 mM solution of **61** in 100 mM NaOD. In our previous studies, 10 mM $Na_2B_4O_7$ was used in the formation of assemblies, while in this project 100 mM NaOD was used in order to simplify the obtained ^{1}H NMR spectra. For instance, assembly of C17 and TEMOA **61** in 10 mM $Na_2B_4O_7$ gave two sets of bound signals, whereas only a single set of signals was observed in 100 mM NaOD (The effect of salt switching assemblies will be discussed in Chapter V). In this study of larger guests C24 through C26, 3 mM host solution was used to ensure full assembly formation. Solutions involving high melting point alkanes (C18 through C26) were heated in an oil bath at 70~80 ˚C. ^{1}H NMR was applied in determination of the stoichiometry of the assemblies. The assembly state was confirmed with PGSE diffusion NMR.

The combination of ^{1}H NMR and PGSE NMR revealed the assembly made up of C14 and 1mM **61** was the kinetically stable 2:1 dimeric complex. The obtained hydrodynamic volume (HV = 11.5 nm^3) and integration confirmed the 2:1 stoichiometry of this assembly. The sufficient size of C14 leads to a dimerization of two units of **61** with complete dehydration of the hydrophobic surface of the guest and binding pockets. With the larger guests C15 and C16, more than one set of signals of bound methyl and methylene groups were observed. This was our first indication that instead of forming kinetically stable 2:1 dimeric complexes, these guests formed more than one assembly (Figure 4-3). These signals were also typically broader than the slow exchange C14, which suggests the exchange rate between each assembled state is faster then the slow binding C14 and the energy difference between each assembled state is relatively small. As we expected, the ^{1}H NMR of the complexes of guests C17 through *n*-eicosane (C20) each appeared as a single set of sharp signals with a methyl group signal showing at -3.33 ppm (for C17). The chemical shifts of bound guest signals followed the typical trend of straight-chain alkanes encapsulated within the nano-capsule. Signal integration and PGSE analysis of the bound host and guest signals confirmed that the host-guest ratio was 2:1, and that the corresponding HV value was 22.5 nm^3 (for C17), a value four times greater than its monomer. In other words, the complex is a 4:2 tetramer. A hint of straight-chain alkanes binding inside capsules from the previous study of hetero-capsular complex formation was that the hetero-capsular complexes were unfavored in the presence of the relative large alkanes C15 and C16. This result is interpreted as that the dimeric homo-TEMOA formation is less stable than homo-OA dimer in the presence of guests C15 and C16. These clear results demonstrate that guests C15 and C16 are too large to form a stable 2:1 dimeric assembly but too small to template a stable 4:2 tetramer, whereas guest C17 leads to very little void space in the 2:1 dimeric assembly but is ideal in the tetrameric assembly. The formation of tetrameric assembly in the presence of C17 can be viewed as the first switch from a low stoichiometry assembly (2:1) to a higher stoichiometry assembly (4:2).

In contrast to C20, guests *n*-heneicosane (C21) through *n*-tricosane (C23) showed both multiple guest and host signals. The broad guest signals again indicated exchange between assembled states faster than the slow exchanging dimeric and tetrameric assemblies. Following the trend of switching a dimeric assembly to a tetrameric assembly, the second switch in assemblies was completed with guest *n*-tetracosane (C24) through *n*-hexacosane (C26). More specifically, this second switch revealed one set of both host and guest signals. Integration of the bound host signals again showed as 2:1 ratio, whereas the diffusion NMR experiment revealed the new assembly as a hexamer (HV = 44.9 nm^3 for C24). The slight broad host signals of its ^1H NMR mirrored the increased HV of free host at this concentration. We attribute this to either a slight aggregation of host at higher concentrations, or the slow diffusion of this large assembly.

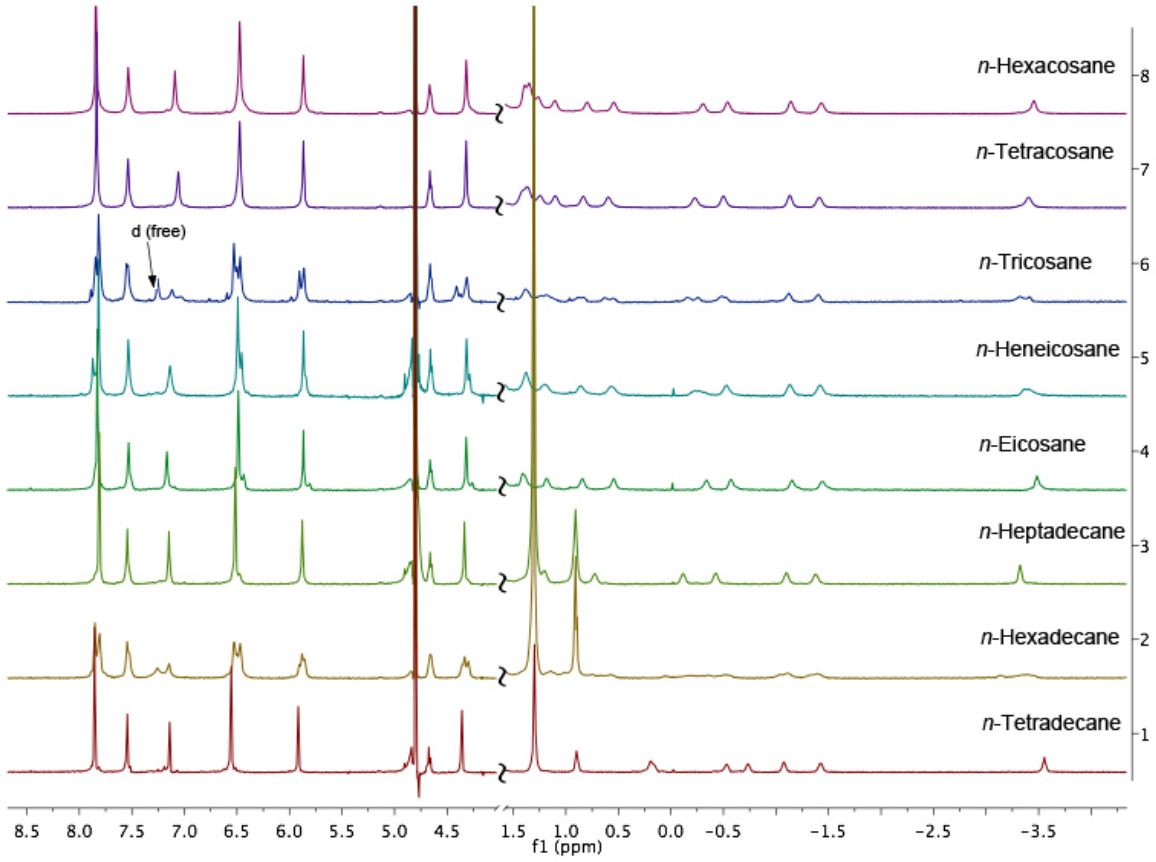

Figure 4-3. ^{1}H NMR spectra of the complexes formed between host **61** and: 1) *n*-tetradecane C14; 2) *n*-hexadecane C16; 3) *n*-heptadecane C17, 4) *n*-eicosane C20; 5) *n*-heneicosane C21; 6) *n*-Tricosane C23; 7) *n*-Tetracosane C24; and 8) *n*-Hexacosane C26. Solutions 1 to 6 were 1 mM complex in D_2O, 100 mM NaOD; solutions 7 and 8 were 3 mM complex in D_2O, 100 mM NaOD.

Although it is evident that straight-chain alkanes adopt well-defined helical conformations in the assemblies constructed by OA **43**[138] and Rebek's cavitand[123]. NOESY NMR did not indicate any well-defined conformation of the guests within these high stoichiometry assemblies. We assume that larger alkanes accommodate a multitude of 'compressed' conformation within the dimeric capsule in order to optimize the packing with less hydrophobic surface exposing to water.

As a complementary support to these studies of the tetrameric assemblies, we designed and synthesized a tetrahedral template **69** and investigated the binding between **69** and host

61. Compound **69** has 8 non-hydrogen atoms on each side chain and one center carbon. It therefore has approximately the same length from Me-to-Me as the straight chain C17. The broad guest signals of the ^{1}H NMR spectrum revealed the exchange rate of the host-guest complex of **61•69** is faster than that of C17 (Figure 4-4). This may be due to the oxygen atoms on each side chain of the guest interacting with water through hydrogen bonding, which reduce with the overall hydrophobicity of the guest. The PGSE diffusion experiment confirmed a tetrameric assembly with the corresponding HV measured at 20.8 nm^3. The slightly lower HV value than that of the *n*-heptadecane tetrameric assembly is most likely due to the less stable assembly. Additionally, the fact that the two chains of the guest are tied together may limit the host-guest interactions at the core of the assembly.

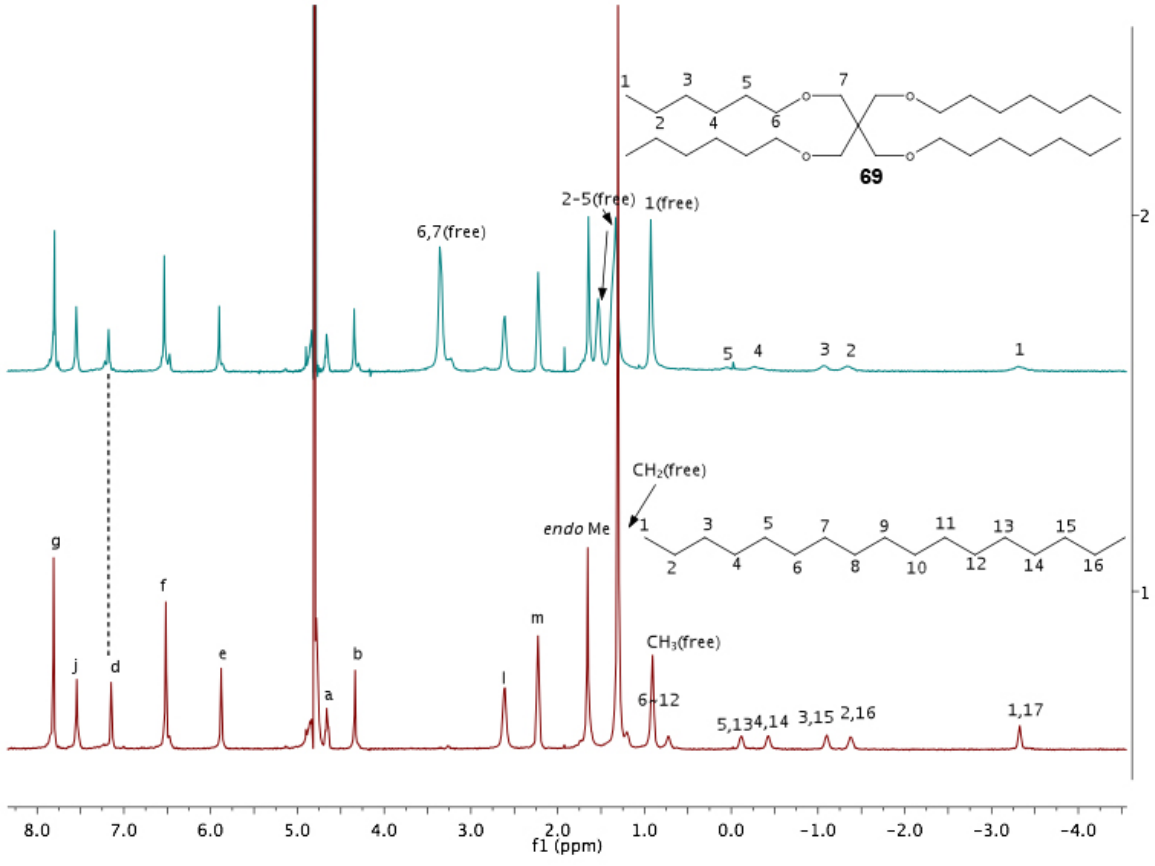

Figure 4-4. ^{1}H NMR of 1) *n*-heptadecane; 2) tetrahedral template **69** in 1 mM TEMOA **61** (100 mM NaOD).

4.2 Determination of the Structure of the High Stoichiometry Assemblies

Our ^{1}H and PGSE diffusion NMR results have demonstrated that TEMOA **61** readily forms higher assemblies. It is important to determine their structures. A few complementary strategies can be applied in this determination, such as X-ray crystallography or dynamic light scattering (DLS). As a method-of-choice, X-ray crystallography can provide direct structural information in the solid state, whereas PGSE diffusion NMR and DLS probe the behavior of the assemblies in the solution phase. We have not obtained any crystals of these different complexes. We will continue to try and grow suitable crystals, and DLS experiments will be carried out in the near future. Consequently, our determination of the possible structures of these large assemblies relied on ^{1}H NMR and PGSE diffusion NMR, as well as computer and CPK models. We discuss the structures below.

The discovery of the tetrameric and hexameric assemblies prompted us to examine their structures on the basis of symmetry. Tetrameric and hexameric assemblies are constructed from four and six identical cavitands, respectively. Here, we define each cavitand as a subunit. This definition allows us to cover all possible symmetries. For a four subunits tetrameric assembly, there are three possible symmetries: D_{2h}, D_{2d}, and T_d (Figure 4-5). D_{2h} symmetry has two pairs of two subunits (one pair constitute on the northern hemisphere and another pair the southern hemisphere) attached at the equator. This is an energetically unstable geometry for the tetrameric assembly due to the existence of electrostatic repulsion of the negatively charged exterior.

The D_{2d} point group is topologically equavilent to a tennis ball, each subunit of this system is symmetrical (Figure 4-5 b). This symmetry is the most ideal structure of the tetrameric assembly. In the case of T_d symmetry, four subunits are placed at the vertices or the

faces of a tetrahedron. We attribute the relative simple aromatic region of the ^{1}H NMR spectrum to a well-defined species with D_{2d} symmetry, but with three rotation of each subunit around it C_{4v} axis giving an average T_d symmetry. In both D_{2d} and T_d symmetry, the four cavitand subunits in this pseudo-spherical system and their aromatic moieties on the upper rim exhibit much of the curvature of this system.

With the aid of Spartan and CPK models, the distance between two top rim aromatic moieties (with 180^o angle) is ca. 1.25 nm which results the edge length (*a*) of internal tetrahedron 1.44 nm (*a* = 1.25/sin 60^o) and the corresponding interior volume is ca. 320 Å^3 ($V = \sqrt{2}a^3/12$). In a T_d symmetry, a well-defined central tetrahedral cavity is constructed by each cavitand subunit with an edge length of ~1.04 nm. The combination of the four folds cavitand volumes and the central tetrahedral void gives a capacity of the assembly of approximate 1500 Å^3.

Unfavored (a) Favored (b)

Figure 4-5. Shells with 4 subunit a) D_{2h} symmetry; b) D_{2d} symmetry (average to T_d symmetry)

In the case of six subunits, three possible symmetries exist: D_{3h}, O_h (I), and O_h (II) (Figure 4-6). In a D_{3h} symmetry, each two subunits cover one third of the surface of a sphere (Figure 4-6 a) and result in 11 vertices. We divide these 11 vertices into two types: type I has three subunits share one vertex and each subunit denotes one of the four carboxylic acid

groups which are appended on the top rim aromatic moieties in the cavitand structure. There are two Type I occupied vertices. Type II has two subunits share one vertex and each subunit denotes one of the four rim carboxylic acid groups. There are nine Type II occupied vertices. The O_h symmetry assembly has six subunits on each face of a cube (Figure 4-6 b). The two possible O_h symmetries have the rim carboxylic acid groups of each cavitand located either at the vertices of a cube (O_h (I)) or at the edges (O_h (II)). CPK models showed all these three symmetries fit with the C_{4v} symmetry of the subunit, while D_{3h} is unfavored due to too much open space exposing to water. We attribute the relative simple aromatic region of the ^{1}H NMR spectrum to a well-defined species with a symmetry averaging between those two O_h symmetries. In the case of O_h (II) symmetry, each cavitand on the face of the cube gives a ca. 1.25 nm edge length of the central cubic hydrophobic cavity, which leads to a total internal volume of 3900 nm^3. This large hydrophobic interior can accommodate approximate 90 non-hydrogen atoms inside the cavity.

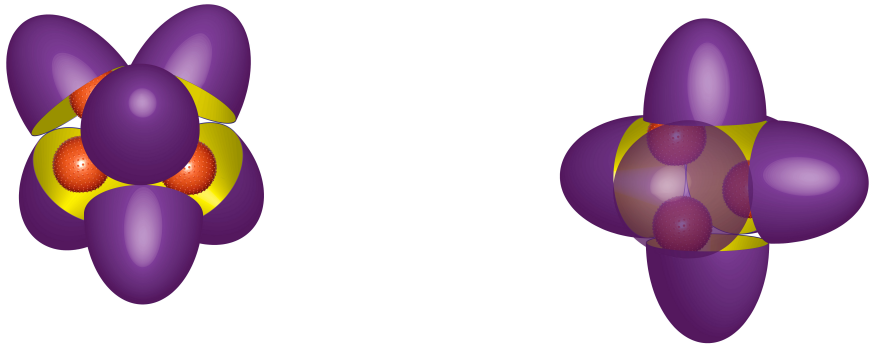

Unfavored
(a)

Favored
(b)

Figue 4-6. Shells with 6 subunit a) D_{3h} symmetry b) O_h symmetry.

^{1} HNMR spectra assists our understanding of the possible structures of these large assemblies. In the case of 1 mM TEMOA in 10 mM $Na_2B_4O_7$ solution involving guests C15 and C16, the “d” protons signals appear approximately at the same chemical shift as in their free

state (δ = 7.25 ppm,), whereas upfield shifted “d” protons were observed in the case of 100 mM NaOD solution (δ = 7.15 ppm, Figure 4-7 (3)). This suggests that the dimeric assemblies involving larger guests result in less π···π stacking of the two hemispheres, and therefore less desolvation of the cavitand hydrophobic rim. This shift of “d” proton signal continued in the higher stoichiometry assemblies, showing at 7.05 ppm in the hexameric assembly of C24.

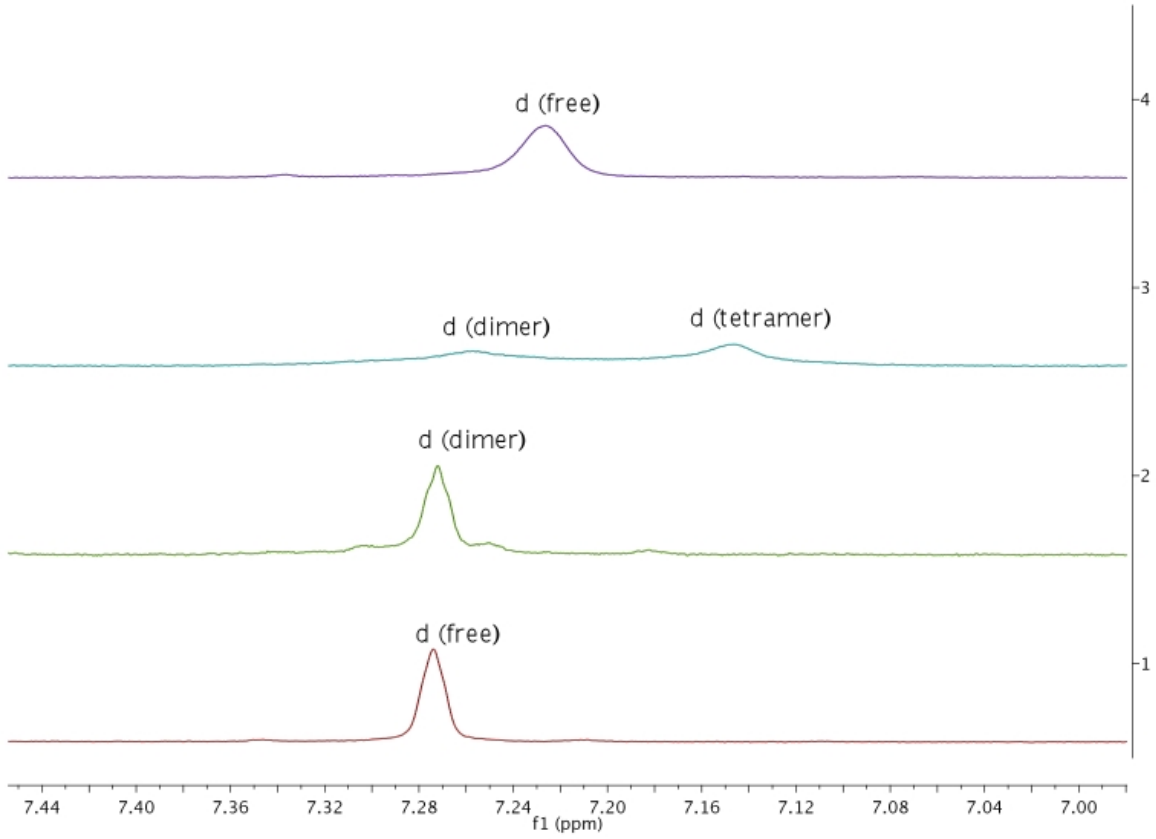

Figure 4-7. Partial ^{1}H NMR aromatic region of 1) 1 mM TEMOA in 10 mM $Na_2B_4O_7$; 2) 1 mM TEMOA in 10 mM $Na_2B_4O_7$ in the presence of *n*-hexadecane; 3) 1 mM TEMOA in 100 mM NaOD in the presence of *n*-hexadecane; 4) 1 mM TEMOA in 100 mM NaOD.

These shifts of “d” proton can be explained by considering the possible assembly structures. Figure 4-8 shows in the D_{4h} symmetry of the dimeric assembly, the “bite angle” of the third row aromatic rings between the north and south hemispheres has large hydrophobic surface being exposed to water, whereas in the tetrameric D_{2d} structure and hexameric Cube

(II) structure this aforementioned angle is smaller and the exposed hydrophobic surface greatly diminished. This may strengthen the π···π stacking between the aromatic units, enhance the van der Waals interactions between the hydrophobic moieties, and result in the more desolvated "d" proton accompanied with upfield-shift. The combination of these weak non-covalent interactions promotes the formation of the more stable higher stoichiometry assembly structures driven by the hydrophobic effect.

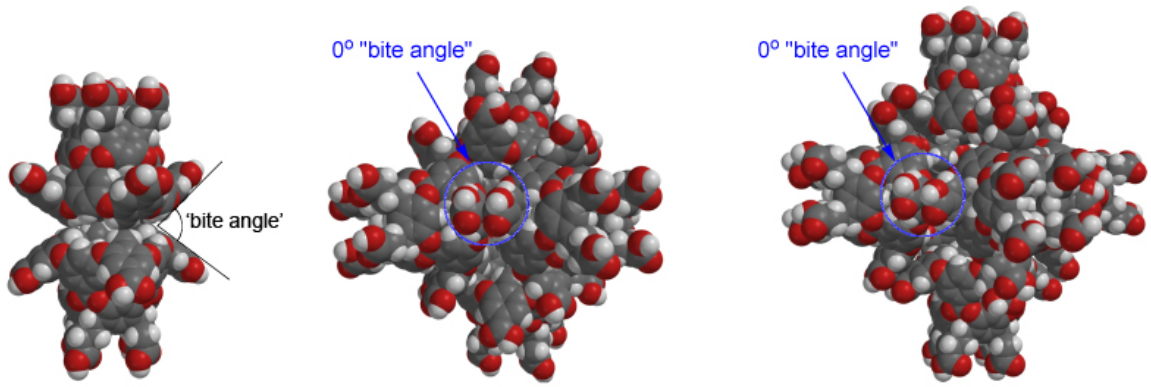

Figure 4-8. Space filling model of TEMOA Left: dimer, D_{4h} symmetry; Middle: tetramer, D_{2d} symmetry; Right: hexamer, Cube(II) symmetry.

In summary, mono-dispersed high stoichiometry assemblies driven by the hydrophobic effect were observed in the presence of large straight-chain alkanes (C15 through C26). They both possess enormous internal hydrophobic cavities, an opportunity of accommodating larger or diverse guest molecules. Two boundaries of the switching indicate the assembled states between dimer and tetramer, tetramer and hexamer are isoenergetic. The conformation of the encapsulated guest alkanes is under further investigation. These mono-dispered water-soluble large assemblies may be in drug delivery, novel separations, and nanoscale reactor development.

V. Salt Mediated Switching Between Self-Assembled States

5.1. The Hofmeister Series

All salts affect the stability and solubility of proteins. Proteins precipitate out in the solution of NaF (salting-out), while they become more soluble in $NaClO_4$ solutions (salting-in). Ions can be rank-ordered on their ability of affecting the physical properties of proteins and other molecules. The order is so named the Hofmeister series,[192,193] a concept that was first proposed more than a century ago (Figure 5-2). According to extensive experimental measures, salting-out or kosmotropic ions are generally small ions of high charge density, they are favorably hydrated in solution and apparently order water and unfavorably interact with hydrophobic solutes. In contrast, salting-in or chaotropic ions are large ions of low charge density, they apparently disorder water and stabilize the solute-water interface thus lead to favorable interacting with hydrophobic solutes.[194] The Hofmeister series is generally observed at high salt concentrations, ca. 1 M. Experiments show the Hofmeister effect is not only found for protein precipitations, but can also be seen in the effect of the solubility of nonpolar solutes in water.[195,196] McDevit *et al.* interpret the Hofmeister effects interms of the first and second-neighbour water shells around ions.[197]

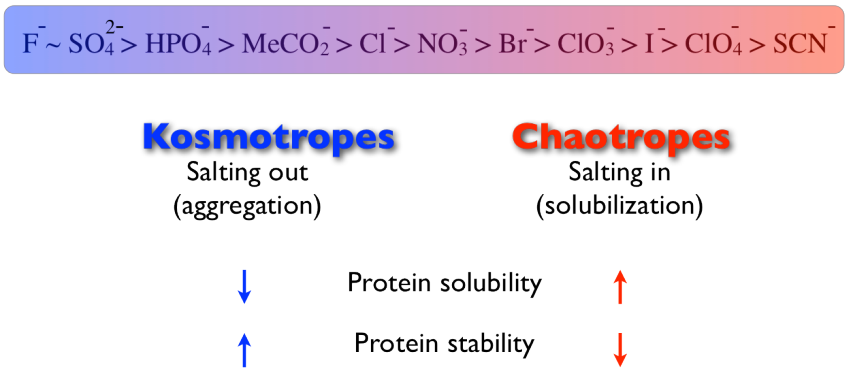

Figure 5-1. The Hofmeister series and the effect of different salts on the physical properties relating to protein folding.

Studies examining the relationship between salt concentration and bulk phenomena such as viscosity,[198] surface tension,[199-201] and solubility[202] on proteins, in combination with *in silico* studies[200,203,204] suggest weak interactions between hydrophobic groups and chaotropes. Little is known about explaining the Hofmeister effect at the molecular level because proteins have structures that are too complex to examine for specific interaction. However, chemists are starting to utilize the designed 'simple' molecules to investigate the Hofmeister effect from the fundamental level. Recently, Gibb *et al.*[205] have revealed for the first time that chaotropic anions have an affinity for hydrophobic concavity (the binding pocket of **43**). The competition for the binding site between the chaotropic anions and a guest molecule leads to an apparent weakening of the hydrophobic effect, which is agreed with the Hofmeister effect (Figure 5-2). The binding between chaotropic anion ClO_4^- and cavitand **43** has the strongest affinity (K_a = 95 M^{-1}) among the investigated Hofmeister series. In the case of cavitand **61** the strongest binding is anion SCN^- of K_a = 78 M^{-1} whilst ClO_4^- is of K_a = 54 M^{-1} and I^- is of K_a < 1 M^{-1}. This suggested to us to investigate whether anions binding to cavitand **61** influences the stability of its different assembled states (*vide infra*).

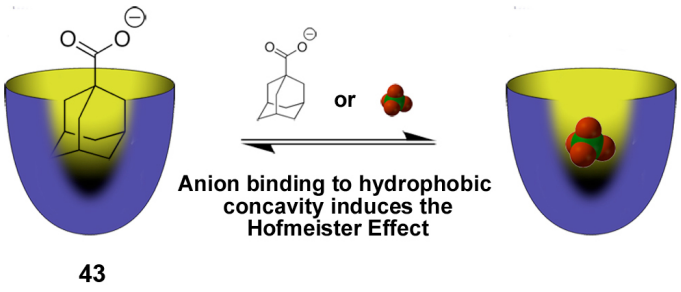

Figure 5-2. Binding competition between anion and adamantanecarboxylic acid to a hydrophobic pocket **43**.[205]

Our previous studies established that we have achieved high stoichiometry assemblies in water. Their Spartan models showed reduced exposure of the hydrophobic rim of the host relative to the dimeric assembly (Figure 4-8). The intrinsic relationship of the Hofmeister effect

and hydration of hydrophobic surfaces intrigued our interests into how external stimuli such as the nature of salts or salt concentrations can influence the switching between self-assembled states. We discuss the effects below.

5.2. Effect of Co-solute Salts on the Stability of a Self-Assembled Host-Guest System

We examined salt effects upon the dimeric assembly state of TEMOA **61** in the presence of C17. All of the subsequent studies involved only C17. The first series of co-solutes were sodium salts of various anions, particularly those that are the most evident in the Hofmeister series. The second series selected were various cations including, both inorganic and organic ions. The general experimental procedure was the titration of salt solution into the 0.8 mM solution of TEMOA **61** in the presence of C17 (in 8 mM NaOD). The combination of ^{1}H NMR and PGSE diffusion NMR was applied to confirm changes in assembly.

5.2.1 Effect of Co-solute Concentration

The ^{1}H NMR titration studies involved titrating a NaCl-D_2O solution into a NaOD solution of dimeric assembly $\mathbf{61_2}$•C17 in D_2O. When the co-solute NaCl was added, a new set of signals appeared at both the host aromatic region and the bound guest region from 0 to -3.5 ppm. By increasing the concentration of co-solute salt in solution, the signals corresponding to the dimeric assembly diminished whereas the new set of signals became predominant (Figure 5-3). The switching phenomenon from the dimeric assembly to the new state was accomplished at a total salt concentration of ca. 90 mM. Specifically, in the host aromatic region, the signal for the rim “d” protons at ca. 7.27 ppm shifted upfield to ca. 7.17 ppm. The guest methyl-H signal in the dimeric assembly occurs at -3.47 ppm, whilst a downfield methyl-H signal at -3.31 ppm was observed upon increasing total salt concentration of the solution.

Integration and PGSE NMR experiments further confirmed that the assembled state at higher salt concentration is a 4:2 tetrameric assembly with a HV = 24.4 nm^3 (cf. free host HV = 5.9 nm^3 at the same salt concentration). The ratio between the dimeric and tetrameric assemblies were extracted from the integration of the guest methyl signals of each assembled states. This ratio was also confirmed by examining the baseline resolved "d" signals in the NMR spectrum at 7.27 ppm (dimer) and 7.17 ppm (tetramer).

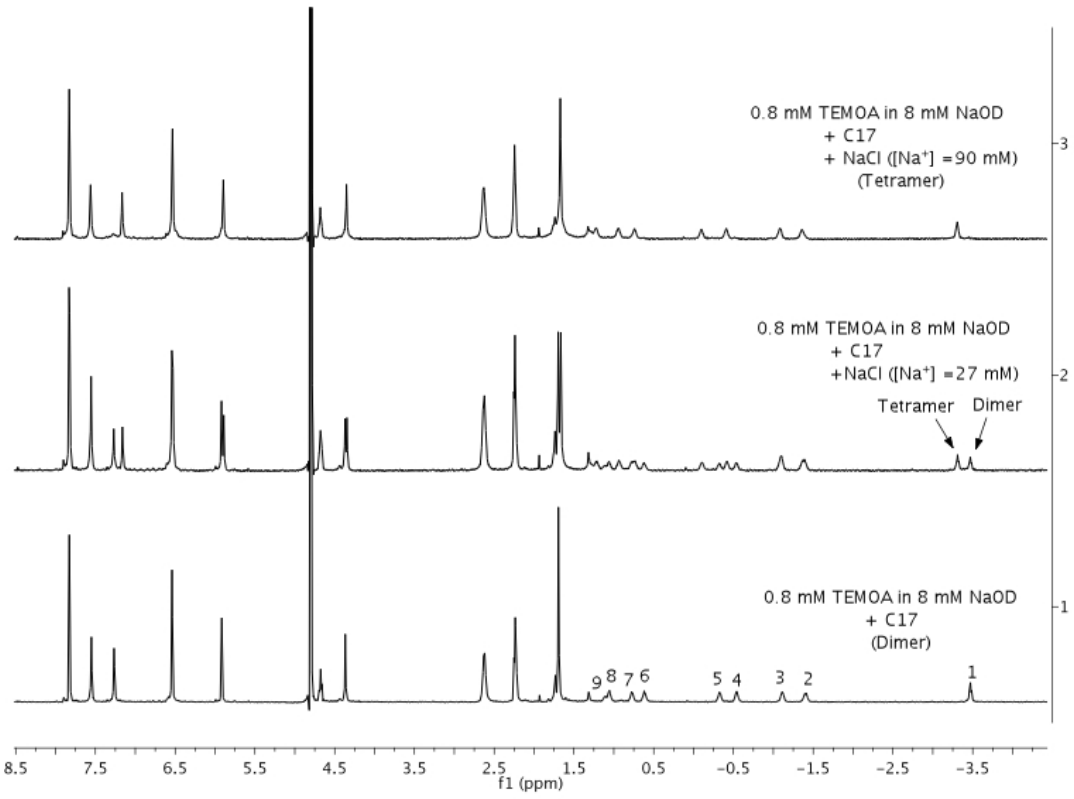

Figure 5-3. ^{1}H NMR spectra of NaCl solution titrate to dimeric assembly **61**$_2$• C17 in 8 mM NaOD. The switching between dimeric assembly and tetrameric assembly was observed by increasing total salt concentration of the solution.

5.2.2 Nature of Anion

Studies repeatedly reveal that the Hofmeister series is most evident with anions.[206] These experimental observations motivated the examination of Hofmeister effect of the switching between self-assembled states in this study.

We examined a series of sodium salts ranging from the kosmotropes to the chaotropes (F^-, OH^-, SO_4^{2-}, Cl^-, ClO_4^-). The selection of SO_4^{2-} is on the basis of investigation of how anions with different charge influence switching. ^1H NMR titration experiments were undertaken. Figure 5-4 shows the relationship between the extent of tetrameric assembly formation and the total salt concentration of the solution in the presence of various anions. To obtain a full switch from dimer to tetramer, a total salt concentration between 70 mM and 90 mM was required. The graph shows that all the investigated anions switch the assembly at a similar way. No distinct variation of the effects of salt on the switching phenomena was observed among those salts. Although the aforementioned study of anion binding to the hydrophobic pocket **61** revealed that anions have different affinity to **61**, the switching phenomenon from dimer to tetramer was observed to be independent of the nature of the anions. A combination of these various weak association constants and the results from the NMR titration experiments leads us to conclude that the Hofmeister effect of anions does not dominate the assembly switching phenomenon.

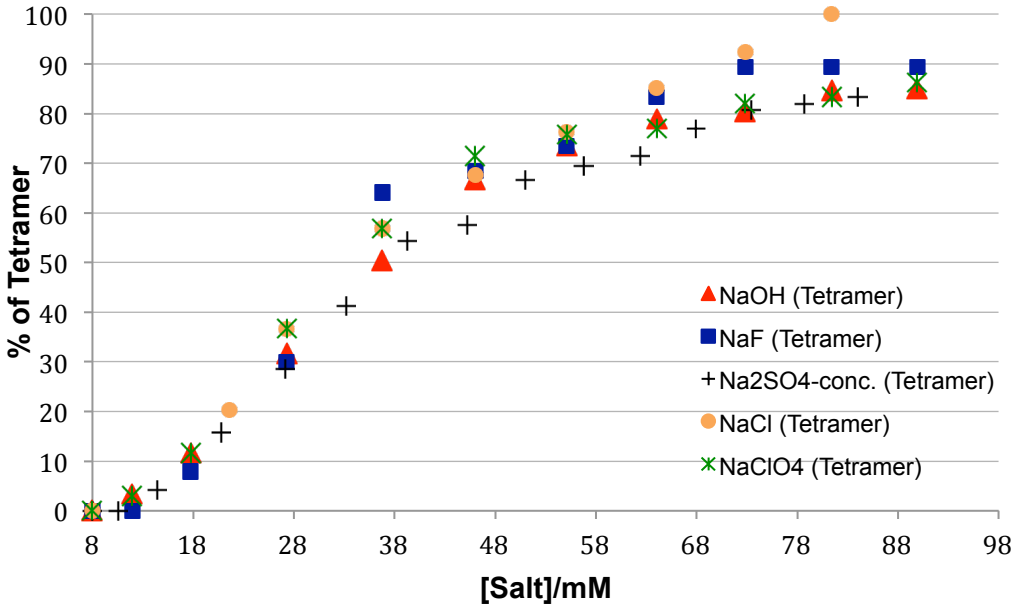

Figure 5-4. The relationship between the extent of tetrameric assembly (**61**$_2$• C17) formation and the total salt concentration of the solution, in the presence of various sodium salts. [Host **61**] = 0.8 mM (in 8 mM NaOD). The product formed in each is noted in parenthesis.

5.2.3 Effect of Cations

Because there was no significant difference of switching between the different anions, we tested whether cations can affect the switching between self-assembled states. A series of chloride salts with variable radius and properties (from inorganic to organic) were examined, including NaCl, KCl, NH_4Cl, Me_4NCl, Et_4NCl, *n*-Pr_4NCl, and *n*-Bu_4NCl. Strikingly, a different scenario was observed for these cations. At the same concentration of the investigated cations, Na^+ and K^+ had similar, and minimal effect on switching, while the switching efficiency dramatically increased in the order $NH_4^+ < Me_4N^+ < Et_4N^+ <$ *n*-Pr_4N^+, *n*-Bu_4N^+ (Figure 5-5, Figure 5-6). More specifically, in order to switch a dimeric assembly to a tetrameric assembly, the total

cationic concentrations were ca. 80 mM in the presence of Na^+ and K^+, whilst for NH_4^+, Me_4N^+, and Et_4N^+, the total cationic concentrations were reduced to ca. 44 mM, 27 mM, and 11 mM, respectively. The most efficient cations, *n*-Pr_4N^+, *n*-Bu_4N^+, can switch the assemblies at ca. 9 mM (ca. 1.8 equiv. of host), which is 10-fold less than Na^+, K^+, and the previous investigated anions.

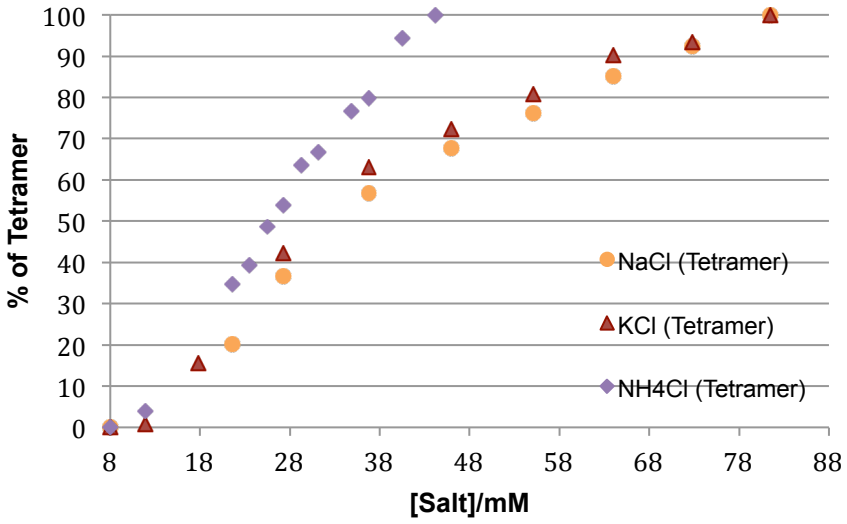

Figure 5-5. The relationship between the extent of tetrameric assembly (**61**$_2$• C17) formation and the total salt concentration of the solution, in the presence of various inorganic chloride salts. [Host] = 0.8 mM (in 8 mM NaOD). The product formed in each is noted in parenthesis.

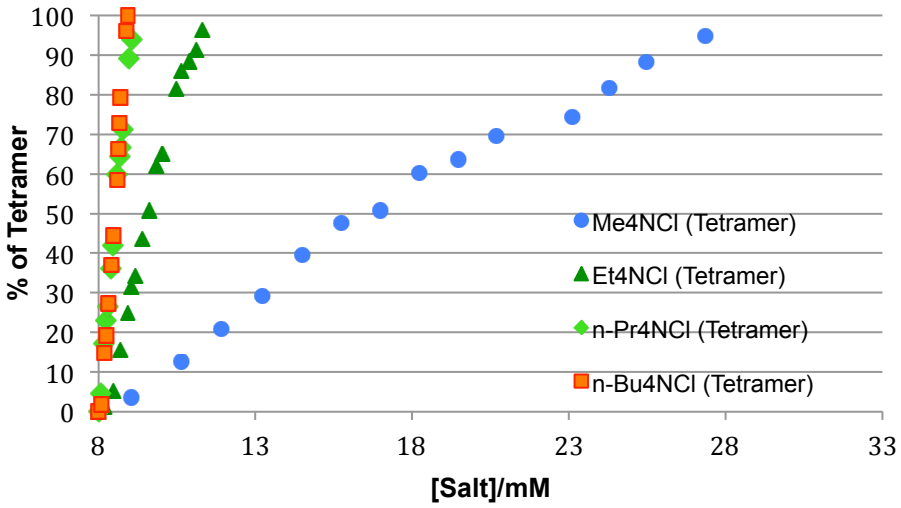

Figure 5-6. The relationship between the extent of tetrameric assembly (**61**$_2$• C17) formation and the total salt concentration of the solution, in the presence of various tetraalkylammonium chloride salts. [Host] = 0.8 mM (in 8 mM NaOD). The product formed in each is noted in parenthesis.

5.3. Binding Studies of Tetraalkylammonium Salt with TEMOA 61 and its self-Assemblied Host-Guest System

5.3.1 Tetraalkylammonium Cations Binding to The Exterior of **61**

The obtained results of tetraalkylammonium cations showed distinct effects on the switching behavior. Our previous study revealed interactions between anions and the hydrophobic pocket of **61**. We were therefore curious to investigate whether these tetraalkylammonium cations show similar binding phenomenon. These cations can either interact with the interior hydrophobic wall through π interactions (cation-π and CH-π) and the hydrophobic effect or the exterior through electrostatic attraction, cation-π interaction, and van der Waals interactions between the alkyl groups and the cavitand hydrophobic moieties. ^{1}H and PGSE diffusion NMR were utilized to investigate the addressed this question.

The ^{1}H NMR (Figure 5-3) demonstrated that no guest exchange occurs during titration.

Furthermore, during the ^{1}H NMR titration experiments there was no observation of peak shifting for the "b" protons, which are located at the bottom of the cavity interior. This indicates that no binding occurs inside the cavity. This has been further confirmed by PGSE diffusion NMR (*vide infra*). The most likely option is therefore that binding occurs on the cavitand exterior. Again however, there were no significant shifts in the host signals suggestive of complexation. Hence, these ^{1}H NMR experiments suggest that there is no binding ot the exterior of the host.

We have illustrated that PGSE diffusion NMR is a powerful tool to determine assembled states. It also can be applied in investigating binding between host and guest molecules. For instance, when binding occurs, the encapsulated guest and host diffuse together as a single entity and their diffusion coefficient are identical.[170,207] In order to further estiablish whether binding of the tetraalkylammonium cations occurs inside or outside the cavity, we further applied PGSE NMR experiments to determine hydrodynamic volumes on the basis of both TEMOA **61** signals and the appropriate salt signals over a range of salt concentration from 0 (no salt) to the identical salt concentrations that were used to induce assembly switching. Control experiments were carried out. We first examined the hydrodynamic volume of salt as a function of concentration in D_2O, this allowed us to evaluate whether the salt could aggregate at higher concentration and thus avoid false positive results in the PGSE diffusion experiments involving assemblies. As we expected, the hydrodynamic volume of salts does not significantly change in the range of concentrations examined (Table 5-1, row 1; *vide infra* Table 7-2). Next we introduced the host TEMOA **61** and screened the corresponding HV values both host and salt over the same salt concentration. The obtained results of the diffusion experiments were surprising and appeared more complex than at first sight. An interesting trend showed that the HV value of the free salt (HV_{salt}) increased in the presence of TEMOA **61**, the longer the alkyl chain, salts giving more pronounced the increases (Table 5-1, row 2). This was also the case with the HV value of the host (HV_{host}) but the increasing is less significant (Table 5-2).

Moreover, we noticed that the determined HV_{host} value (HV_{host} = 8.1 nm^3 for *n*-Bu_4N^+) were much higher than the HV_{salt} (HV_{salt} = 4.3 nm^3), an indication of no encapsulation of tetraalkylammonium salts inside the cavity, but weak association outside the cavity. We sought to determine this binding constant using the diffusion constant. In order to obtain a reliable binding constant from diffusion titration experiments,[170] the titration curve should reach to a plateau. This requires higher guest (salt) concentration for full association. However, increasing the salt concentration prevent us from obtaining reliable binding constant due to the binding competition at the two binding sites (both inside and outside the cavity). We interpreted the increasing HV of both host and salts as follows. First, ion pairing interactions between the electronegative charged portion of TEMOA **61** and the electropositive charged tetraalkylammonium cations induced weak association on the exterior of the cavitand. Also, the hydrophobic properties of salt enhanced the van der Waals interactions between the alkyl chain of salts and the hydrophobic surface of the cavitand. These two aspects resulted in the increasing of HV as a function of the length of alkyl chain of salts, the longer the alkyl chain, the greater contribution of the van der Waals interactions, thus the larger the HV.

Table 5-1. Hydrodynamic volumes of tetraalkylammonium salts obtained from PGSE NMR experiments (unit in nm^3)

	Me_4NCl	Et_4NCl	*n*-Bu_4NCl
HV_{salt} (No TEMOA **61**)	0.2	0.3	0.8
HV_{salt} (+TEMOA **61**)	0.1	0.5	4.3

HV_{salt} values showing are on the basis of salt alkyl signals within experimental error.

Table 5-2. Hydrodynamic volumes of TEMOA **61** obtained from PGSE NMR experiments in the presence of tetraalkylammonium salts and NaCl (unit in nm^3)

	TEMOA **61**	**61** + Me_4NCl	**61** +Et_4NCl	**61** +*n*-Bu_4NCl	**61** + *NaCl*
HV_{host}	6.4	5.9	6.2	8.1	5.9

HV_{host} values are average on the basis of host aromatic “j”, “d”, “f” signals.

5.3.2 Tetraalkylammonium Cations Binding to The Exterior of Assemblies

We have revealed that tetraalkylammonium cations can weakly interact with TEMOA **61** on the cavitand exterior. This result assists us to review the HV of larger assemblies induced by salts. A noteworthy aspect is that hydrodynamic volume of the larger assembly correlates with the nature of the present tetraalkylammonium cations (Table 5-3). The HV_{host} value increased in the order of Na^+ < Me_4N^+ < Et_4N^+ < *n*-Bu_4N^+, which is the same order as that observed in switching efficiency. In the case of the large assembly involving *n*-Bu_4N^+, the HV_{salt} value (HV_{salt} = 28.6 nm^3) is close to the value of host (HV_{host} = 39.5 nm^3), which is a dramatically larger compared to the HV_{salt} in the free TEMOA **61** solution (HV_{salt} = 4.3 nm^3). To determine whether the association of tetraalkylammonium cations only correlates with the larger assembly, we examined whether this phenomenon exists in the dimeric assembly. We selected the dimeric assembly of TEMOA **61** in the presence of C12 for this examination because this guest has sufficient size to template a kinetically stable dimeric assembly, but it is too small to trigger a tetrameric assembly. As we expected, at the identical concentration of *n*-Bu_4N^+ as the experiment involving C17, we did not observe encapsulation of this hydrophobic cation. Moreover, the obtained HV_{salt} increased as in the case of the larger assembly whereas the HV_{host} has no significant difference. Specifically, the obtained HV_{salt} in the dimeric assembly solution is 10.8 nm^3, which is smaller than HV_{salt} in the tetrameric assembly solution whilst greater than HV_{salt} in the free host solution (Table 5-4). These results illustrated that first, co-solute with hydrophobic properties can interact with the external surface of the assemblies (both dimer and tetramer); second, the longer the alkyl chain of salts, the greater the interaction.

Table 5-3. Hydrodynamic volumes of both salt and host obtained from PGSE NMR experiments for TEMOA **61**-C17 tetrameric assembly. (unit in nm^3)

	TEMOA **61**	**61** + Me_4NCl	**61** +Et_4NCl	**61** +*n*-Bu_4NCl	**61** + NaCl
HV_{salt} (**61**-C17)	-	0.2	0.8	28.6	-
HV_{host} (**61**-C17)	15.9	26.5	33.1	39.5	24.4

Table 5-4. Hydrodynamic volumes of both salt and host obtained from PGSE NMR experiments for TEMOA **61**-C12 dimer and TEMOA **61**-C17 tetramer. (unit in nm^3)

		TEMOA	TEMOA + C17	TEMOA + C12
No Salt	HV_{host} (nm^3)	6.4	16.8 (dimer)	17.5
	HV_{salt} (nm^3)	4.3	28.6	10.8
n-Bu_4N^+	HV_{host} (nm^3)	8.1	39.5	18.1

HV_{host} values are average on the basis of host aromatic "j", "d", "f" signals. HV_{salt} values are average on the basis of *n*-Bu_4N^+ signals.

5.3.3 Thermodynamic consideration of the large assembly formation

In order to provide a plausible explanation of our results, we undertook a thermodynamic consideration of the hydration of molecular ions, especially those have both hydrophobic and electrostatic properties. In the literature, a variety of models have been applied in computer simulations of the water structure around solvated solutes. We are aware of the debate between each computational model,[208,209] however our attention has centered on the thermodynamic properties of the hydrated ions and neglected the aspect of water structure using a specific model. Chloride salts with simple cations, such as Na^+, K^+, NH_4^+ investigated in this study, dissociate in water and are fully solvated by water molecules through ion-dipole interaction. Small ions can reach closest to the dipole of a water molecule, thus this interaction is the strongest. Water molecules are ordered predominantly around a small ion and the hydration heat capacity change of the small ions are usually negative.[2] However, around large

ions this electrostatic interaction is weaker due to the relative large distance between ions and the dipole of water molecules. Thus water-water hydrogen bondings dominate in the solvation shell of large ions such as tetraalkylammonium ions, tend to increases water-structure and have large positive heat capacity changes. This combination results in the increase in free energy. In that regard, the hydration of large ions can also be viewed as hydration of nonpolar solutes. These symmetric tetraalkylammonium halides have been applied as models for studying hydrophobic phenomena, especially the water-water interaction. With different length of the alkyl chains, they offer different ratios of polar to nonpolar groups, thus their thermodynamic properties vary (Table 5-5).[210] The hydrophobic and ionic groups of tetraalkylammonium halides lead to both the hydrophobic effect and electrostatic interactions in water. As the alkyl chain length increases, the ion-dipole interactions diminish and the hydrophobic effect becomes dominant. The investigation of heat capacity changes as a function of the chain length provided a further insight of the hydration of these large cations. The large and positive heat capacity increased almost linearly from Me_4N^+ to *n*-Bu_4N^+.[211] It is also the case that an increase in switching efficiency as the chain length of tetraalkylammonium salts increases. Tetraalkylammonium halides are also known to possess a capacity to destabilize proteins.[212] The concept of overlap of the hydration co-sphere of the salts and the nonpolar groups of co-solute can also assist us to rationalize our results.[208,213] In a system of the TEMOA-C17 dimeric assembly and water, introducing the tetraalkylammonium salt results in the two separate particles merging to reduce the exposed hydrophobic surface area.[214] A hydrophobic hydration co-sphere was created through van der Waals interactions between the overlap of dimeric assembly exterior and those salts, which resulted in enhanced hydrophobic effect, thus favored the higher assembly state. The greater effect in *n*-Bu4NCl may due to the presence of longer alkyl chain induced maximum hydrophobic effect of the assembly exterior.[208,213] This hydrophobic effect donated from the tetraalkylamminum salts was more distinct in the system of larger assembly than in the lower stoichiometry assembly. This also explained the less

increased HV of salt in the solution of free TEMOA and dimeric assembly than in tetrameric assembly.

Table 5-5. Cation radius (in pm) and heat capacity changes on hydration (in J K^{-1} mol^{-1}).[2]

	Na^+	K^+	NH_4^+	Me_4N^+	Et_4N^+	n-Pr_4N^+	n-Bu_4N^+
r	102	138	148	280	337	379	413
$\Delta_{Hydr}C_p$	-49	-79	-36	67	252	569	893

Although it is not quite clear what position the *n*-Bu_4NCl adopts when associate with the assemblies, much support from the CPK model and Spartan space filling model estimated that *n*-Bu_4N^+ attracted at the eight corners of the D_{2d} symmetry of the tetramer through electrostatic interactions, which results in the ratio of 2:1 between *n*-Bu_4N^+ and TEMOA monomer. Consistent with this notion, the previous salt titration experiments revealed that 1.8 equiv. of *n*-Bu_4NCl assists the total assembly switching.

In summary, this work offers the first example of switching between self-assembled states driven by the hydrophobic effect. Our data firmly establishes that co-solute salt can effectively stabilize the higher stoichiometry assemblies by reducing the exposed hydrophobic surface of hosts. Interestingly, the Hofmeister series are more evident with cations by contrast of anions. The effect of tetraalkylammonium salts on the switching phenomena has been explained in terms of swing between electrostatic and hydrophobic effect. The switching efficiency is highly dependent on the length scale of the alkyl chain of tetraalkylammonium salts. Further investigation of applying dynamic light scattering experiments is under way.

VI. Conclusion

Overall, this dissertation is focus on exploring the binding and assembly properties of a novel water-soluble deep-cavity cavitand TEMOA driven by the hydrophobic effect. The four *endo* methyl groups on the top rim narrowed the portal of the cavitand but also deepened the cavity. The resulted cavity has similar internal volume as a previous well-studied water-soluble deep-cavity cavitand OA. Due to this subtle change in structure, TEMOA is less predisposed to dimerize and aggregate than OA. Moreover, TEMOA has much different assembly properties than OA. First of all, we discussed the observation of an unusual, non-monotonic assembly profile of binding between straight chain alkanes methane through *n*-tetradecane and TEMOA. Second, mix these two water-soluble hosts OA and TEMOA we investigated guest size controlled self-sorting in assemblies driven by the hydrophobic effect and reviewed that hydrogen bonding and metal-ligand coordination bond are not a prerequisite to conduct molecular self-sorting. Last, higher stoichiometry assemblies involving TEMOA and larger straight-chain alkanes were achieved either by adjust the size of guests or by introducing salt to switch a lower assembled state to a higher states with smooth transition. These large assemblies are truly water-soluble mono-dispersed particles. They may provide unprecedented opportunity in the studies of nano-scale reactors, drug delivery, and novel separation in the future. The investigation of salt switching assembly between states may shed light on the protein studies involving hydrophobic effect and the Hofmeister effect.

VII. Experimental Section

7.1. Synthesis of TEMOA 61

The synthesis of **61** is shown in Scheme 2-1. Known octabromide **62** was subjected to an eight-fold Ullmann ether reaction with 3,5-dihydroxy-4-methylbenzyl alcohol to yield cavitand **63**. Potassium permanganate was then used to oxidize cavitand **63** to give crude octa-acid **61** of an estimated 60% purity. Pure **61** was obtained by an esterification (to yield **64**) and hydrolysis procedure.

7.2. Characterization of intermediates and TEMOA 61

7.2.1 Synthesis of 3,5-dihydroxy-4-Methylbenzyl alcohol

To a stirring solution of BH_3-Me_2S (2.26 mL, 23.8 mmol) and $B(OMe)_3$ (6mL, 53.8 mol) in 60 mL THF at 0 ˚C was slowly (30 min.) added a solution of 3,5-dihydroxy-4-methyl benzoic acid (2.0 g, 11.9 mmol) in 16 mL THF. After the addition, the mixture was heated to reflux for 24 h and then quenched with 30 mL methanol. The solvent was then removed under reduced pressure. Crystallization from chloroform afforded the benzyl alcohol as white crystals (1.7 g, yield: 87%). m.p. 153-155 ˚C. ^{1}H NMR (Acetone-d_6, 500 MHz) δ (ppm) 2.82 (s, 3H), 3.91 (t, J = 5.75 Hz, 1H), 4.41 (d, J = 5.98 Hz, 2H), 6.39 (s, 2H), 7.97 (s, 2H). MS (ESI): Calcd. 155.1 $[M+H]^+$, Found: 155.2 $[M+H]^+$. Anal. Calcd. for $C_8H_{10}O_3$: C, 62.33; H, 6.54. Found: C, 62.35; H, 6.43.

7.2.2 Synthesis of Crude Octol **63**

For 5 min N_2 was bubbled through a suspension of octa bromide **62** (2.0 g, 1.21 mmol), 3,5-dihydroxy-4-methyl benzyl alcohol (1.12 g, 5.45 mmol), and anhydrous K_2CO_3 (1.97 g, 14.3 mmol) in 125 mL pyridine. CuO (1.12g, 14.3 mmol) was then added and the stirring mixture was vigorously refluxed for 7 d. After this time, the mixture was cooled and the solvent was removed under reduced pressure. The crude material was dried under reduced pressure for 1 hour (excessive drying and/or exposing the mixture to air for extended periods led to greatly reduced yields). Subsequently, 150 mL of THF was added and the reaction mixture sonicated for 30 min. The mixture was then filtered through THF-wet Celite and the solvent of the filtrate evaporated under reduced pressure to give a brown crude solid. This material was dried at rt overnight under reduced pressure. To the dried solid was added 20 mL of $CHCl_3$ and the suspension sonicated for 20 min. The solid obtained after filtration (the filtrate was green) was suspended once again in $CHCl_3$, sonicated for 20 min., and dried under vacuum overnight at 120°C to give ~ 1.0 g crude octol **63** as an off-white powder (yield by weight: 45%, ca. 75% purity by NMR, therefore, 34% estimated yield). m.p. > 250°C. ^{1}H NMR (DMSO-d_6, 500 MHz) δ (ppm) 1.40 (m, 8H), 1.54 (s, 12H), 2.38 (m, 8H), 3.46 (m, 8H), 4.40 (s, 4H), 4.48 (t, *J* = 5.01 Hz, 4H), 4.52 (t, *J* = 8.17 Hz, 4H), 4.58 (d, *J* = 5.74 Hz, 8H), 5.43 (t, *J* = 5.83 Hz, 4H), 5.74 (s, 4H), 6.40 (d, *J* = 1.56 Hz, 8H), 7.12 (s, 4H), 7.25 (s, 8H), 7.69 (s, 4H).

7.2.3 Crude TEMOA **61**

To a solution of 0.8 g (0.48 mmol) of crude octol **63** in 80 mL degassed DMA and 80 mL of *t*-BuOH was added 2.12 g (13.41 mmol) of $KMnO_4$. The resulting purple solution was stirred at rt for 2 d. The reaction mixture was filtered and the solid washed thoroughly with 4 × 80 mL distilled water. The combined filtrate was evaporated under reduced pressure and dried at rt for

16 h. 8 mL of 20% HCl was then added to the solid and the suspension sonicated for 5 min. Following filtration, the solid was shaken with 50 mL of distilled water. Filtration and washing with water gave crude host **61** which was dried at 120 °C for overnight (~ 0.78 g).

7.2.4 Octa-Ester **64**

HCl gas was bubbled through a solution of 0.8 g of crude **61** in 63 mL of ethanol for ~2 minutes. To this suspension was added 25.7 mL of $CHCl_3$ and the solution heated up to reflux for 4 days. The solvent was then removed and 10 mL of ethanol added to the residue, the resulting suspension shaken, and then filtered. The resulting off-white solid was dried at 120 °C under reduced pressure for 16 h. Chromatography of the crude product afforded the main products octa-ester **64** (345 mg). R_f = 0.33 ($CHCl_3$/Acetone, 40:1, v/v). mp > 250 °C. ^{1}H NMR (Methylene Chloride-d_2, 500 MHz) δ (ppm) 1.21 (t, *J* = 7.14 Hz, 12H), 1.39 (t, *J* = 7.13 Hz, 12H), 2.30 (t, *J* = 7.38 Hz, 8H), 2.59 (q, *J* = 8.01 Hz, 8H), 4.09 (q, *J* = 7.14 Hz, 8H), 4.37 (m, 12H), 4.75 (t, *J* = 8.28 Hz, 4H), 5.88 (s, 4H), 6.48 (d, *J* = 1.88 Hz, 8H), 7.11(d, *J* = 2.24 Hz, 4H), 7.24 (s, 4H), 7.91 (s, 8H). MS (MALDI): Calcd. 2117.6 $[M + Ag]^+$, Found: 2117.6 $[M + Ag]^+$. Anal. Calcd. for $C_{116}H_{104}O_{32}$: C, 69.32; H, 5.22 Found: C, 68.25; H, 5.04.

7.2.5 Pure TEMOA **61**

To 345 mg (0.17 mmol) of octa-ester **64** in 35 mL DMA was added 0.76 mL of 2.0 M (1.5 mmol) aqueous LiOH solution. The solution was heated to 50 ˚C and small amounts of distilled water added until the precipitate fully dissolved. The resulting clear solution was stirred at 50˚C for 24 h. After this time the solution was filtered, the solvent removed under reduced pressure and the residue dried for 2 h. Subsequently, 5 mL of 20% HCl was added to the solid and the suspension sonicated for 1 min before a further 20 mL of water was added and the suspension

shook. Filtration and washing with water gave octa-acid **61**, which was dried at RT under reduced pressure for 3 h. 5 mL of acetone was then added to the solid, the mixture sonicated for 2 min, and then left to stand for 2 h. Filtration, and drying at 120 °C under reduced pressure for 48 h afforded pure octa-acid **61** as a white solid in 91% yield. m.p, > 250 °C. ^{1}H NMR (DMSO-d_6, 500 MHz) δ (ppm) 1.65 (s, 12H), 2.19 (t, J = 6.98 Hz, 8H), 2.60 (q, J = 6.96 Hz, 8H), 4.37 (s, 4H), 4.57 (t, J = 8.07 Hz, 4H), 5.96 (s, 4H), 6.36 (s, 8H), 7.24 (s, 4H), 7.70 (s, 4H), 7.82 (s, 8H), 12.17 (broad s, 4H), 13.51 (broad s, 4H). MS (MALDI): Calcd. 1983.5 $[M + Ag]^+$, Found: 1983.7 $[M + Ag]^+$. Anal. Calcd. for $C_{100}H_{72}O_{32} \bullet 9H_2O$: C, 61.66; H, 4.66. Found: C, 60.94; H, 4.19.

7.3. ^{1}H NMR data for binding between 61 and methane through *n*-hexacosane

^{1}H NMR spectra were recorded on an INOVA 500 MHz (Varian Inc.) instrument at 25 ˚C. In all cases, 1 mM host **61** in 10 mM sodium tetraborate was used. For the gaseous hydrocarbons, 345 µL (20 eq.) of the appropriate gas was added to 0.7 mL host **61** through a septum and the contents of the vial allowed to equilibrate for 16 hours at room temperature. For the guest *n*-pentane through *n*-tetradecane an excess of guest (10 mL) was added to 0.6 mL of the solution of host **61**. The NMR spectrum was recorded. Integration for the host peaks versus the bound guest methyl peaks gave the ratio of host and guest.

In all cases of hetero-capsule formation, an excess of guest was added to the mixture of host **43** and **61**. To a mixture of 0.275 mL of 1 mM host **43** and 0.275 mL of 1 mM host **61** (both in 10 mM sodium tetraborate), 10 µL of the guest was added and the NMR spectra recorded. The samples were then briefly sonicated to ensure maximal dissolution of the guest. The 1H NMR spectra for all the guests investigated are shown in Figure 3-3. Integration of the host peaks versus the bound guest methyl peaks gave ratio of host to guest. The, “island” of

kinetic instability for the complexes formed by the guests, *n*-hexane to *n*-nonane is apparent in the high field, bound guest, region of the NMR. For clarity, the ^{1}H NMR spectra of the complexes formed by *n*-pentane, *n*-octane, *n*-decane are reproduced in Figure 3-6 along with the assignments for the 'd', endo-methyl, and bound guest signals. These examples emphasize how small *n*-pentane and large *n*-decane form kinetically stable complexes, but that intermediate sized *n*-octane forms a less stable complex.

The *n*-pentane complex showed an unexpected property, namely a 'disappearing' guest methyl signal (Figure 3-7). ^{1}H NMR spectra recorded at two different host concentrations are shown in Figure 3-7. In the mixture of the hosts at a total concentration of 1 mM, the signal for the methyl groups of the bound guest in the $\mathbf{43}_2$ homo complex are barely visible at ca. -1.75 ppm. However, at 2 mM host complexation this same signal is readily apparent. This phenomenon suggests that at low host concentration the exchanging rate of the methyl groups in this complex is on the NMR time scale.

7.4. PGSE Diffusion NMR Experiments

Diffusion measurements were performed on an INOVA 500 MHz (Varian Inc.) instrument equipped with a Performa II pulsed field gradient (PFG) module capable of producing pulses up to 52 gauss/cm. The experiments were carried out on a 5 mm PFG indirect detection probe. The STE (stimulated echo) diffusion experiment using the Varian pulse sequence "pge" (stimulated option on) were performed with pulse gradients of 2 ms in duration separated by 155 ms. Calibration utilized D_2O samples with a diffusion constant of 1.88×10^{-5} cm^2/s. The data was analyzed using the optional Varian diffusion software. Figure 2-2 shows a typical plot of the ln(amplitude) versus the square of the gradient strength applied that was obtained (in this case for *n*-tetradecane). The experiments were run at 25°C, at a host concentration of 1 mM in 10

mM sodium tetraborate. The given diffusion constants (Table 6-1) were an average of measurements of host signals.

In the study of salt mediate switching between assembled states, all salts were purchased from Aldrich Chemical Company and were used as received without further purification. Tetraalkylammonium chlorides were measured in air-free glove box. Salt solutions were prepared in D_2O. The percentage of tetramer formation is calculated from the integration of terminal methyl-H signals applying the iNMR® deconvolution program. The given diffusion constants were an averate of measurements of host "j", "d", "f" signals. Table 6-2 are blank test assembly in the presence of NaCl and tetraalkylammonium chlorides.

Table 7-1. Diffusion constants for the complexes formed between host **61** and the guest methane through n-tetradecane.

Species	Free host	CH_4	C_2H_6	C_3H_8	C_4H_{10}	C_5H_{12}	C_6H_{14}	C_7H_{16}
Diffusion Constant (D, $cm^2\ s^{-1} \times 10^6$)	1.90	1.91	1.79	1.62	1.60	1.51	1.63	1.79
Species	C_8H_{18}	C_9H_{20}	$C_{10}H_{22}$	$C_{11}H_{24}$	$C_{12}H_{26}$	$C_{13}H_{28}$	$C_{14}H_{30}$	
Diffusion Constant (D, $cm^2\ s^{-1} \times 10^6$)	1.75	1.49	1.45	1.42	1.40	1.40	1.41	

Table 7-2. Values of hydrodynamic volume of tetraalkylammonium salts at various concentrations.

[Me_4NCl] (mM)	3.77	7.45	11.03	14.53	
HV (nm^3)	0.2	0.2	0.2	0.2	
[Et_4NCl] (mM)	0.75	1.49	2.21	2.91	3.59
HV (nm^3)	0.3	0.3	0.3	0.3	0.3
[*n*-Bu_4NCl] (mM)	0.27	0.54	0.80	1.05	1.30
HV (nm^3)	0.8	0.8	0.8	0.8	0.8

Table 7-3. Diffusion constants, particle radius, and hydrodynamic volumes of TEMOA and TEMOA tetramer in various salts.

	D (m2/s) (j, d, f)	Radius (nm)	HV (nm3)
TEMOA	1.90E-10	1.15E+00	6.36E+00
TEMOA + C17	1.38E-10	1.59E+00	1.68E+01
TEMOA + NaCl	1.95E-10	1.12E+00	5.91E+00
TEMOA+ NaCl + C17	1.21E-10	1.80E+00	2.44E+01
TEMOA + Me4NCl	1.95E-10	1.12E+00	5.85E+00
TEMOA+ Me4NCl + C17	1.18E-10	1.86E+00	2.68E+01
TEMOA + Et4NCl	1.92E-10	1.14E+00	6.16E+00
TEMOA + Et4NCl + C17	1.10E-10	1.99E+00	3.31E+01
TEMOA + Bu4NCl	1.75E-10	1.25E+00	8.09E+00
TEMOA+ Bu4NCl + C17	1.03E-10	2.11E+00	3.95E+01
TEMOA + C12	1.36E-10	1.61E+00	1.73E+01
TEMOA + Bu4NCl +C12	1.34E-10	1.63E+00	1.81E+01
1 mM SOA + 100 mM NaOD	1.95E-10	1.12E+00	5.88E+00
1 mM SOA + 100 mM NaOD + C17	1.25E-10	1.75E+00	2.25E+01
3 mM SOA + 100 mM NaOD	1.79E-10	1.22E+00	7.60E+00
3 mM SOA + 100 mM NaOD+ C24	9.90E-11	2.21E+00	4.49E+01

7.5. Isothermal Titration Calorimetry (ITC) Experiments

A Microcal VP-ITC calorimeter (cell volume = 1.4711 mL) was used for all titrations. All experiments were run at 25 ˚C. The curve-fitting model used was the single set of identical sites (SSIS) model, and the obtained curve analyzed using Origin 7.0. All of the ITC-titration

experiments applied the 25-injection procedure in D_2O. An interval of 250 seconds was allowed between each injection, and the stirring speed was set at 450 rpm. A solution of 150 mM of host prepared in 10 mM LiOH was loaded in the measuring cell. This solution was titrated with 25 injections of 9 µl of a 1.5 mM appreciate guest prepared in an identical buffer solution (Figure 3-10).

VIII. Appendix

8.1 Copyright Permission

Figure 1-3 Reprinted with permission from ref 8 (Sharp, K. A.; Vanderkooi, J. M. *Acc. Chem. Res.* **2010**, 231.). Copyright 2010 American Chemical Society.

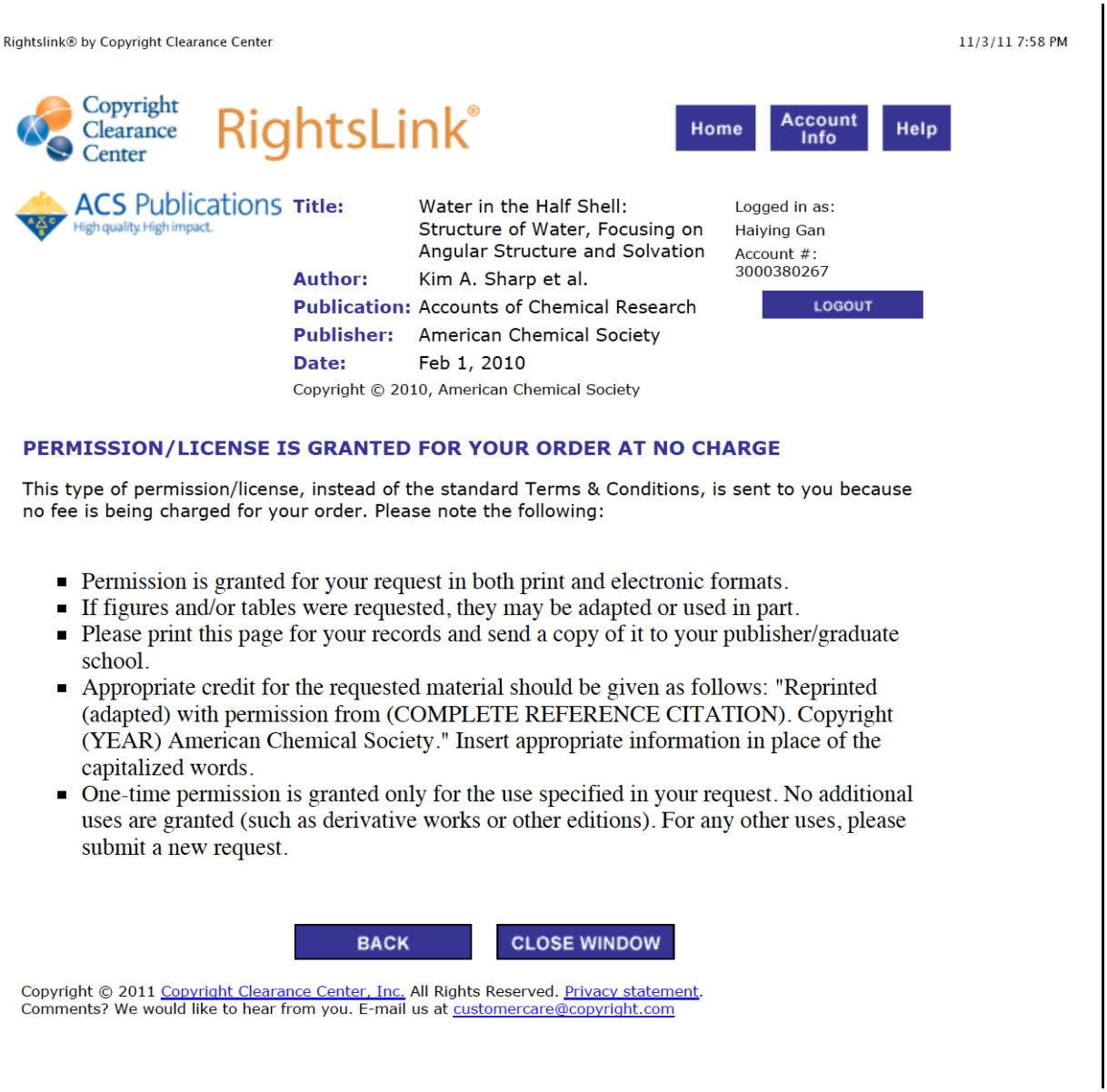

Rightslink® by Copyright Clearance Center 11/3/11 7:58 PM

Copyright Clearance Center RightsLink® Home Account Info Help

ACS Publications High quality. High impact.

Title:	Water in the Half Shell: Structure of Water, Focusing on Angular Structure and Solvation	Logged in as: Haiying Gan Account #: 3000380267
Author:	Kim A. Sharp et al.	
Publication:	Accounts of Chemical Research	LOGOUT
Publisher:	American Chemical Society	
Date:	Feb 1, 2010	

Copyright © 2010, American Chemical Society

PERMISSION/LICENSE IS GRANTED FOR YOUR ORDER AT NO CHARGE

This type of permission/license, instead of the standard Terms & Conditions, is sent to you because no fee is being charged for your order. Please note the following:

- Permission is granted for your request in both print and electronic formats.
- If figures and/or tables were requested, they may be adapted or used in part.
- Please print this page for your records and send a copy of it to your publisher/graduate school.
- Appropriate credit for the requested material should be given as follows: "Reprinted (adapted) with permission from (COMPLETE REFERENCE CITATION). Copyright (YEAR) American Chemical Society." Insert appropriate information in place of the capitalized words.
- One-time permission is granted only for the use specified in your request. No additional uses are granted (such as derivative works or other editions). For any other uses, please submit a new request.

BACK CLOSE WINDOW

Copyright © 2011 Copyright Clearance Center, Inc. All Rights Reserved. Privacy statement.
Comments? We would like to hear from you. E-mail us at customercare@copyright.com

Figure 1-7 Reprinted with permission from ref 38 (Rekharsky, M. V.; Inoue, Y. *Chem. Rev.* **1998**, *98*, 1875.). Copyright 1998 American Chemical Society.

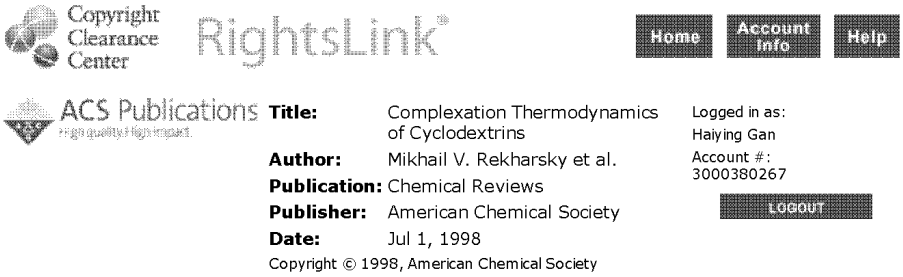

Copyright Clearance Center RightsLink®

Home | Account Info | Help

ACS Publications

Title: Complexation Thermodynamics of Cyclodextrins
Author: Mikhail V. Rekharsky et al.
Publication: Chemical Reviews
Publisher: American Chemical Society
Date: Jul 1, 1998
Copyright © 1998, American Chemical Society

Logged in as:
Haiying Gan
Account #:
3000380267
LOGOUT

Order Completed

Thank you very much for your order.

This is a License Agreement between Haiying Gan ("You") and American Chemical Society ("American Chemical Society"). The license consists of your order details, the terms and conditions provided by American Chemical Society, and the payment terms and conditions.

Get the printable license.

License Number	2622161300884
License Date	Mar 04, 2011
Licensed content publisher	American Chemical Society
Licensed content publication	Chemical Reviews
Licensed content title	Complexation Thermodynamics of Cyclodextrins
Licensed content author	Mikhail V. Rekharsky et al.
Licensed content date	Jul 1, 1998
Volume number	98
Issue number	5
Type of Use	Thesis/Dissertation
Are you the Author of original article?	No
Format	Electronic
Portion	Table/Figure/Micrograph
Number of Tables/Figures /Micrographs	1
Order reference number	1
Title of the thesis / dissertation	Hydrophobically Driven Assemblies in Water
Expected completion date	Jun 2011
Estimated size(pages)	150
Billing Type	Invoice
Billing address	Department of Chemistry University of New Orleans New Orleans, LA 70148 United States
Customer reference info	
Permissions price	0.00 USD

ORDER MORE... CLOSE WINDOW

Figure 1-8. Reprinted with permission.

AMERICAN CHEMICAL SOCIETY LICENSE
TERMS AND CONDITIONS

Mar 14, 2011

This is a License Agreement between Haiying Gan ("You") and American Chemical Society ("American Chemical Society") provided by Copyright Clearance Center ("CCC"). The license consists of your order details, the terms and conditions provided by American Chemical Society, and the payment terms and conditions.

All payments must be made in full to CCC. For payment instructions, please see information listed at the bottom of this form.

License Number	2627791097898
License Date	Mar 14, 2011
Licensed content publisher	American Chemical Society
Licensed content publication	Journal of the American Chemical Society
Licensed content title	New Cucurbituril Homologues: Syntheses, Isolation, Characterization, and X-ray Crystal Structures of Cucurbit[n]uril (n = 5, 7, and 8)
Licensed content author	Jaheon Kim et al.
Licensed content date	Jan 1, 2000
Type of Use	Thesis/Dissertation
Requestor type	Not specified
Format	Electronic
Portion	Table/Figure/Micrograph
Number of Table/Figure /Micrographs	1
Author of this ACS article	No
Order reference number	
Title of the thesis / dissertation	Hydrophobically Driven Assemblies in Water
Expected completion date	Jun 2011
Estimated size(pages)	150
Billing Type	Invoice
Billing Address	Department of Chemistry University of New Orleans New Orleans, LA 70148 United States
Customer reference info	
Total	0.00 USD
Terms and Conditions	

Thesis/Dissertation

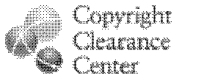

Home | Account Info | Help

Title: Cucurbituril
Author: W. A. Freeman et al.
Publication: Journal of the American Chemical Society
Publisher: American Chemical Society
Date: Dec 1, 1981

Logged in as:
Haiying Gan
Account #:
3000380267
LOGOUT

Order Completed

Thank you very much for your order.

This is a License Agreement between Haiying Gan ("You") and American Chemical Society ("American Chemical Society"). The license consists of your order details, the terms and conditions provided by American Chemical Society, and the payment terms and conditions.

Get the printable license.

License Number	2642181099119
License Date	Apr 04, 2011
Licensed content publisher	American Chemical Society
Licensed content publication	Journal of the American Chemical Society
Licensed content title	Cucurbituril
Licensed content author	W. A. Freeman et al.
Licensed content date	Dec 1, 1981
Volume number	103
Issue number	24
Type of Use	Thesis/Dissertation
Are you the Author of original article?	No
Format	Electronic
Portion	Table/Figure/Micrograph
Number of Tables/Figures /Micrographs	1
Order reference number	
Title of the thesis / dissertation	Hydrophobically Driven Assemblies in Water
Expected completion date	Jun 2011
Estimated size(pages)	150
Billing Type	Invoice
Billing address	Department of Chemistry University of New Orleans New Orleans, LA 70148 United States
Customer reference info	
Permissions price	0.00 USD

ORDER MORE... CLOSE WINDOW

Figure 1-10. Reprinted with permission.

AMERICAN CHEMICAL SOCIETY LICENSE
TERMS AND CONDITIONS

Apr 06, 2011

This is a License Agreement between Haiying Gan ("You") and American Chemical Society ("American Chemical Society") provided by Copyright Clearance Center ("CCC"). The license consists of your order details, the terms and conditions provided by American Chemical Society, and the payment terms and conditions.

All payments must be made in full to CCC. For payment instructions, please see information listed at the bottom of this form.

License Number	2643240970294
License Date	Apr 06, 2011
Licensed content publisher	American Chemical Society
Licensed content publication	Accounts of Chemical Research
Licensed content title	Cucurbituril Homologues and Derivatives: New Opportunities in Supramolecular Chemistry
Licensed content author	Jae Wook Lee et al.
Licensed content date	Aug 1, 2003
Volume number	36
Issue number	8
Type of Use	Thesis/Dissertation
Requestor type	Not specified
Format	Print and Electronic
Portion	Table/Figure/Micrograph
Number of Table/Figure /Micrographs	1
Author of this ACS article	No
Order reference number	
Title of the thesis / dissertation	Hydrophobically Driven Assemblies in Water
Expected completion date	Jun 2011
Estimated size(pages)	150
Billing Type	Invoice
Billing Address	Department of Chemistry University of New Orleans New Orleans, LA 70148 United States
Customer reference info	
Total	0.00 USD
Terms and Conditions	

Scheme 1-5. Reprinted with permission.

THE AMERICAN ASSOCIATION FOR THE ADVANCEMENT OF SCIENCE LICENSE TERMS AND CONDITIONS

Apr 06, 2011

This is a License Agreement between Haiying Gan ("You") and The American Association for the Advancement of Science ("The American Association for the Advancement of Science") provided by Copyright Clearance Center ("CCC"). The license consists of your order details, the terms and conditions provided by The American Association for the Advancement of Science, and the payment terms and conditions.

All payments must be made in full to CCC. For payment instructions, please see information listed at the bottom of this form.

License Number	2643280065525
License date	Apr 06, 2011
Licensed content publisher	The American Association for the Advancement of Science
Licensed content publication	Science
Licensed content title	Diels-Alder in Aqueous Molecular Hosts: Unusual Regioselectivity and Efficient Catalysis
Licensed content author	Michito Yoshizawa, Masazumi Tamura, Makoto Fujita
Licensed content date	Apr 14, 2006
Volume number	312
Issue number	5771
Type of Use	Thesis / Dissertation
Requestor type	Other Individual
Format	Print and electronic
Portion	Figure
Number of figures/tables	2
Order reference number	
Title of your thesis / dissertation	Hydrophobically Driven Assemblies in Water
Expected completion date	Jun 2011
Estimated size(pages)	150
Total	0.00 USD
Terms and Conditions	

American Association for the Advancement of Science TERMS AND CONDITIONS

Regarding your request, we are pleased to grant you non-exclusive, non-transferable permission, to republish the AAAS material identified above in your work identified above, subject to the terms and conditions herein. We must be contacted for permission for any uses other than those specifically identified in your request above.

The following credit line must be printed along with the AAAS material: "From [Full Reference Citation]. Reprinted with permission from AAAS."

Figure 1-12. Reprinted with permission.

AMERICAN CHEMICAL SOCIETY LICENSE
TERMS AND CONDITIONS

Apr 06, 2011

This is a License Agreement between Haiying Gan ("You") and American Chemical Society ("American Chemical Society") provided by Copyright Clearance Center ("CCC"). The license consists of your order details, the terms and conditions provided by American Chemical Society, and the payment terms and conditions.

All payments must be made in full to CCC. For payment instructions, please see information listed at the bottom of this form.

License Number	2643411278484
License Date	Apr 06, 2011
Licensed content publisher	American Chemical Society
Licensed content publication	Journal of the American Chemical Society
Licensed content title	Endohedral Clusterization of Ten Water Molecules into a "Molecular Ice" within the Hydrophobic Pocket of a Self-Assembled Cage
Licensed content author	Michito Yoshizawa et al.
Licensed content date	Mar 1, 2005
Volume number	127
Issue number	9
Type of Use	Thesis/Dissertation
Requestor type	Not specified
Format	Print and Electronic
Portion	Table/Figure/Micrograph
Number of Table/Figure /Micrographs	1
Author of this ACS article	No
Order reference number	
Title of the thesis / dissertation	Hydrophobically Driven Assemblies in Water
Expected completion date	Jun 2011
Estimated size(pages)	150
Billing Type	Invoice
Billing Address	Department of Chemistry University of New Orleans New Orleans, LA 70148 United States
Customer reference info	
Total	0.00 USD
Terms and Conditions	

Scheme 1-8. Reprinted with permission.

AMERICAN CHEMICAL SOCIETY LICENSE
TERMS AND CONDITIONS

Apr 07, 2011

This is a License Agreement between Haiying Gan ("You") and American Chemical Society ("American Chemical Society") provided by Copyright Clearance Center ("CCC"). The license consists of your order details, the terms and conditions provided by American Chemical Society, and the payment terms and conditions.

All payments must be made in full to CCC. For payment instructions, please see information listed at the bottom of this form.

License Number	2643431041719
License Date	Apr 07, 2011
Licensed content publisher	American Chemical Society
Licensed content publication	Journal of the American Chemical Society
Licensed content title	The Hydrophobic Effect Drives the Recognition of Hydrocarbons by an Anionic Metal−Ligand Cluster1
Licensed content author	Shannon M. Biros et al.
Licensed content date	Oct 1, 2007
Volume number	129
Issue number	40
Type of Use	Thesis/Dissertation
Requestor type	Not specified
Format	Print and Electronic
Portion	Table/Figure/Micrograph
Number of Table/Figure /Micrographs	1
Author of this ACS article	No
Order reference number	
Title of the thesis / dissertation	Hydrophobically Driven Assemblies in Water
Expected completion date	Jun 2011
Estimated size(pages)	150
Billing Type	Invoice
Billing Address	Department of Chemistry University of New Orleans New Orleans, LA 70148 United States
Customer reference info	
Total	0.00 USD
Terms and Conditions	

Figure 1-18. Reprinted with permission

THE AMERICAN ASSOCIATION FOR THE ADVANCEMENT OF SCIENCE LICENSE TERMS AND CONDITIONS

Apr 07, 2011

This is a License Agreement between Haiying Gan ("You") and The American Association for the Advancement of Science ("The American Association for the Advancement of Science") provided by Copyright Clearance Center ("CCC"). The license consists of your order details, the terms and conditions provided by The American Association for the Advancement of Science, and the payment terms and conditions.

All payments must be made in full to CCC. For payment instructions, please see information listed at the bottom of this form.

License Number	2643750132214
License date	Apr 07, 2011
Licensed content publisher	The American Association for the Advancement of Science
Licensed content publication	Science
Licensed content title	Helical Conformation of Alkanes in a Hydrophobic Cavitand
Licensed content author	Laurent Trembleau, Julius Rebek, Jr.
Licensed content date	Aug 29, 2003
Volume number	301
Issue number	5637
Type of Use	Thesis / Dissertation
Requestor type	Other Individual
Format	Print and electronic
Portion	Figure
Number of figures/tables	1
Order reference number	
Title of your thesis / dissertation	Hydrophobically Driven Assemblies in Water
Expected completion date	Jun 2011
Estimated size(pages)	150
Total	0.00 USD
Terms and Conditions	

American Association for the Advancement of Science TERMS AND CONDITIONS

Regarding your request, we are pleased to grant you non-exclusive, non-transferable permission, to republish the AAAS material identified above in your work identified above, subject to the terms and conditions herein. We must be contacted for permission for any uses other than those specifically identified in your request above.

The following credit line must be printed along with the AAAS material: "From [Full Reference Citation]. Reprinted with permission from AAAS."

Figure 1-19. Reprinted with permission from ref 126 (Hooley, R. J.; Van Anda, H. J.; Rebek, J. J. *J. Am. Chem. Soc.* **2006**, *128*, 3894). Copyright 2006 American Chemical Society.

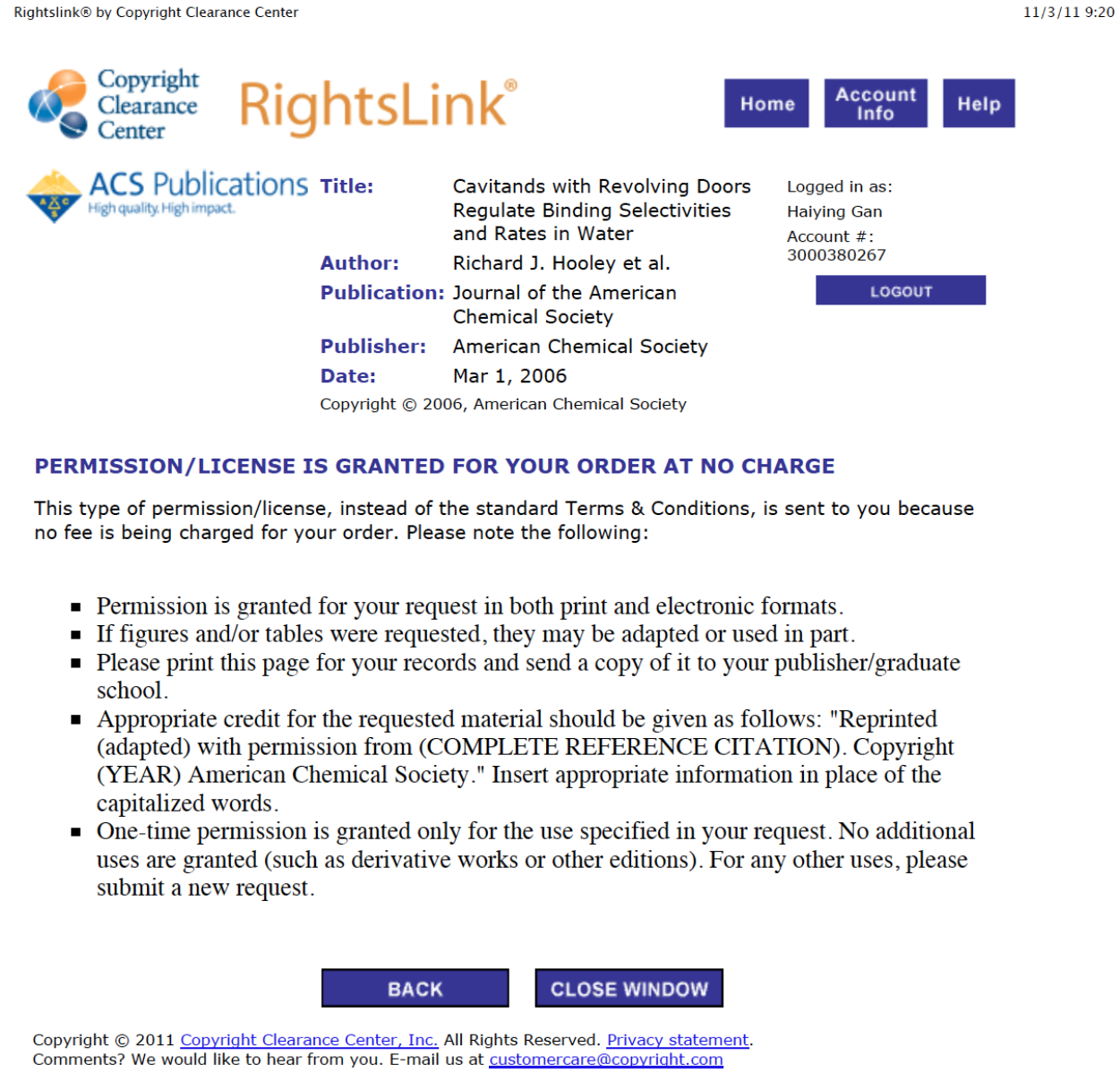

Rightslink® by Copyright Clearance Center 11/3/11 9:20

Copyright Clearance Center RightsLink®

Home | Account Info | Help

ACS Publications High quality. High impact.

Title: Cavitands with Revolving Doors Regulate Binding Selectivities and Rates in Water

Author: Richard J. Hooley et al.

Publication: Journal of the American Chemical Society

Publisher: American Chemical Society

Date: Mar 1, 2006

Copyright © 2006, American Chemical Society

Logged in as:
Haiying Gan
Account #:
3000380267

LOGOUT

PERMISSION/LICENSE IS GRANTED FOR YOUR ORDER AT NO CHARGE

This type of permission/license, instead of the standard Terms & Conditions, is sent to you because no fee is being charged for your order. Please note the following:

- Permission is granted for your request in both print and electronic formats.
- If figures and/or tables were requested, they may be adapted or used in part.
- Please print this page for your records and send a copy of it to your publisher/graduate school.
- Appropriate credit for the requested material should be given as follows: "Reprinted (adapted) with permission from (COMPLETE REFERENCE CITATION). Copyright (YEAR) American Chemical Society." Insert appropriate information in place of the capitalized words.
- One-time permission is granted only for the use specified in your request. No additional uses are granted (such as derivative works or other editions). For any other uses, please submit a new request.

BACK | CLOSE WINDOW

Copyright © 2011 Copyright Clearance Center, Inc. All Rights Reserved. Privacy statement.
Comments? We would like to hear from you. E-mail us at customercare@copyright.com

Figure 1-20. Reprinted with permission.

AMERICAN CHEMICAL SOCIETY LICENSE
TERMS AND CONDITIONS

Apr 07, 2011

This is a License Agreement between Haiying Gan ("You") and American Chemical Society ("American Chemical Society") provided by Copyright Clearance Center ("CCC"). The license consists of your order details, the terms and conditions provided by American Chemical Society, and the payment terms and conditions.

All payments must be made in full to CCC. For payment instructions, please see information listed at the bottom of this form.

License Number	2643760581673
License Date	Apr 07, 2011
Licensed content publisher	American Chemical Society
Licensed content publication	Journal of the American Chemical Society
Licensed content title	Guest Encapsulation in a Water-Soluble Molecular Capsule Based on Ionic Interactions
Licensed content author	Francesca Corbellini et al.
Licensed content date	Aug 1, 2003
Volume number	125
Issue number	33
Type of Use	Thesis/Dissertation
Requestor type	Not specified
Format	Print and Electronic
Portion	Table/Figure/Micrograph
Number of Table/Figure /Micrographs	1
Author of this ACS article	No
Order reference number	
Title of the thesis / dissertation	Hydrophobically Driven Assemblies in Water
Expected completion date	Jun 2011
Estimated size(pages)	150
Billing Type	Invoice
Billing Address	Department of Chemistry University of New Orleans New Orleans, LA 70148 United States
Customer reference info	
Total	0.00 USD
Terms and Conditions	

Chapter II. Reprinted with permission

AMERICAN CHEMICAL SOCIETY LICENSE
TERMS AND CONDITIONS

Apr 07, 2011

This is a License Agreement between Haiying Gan ("You") and American Chemical Society ("American Chemical Society") provided by Copyright Clearance Center ("CCC"). The license consists of your order details, the terms and conditions provided by American Chemical Society, and the payment terms and conditions.

All payments must be made in full to CCC. For payment instructions, please see information listed at the bottom of this form.

License Number	2643820276311
License Date	Apr 07, 2011
Licensed content publisher	American Chemical Society
Licensed content publication	Journal of the American Chemical Society
Licensed content title	Nonmonotonic Assembly of a Deep-Cavity Cavitand
Licensed content author	Haiying Gan et al.
Licensed content date	Apr 1, 2011
Volume number	133
Issue number	13
Type of Use	Thesis/Dissertation
Requestor type	Not specified
Format	Electronic
Portion	50% or more of original article
Author of this ACS article	Yes
Order reference number	
Title of the thesis / dissertation	Hydrophobically Driven Assemblies in Water
Expected completion date	Jun 2011
Estimated size(pages)	150
Billing Type	Invoice
Billing Address	Department of Chemistry University of New Orleans New Orleans, LA 70148 United States
Customer reference info	
Total	0.00 USD
Terms and Conditions	

Thesis/Dissertation

Figure 4-1. Reprinted with permission.

NATURE PUBLISHING GROUP LICENSE
TERMS AND CONDITIONS

Nov 03, 2011

This is a License Agreement between Haiying Gan ("You") and Nature Publishing Group ("Nature Publishing Group") provided by Copyright Clearance Center ("CCC"). The license consists of your order details, the terms and conditions provided by Nature Publishing Group, and the payment terms and conditions.

All payments must be made in full to CCC. For payment instructions, please see information listed at the bottom of this form.

License Number	2781680243388
License date	Nov 03, 2011
Licensed content publisher	Nature Publishing Group
Licensed content publication	Nature
Licensed content title	A chiral spherical molecular assembly held together by 60 hydrogen bonds
Licensed content author	Leonard R. MacGillivray and Jerry L. Atwood
Licensed content date	Oct 2, 1997
Volume number	389
Issue number	6650
Type of Use	reuse in a thesis/dissertation
Requestor type	academic/educational
Format	print and electronic
Portion	figures/tables/illustrations
Number of figures/tables/illustrations	1
Figures	Figure 4-1
Author of this NPG article	no
Your reference number	175
Title of your thesis / dissertation	Self-Assemblies Driven by the Hydrophobic Effect
Expected completion date	Nov 2011
Estimated size (number of pages)	150
Total	0.00 USD

Terms and Conditions

References

(1) Anslyn, E. V.; Dougherty, D. A. *Modern Physical Organic Chemistry*; University Science Books: Sausalito, 2006.

(2) Marcus, Y. In *Ion properties*; Marcel Dekker: New York, 1997.

(3) Krienke, H.; Vlachy, V.; Ahn-Ercan, G.; Bako, I. *J. Phys. Chem. B* **2009**, *113*, 4360.

(4) *Thermodynamic of Solvation*; Krestov, G. A., Ed.; New York: Elliss Horwood: New Orleans, 1991.

(5) Marcus, Y. *Chem. Rev.* **2009**, *109*, 1346.

(6) Steed, J. W.; Atwood, J. L. *Supramolecular Chemistry*; John Wiley and Sons, Ltd: Chichester, 2000.

(7) Israelachvili, J. *Intermolecular & Surface Forces*; Academic Press: San Diego, 1991.

(8) Sharp, K. A.; Vanderkooi, J. M. *Acc. Chem. Res.* **2010**, 231.

(9) Gallagher, K. R.; Sharp, K. A. *J. Am. Chem. Soc.* **2003**, *125*, 9853.

(10) Gomez, J.; Hilser, V. J.; Xie, D.; Freire, E. *Protein Sci.* **1995**, *22*, 404.

(11) Spolar, R. S.; Livingstone, J. R.; Record, M. T., Jr. *Biochemistry* **1992**, *31*, 3947.

(12) Southall, N. T.; Dill, K. A.; Haymet, A. D. J. *J. Phys. Chem. B* **2002**, *106*, 521.

(13) Fisicaro, E.; Compari, C.; Braibanti, A. *Phys . Chem. Chem. Phys .* **2004**, *6*, 4156.

(14) Guillot, B.; Giussani, Y. *J. Chem. Phys.* **1993**, *99*, 8075.

(15) Chandler, D. *Nature* **2005**, *437*, 640.

(16) Ewell, J.; Gibb, B. C.; Rick, S. W. *J. Phys. Chem. B* **2008**, *112*, 10272.

(17) Pedersen, C. J. *J. Am. Chem. Soc.* **1967**, *89*, 2495.

(18) Georgiadis, T. M.; Georgiadis, M. M.; Diederich, F. *J. Org. Chem.* **1991**, *56*, 3362.

(19) Yoon, J.; Kim, S. K.; Singh, N. J.; Kim, K. S. *Chem. Soc. Rev.* **2006**, *35*, 355.

(20) Setter, H.; Roos, E. E. *Chem. Ber.* **1955**, *88*, 1390.

(21) Odashima, K.; Itai, A.; Iitaka, Y.; Koga, K. *J. Am. Chem. Soc.* **1980**, *102*, 2504.

(22) Ray, F. E.; L., S. *J. Org. Chem.* **1950**, *15*, 1037.

(23) Atilgan, S.; Akkaya, E. U. *Tetra. Lett.* **2004**, *45*, 9269.

(24) Fabbrizzi, L.; Leone, A.; Taglietti, A. *Angew. Chem. Int. Ed.* **2001**, *40*, 3066.

(25) Fabbrizzi, L.; Pallavicini, P.; Parodi, L.; Taglietti, A. *Inorganica Chimica Acta* **1995**, *238*, 5.

(26) Fabbrizzi, L.; Marcotte, N.; Stomeo, F.; Taglietti, A. *Angew. Chem. Int. Ed.* **2002**, *41*, 3811.

(27) Marcotte, N.; Taglietti, A. *Supramolecular Chemistry* **2003**, *15*, 617.

(28) Bender, M. L.; Komiyama, M. *Cyclodextrin Chemistry*; Springer-Verlag: Berlin, 1978.

(29) Szejtli, J.; Pergamon: Oxford, 1996; Vol. 3.

(30) Connors, K. A. *Chem. Rev.* **1997**, *97*, 1325.

(31) Stoddart, J. F. *Carbohydr. Res.* **1989**, *192*, xii.

(32) Bom, A.; Bradley, M.; Cameron, K.; Clark, J. K.; van Egmond, J.; Feilden, H.; MacLean, E. J.; Muir, A. W.; Palin, R.; Rees, D. C.; Zhang, M.-Q. *Angew. Chem. Int. Ed.* **2002**, *41*, 265.

(33) Coleman, A. W.; Nicolis, I.; Keller, N.; Dalbiez, J. P. *J. Incl. Phenom. Mol. Recogn. Chem.* **1992**, *13*, 139.

(34) Jozwiakowski, M. J.; Connors, K. A. *Carbohydr. Res.* **1985**, *143*, 51.

(35) Szejtli, J. *Cyclodextrin Technology*; Kluwer: Dordecht, 1988.

(36) Breslow, R.; Halfon, S.; Zhang, B. *Tetrahedron* **1995**, *51*, 377.

(37) Breslow, R.; Zhang, B. *J. Am. Chem. Soc.* **1996**, *118*, 8495.

(38) Rekharsky, M. V.; Inoue, Y. *Chem. Rev.* **1998**, *98*, 1875.

(39) Chen, Y.-F.; Banerjee, I. A.; Yu, L.; Djalali, R.; Matsui, H. *Langmuir* **2004**, *20*, 8409.

(40) Kim, H.-S.; Jeon, S.-J. *Chem. Commun.* **1996**, 817.

(41) Dong, S. D.; Breslow, R. *Tetra. Lett.* **1998**, *39*, 9343.

(42) Villalonga, R.; Cao, R.; Fragoso, A. *Chem. Rev.* **2007**, *107*, 3088.

(43) Piel, G.; Piette, M.; Barillaro, V.; Castagne, D.; Evrard, B.; Delattre, L. *Int. J. Pharm.* **2007**, *338*, 35.

(44) Rasheed, A.; Kumar, A. C. K.; Sravanthi, V. V. N. S. S. *Sci. Pharm.* **2008**, *76*, 567.

(45) Uekama, K.; Hirayama, F.; Irie, T. *Chem. Rev.* **1998**, *98*, 2045.

(46) Hallen, D.; Schon, A.; Shehatta, I.; Wadso, I. *J. Chem. Soc., Faraday Trans.* **1992**, *88*, 2859.

(47) Barone, G.; Castronuovo, G.; Delvecchio, P.; Elia, V.; Muscetta, M. *Journal of the Chemical Society-Faraday Transactions I* **1986**, *82*, 2089.

(48) Fujiwara, H.; Arakawa, H.; Murata, S.; Sasaki, Y. *Bulletin of the Chemical Society of Japan* **1987**, *60*, 3891.

(49) Behrend, R.; Meyer, E.; Rusche, F. *Liebigs Ann. Chem.* **1905**, *339*, 1.

(50) Lee, J. W.; Samal, S.; Selvapalam, N.; Kim, H.-J.; Kim, K. *Acc. Chem. Res.* **2003**, *36*, 621.

(51) Freeman, W. A.; Mock, W. L.; Shih, N.-Y. *J. Am. Chem. Soc.* **1981**, *103*, 7367.

(52) Lagona, J.; Mukhopadhyay, P.; Chakrabarti, S.; Isaacs, L. *Angew. Chem. Int. Ed.* **2005**, *44*, 4844.

(53) Liu, S.; Zavalij, P. Y.; Isaacs, L. *J. Am. Chem. Soc.* **2005**, *127*, 16798.

(54) Day, A. I.; Blanch, R. J.; Arnold, A. P.; Lorenzo, S.; Lewis, G. R.; Dance, I. *Angew. Chem. Int. Ed.* **2002**, *41*, 275.

(55) Buschmann, H.-J.; Jansen, K.; Schollmeyer, E. *Thermochim. Acta* **2000**, *346*, 33.

(56) Fujiwara, H.; Arakawa, H.; Murata, S.; Sasaki, Y. *Bull. Chem.Soc. Jpn.* **1987**, *60*, 3891.

(57) Angelos, S.; Yang, Y.-W.; Khashab, N. M.; Stoddart, J. F.; Zink, J. I. *J. Am. Chem. Soc.* **2009**, *131*, 11344.

(58) Angelos, S.; Khashab, N. M.; Yang, Y.-W.; Trabolsi, A.; Khatib, H. A.; Stoddart, J. F.; Zink, J. I. *J. Am. Chem. Soc.* **2009**, *131*, 12912.

(59) Moon, K.; Kaifer, A. E. *Org. Lett.* **2004**, *6*, 185.

(60) Sindelar, V.; Moon, K.; Kaifer, A. E. *Org. Lett.* **2004**, *6*, 2665.

(61) Constabel, F.; Geckeler, K. E. *Tetrahedron Lett.* **2004**, *45*, 2071.

(62) Xu, L.; Liu, S.-M.; Wu, C.-T.; Feng, Y.-Q. *Electrophoresis* **2004**, *25*, 3300.

(63) Lorenzo, S.; Day, A.; Craig, D.; Blanch, R.; Arnold, A.; Dance, I. *CrystEngComm.* **2001**, *49*, 1.

(64) Yan, K.; Huang, Z.-X.; Liu, S.-M.; Feng, L.; Wu, C.-T. *Wuhan Univ. J. Nat. Sci.* **2004**, 99.

(65) Wheate, N. J.; Day, A. I.; Blanch, R. J.; Arnold, A. P.; Cullinane, C.; Collins, J. G. *Chem. Commun.* **2004**, 1424.

(66) Fujita, M.; Oguro, D.; Mlyazawa, M.; Oka, H.; Yamaguchi, K.; Ogura, K. *Nature* **1995**, *378*, 469.

(67) Kusukawa, T.; Fujita, M. *J. Am. Chem. Soc.* **2002**, *124*, 13576.

(68) Yoshizawa, M.; Tamura, M.; Fujita, M. *Science* **2006**, *312*, 251.

(69) Yoshizawa, M.; Klosterman, J. K.; Fujita, M. *Angew. Chemie* **2009**, *48*, 3418.

(70) Fringuelli, F.; Taticchi, A. *The Diels-Alder Reaction: Selected Practical Methods*; Wiley: Chichester, UK, 2002.

(71) Breslow, R. *Acc. Chem. Res.* **1991**, *24*, 159.

(72) Stuhlmann, F.; Ja¨schke, A. *J. Am. Chem. Soc.* **2002**, *124*, 3238.

(73) Cheng, M.-F.; Li, W.-K. *Chem. Phys. Lett.* **2003**, *368*, 630.

(74) Furutani, Y.; Kandori, H.; Kawano, M.; Nakabayashi, K.; Yoshizawa, M.; Fujita, M. *J. Am. Chem. Soc.* **2009**, *131*, 4764.

(75) Yoshizawa, M.; Kusukawa, T.; Kawano, M.; Ohhara, T.; Tanaka, I.; Kurihara, K.; Niimura, N.; Fujita, M. *J. Am. Chem. Soc.* **2005**, *127*, 2798.

(76) Eisenberg, D.; Kauzmann, W. *The Structure and Properties of Water*; Oxford University Press: New York, 1969.

(77) Stillinger, F. H. *Science* **1980**, *309*, 451.

(78) Dang, L. X. *J. Chem. Phys.* **1999**, *110*, 1526.

(79) Sadlej, J.; Buch, V.; Kazimirski, J. K.; Buck, U. *J. Phys. Chem. A* **1999**, *103*, 4933.

(80) Kang, J.; Rebek, J. J. *Nature* **1996**, *382*, 239.

(81) Parac, T. N.; Caulder, D. L.; Raymond, K. N. *J. Am. Chem. Soc.* **1998**, *120*, 8003.

(82) Rekharsky, M.; Inoue, Y.; Tobey, S.; Metzger, A.; Anslyn, E. V. *J. Am. Chem. Soc.* **2002**, *124*, 14959.

(83) Pluth, M. D.; Raymond, K. N. *Chem. Soc. Rev.* **2007**, *36*, 161.

(84) Davis, A. V.; Fiedler, D.; Ziegler, F. E.; Terpin, A.; Raymond, K. N. *J. Am. Chem. Soc.* **2007**, *129*, 15354.

(85) Davis, A. V.; Raymond, K. N. *J. Am. Chem. Soc.* **2005**, *127*, 7912.

(86) Pluth, M. D.; Johnson, D. W.; Szigethy, G.; Davis, A. V.; Teat, S. J.; Oliver, A. G.; Bergman, R. G.; Raymond, K. N. *Inorg. Chem.* **2009**, *48*, 111.

(87) Caulder, D. L.; Raymond, K. N. *J. Chem. Soc., Dalton Trans.* **1999**, 1185.

(88) Kersting, B.; Telford, J. R.; Meyer, M.; Raymond, K. N. *J. Am. Chem. Soc.* **1996**, *118*, 5712.

(89) Terpin, A. J.; Ziegler, M.; Johnson, D. W.; Raymond, K. N. *Angew. Chem. Int. Ed.* **2001**, *40*, 157.

(90) Ziegler, F. E.; Davis, A.; John, D.; Raymond, K. N. *Angew. Chem. Int. Ed.* **2003**, *42*.

(91) Brumaghim, J. L.; Michels, M.; Pagliero, D.; Raymond, K. N. *Eur. J. Org. Chem.* **2004**, 5115.

(92) Brumaghim, J. L.; Michels, M.; Pagliero, D.; Raymond, K. N. *Eur. J. Org. Chem* **2004**, 4552.

(93) Dong, V. M.; Fiedler, D.; Carl, B.; Bergman, R. G.; Raymond, K. N. *J. Am. Chem. Soc.* **2006**, *128*, 14464.

(94) Pluth, M. D.; Bergman, R. G.; Raymond, K. N. *J. Am. Chem. Soc.* **2007**, *129*, 11459.

(95) Pluth, M. D.; Bergman, R. G.; Raymond, K. N. *J. Am. Chem. Soc.* **2008**, *130*, 6362.

(96) Pluth, M. D.; Bergman, R. G.; Raymond, K. N. *Acc. Chem. Res.* **2009**, *42*, 1650.

(97) Pluth, M. D.; Bergman, R. G.; Raymond, K. N. *Science* **2007**, *316*, 85.

(98) Biros, S. M.; Bergman, R. G.; Raymond, K. N. *J. Am. Chem. Soc.* **2007**, *129*, 12094.

(99) Hastings, C. J.; Pluth, M. D.; Biros, S. M.; Bergman, R. G.; Raymond, K. N. *Tetrahedron* **2008**, *64*, 8362.

(100) Palmer, L. C.; Rebek, J. J. *Org. Lett.* **2005**, *7*, 787.

(101) Baeyer, A. *Ber. Dtsch. Chem. Ges* **1872**, *5*, 25.

(102) Fabre, R. *Ann. Chim. (Paris)* **1922**, *18*, 82.

(103) Liebermann, C.; Lindenbaum, S. *Ber. Dtsch. Chem. Ges.* **1904**, *37*, 2728.

(104) Liebermann, C.; Lindenbaum, S.; Glawe, A. *Ber. Dtsch. Chem. Ges.* **1904**, *37*, 1171.

(105) Mertens, E.; Fonteyn, M. *Bull. Soc. Chim. Belg* **1936**, *45*, 186.

(106) Michael, A. *Am. Chem. J.* **1883**, *5*, 338.

(107) Michel, A.; Ryder, J. P. *Ber. Dtsch. Chem. Ges.* **1886**, *19*, 1388.

(108) Niederl, J. B.; Vogel, H. J. *J. Am. Chem. Soc.* **1940**, *62*, 2512.

(109) Erdtman, H.; Högberg, S.; Abrahamsson, S.; Nilsson, B. *Tetrahedron Lett.* **1968**, *9*, 1679.

(110) Högberg, A. G. S. *J. Am. Chem. Soc.* **1980**, *102*, 6046.

(111) Högberg, A. G. S. *J. Org. Chem.* **1980**, *45*, 4498.

(112) Schneider, H.-J.; Gu¨ ttes, D.; Schneider, U. *Angew. Chem. Int. Ed.* **1986**, *25*, 647.

(113) Pellet-Rostaing, S.; Nicod, L.; Chitry, F.; Lemaire, M. *Tetrahedron Lett.* **1999**, *40*, 8793.

(114) Park, S. J.; Hong, J.-I. *Tetrahedron Lett.* **2000**, *41*, 8311.

(115) Grote Gansey, M. H. B.; Bakker, F. K. G.; Feiters, M. C.; Geurts, H. P. M.; Verboom, W.; Reinhoudt, D. N. *Tetrahedron* **1998**, *39*, 5447.

(116) Biros, S. M.; Rebek, J. J. *Chem. Soc. Rev.* **2007**, *36*, 93.

(117) Ahn, D.-R.; Kim, T. W.; Hong, J.-I. *Tetrahedron lett.* **1999**, *40*, 6045.

(118) Sebo, L.; Diederich, F. *Helv. Chim. Acta* **2000**, *83*, 93.

(119) Haino, T.; Rudkevich, D. M.; Rebek, J. J. *J. Am. Chem. Soc.* **1999**, *121*, 11253.

(120) Haino, T.; Rudkevich, D. M.; Shivanyuk, A.; Rissanen, K.; Rebek, J. J. *Chem. Eur. J.* **2000**, *6*, 3797.

(121) Cram, D. J.; Heung-Jin, C.; Bryant, J. A.; Knobler, C. B. *J. Am. Chem. Soc.* **1992**, *114*, 7748.

(122) Hof, F.; Trembleau, L.; Ullrich, E. C.; Rebek, J. J. *Angew. Chem. Int. Ed.* **2003**, *42*, 3150.

(123) Trembleau, L.; Rebek, J. J. *Science* **2003**, *301*, 1219.

(124) Biros, S. M.; Ullrich, E. C.; Hof, F.; Trembleau, L.; Rebek, J. J. *J. Am. Chem. Soc.* **2004**, *126*, 2870.

(125) Hooley, R. J.; Van Anda, H. J.; Rebek, J. J. *J. Am. Chem. Soc.* **2006**, *128*, 3894.

(126) Corbellini, F.; Fiammengo, R.; Timmerman, P.; Crego-Calama, M.; Versluis, K.; Heck, A. J. R.; Luyten, I.; Reinhoudt, D. N. *J. Am. Chem. Soc.* **2002**, *124*, 6569.

(127) Corbellini, F.; Di Costanzo, L.; Crego-Calama, M.; Geremia, S.; Reinhoudt, D. N. *J. Am. Chem. Soc.* **2003**, *125*, 9946.

(128) Xi, H.; Gibb, C. L. D.; Stevens, E. D.; Gibb, B. C. *Chem. Commun.* **1998**, 1743.

(129) Xi, H.; Gibb, C. L. D.; Gibb, B. C. *J. Org. Chem.* **1999**, *64*, 9286.

(130) Green, J. O.; Baird, J.-H.; Gibb, B. C. *Org. Lett.* **2000**, *2*, 3845.

(131) Gibb, C. L. D.; Stevens, E. D.; Gibb, B. C. *J. Am. Chem. Soc.* **2001**, *123*, 5849.

(132) Laughrey, Z. R.; Gibb, C. L. D.; Senechal, T.; Gibb, B. C. *Chem. Eur. J.* **2003**, *9*, 130.

(133) Laughrey, Z. R.; Gibb, B. C. *J. Org. Chem.* **2006**, *71*, 1289.

(134) Gibb, C. L. D.; Gibb, B. C. *J. Am. Chem. Soc.* **2004**, *126*, 11408.

(135) Liu, S.; Gibb, B. C. *Chem. Commun.* **2008**, 3709.

(136) Gibb, C. L. D.; Gibb, B. C. *J. Am. Chem. Soc.* **2006**, *128*, 16498.

(137) Gibb, C. L. D.; Gibb, B. C. *Tetrahedron* **2009**, *65*, 7240.

(138) Gibb, C. L. D.; Gibb, B. C. *Chem. Commun.* **2007**, 1635.

(139) Sun, H.; Gibb, C. L. D.; Gibb, B. C. *Supramol. Chem.* **2008**, *20*, 141.

(140) Chandler, D. *Nature* **2002**, *417*, 491.

(141) Tanford, C. *The Hydrophobic Effect. Formation of Micelles & Biological Membranes*; 2 ed.; John Wiley & Sons: New York, 1980.

(142) Rowan, S. J.; Hamilton, D. G.; Brady, P. A.; Sanders, J. K. M. *J. Am. Chem. Soc.* **1997**, *119*, 2578.

(143) Kaanumalle, L. S.; Gibb, C. L. D.; Gibb, B. C.; Ramamurthy, V. *J. Am. Chem. Soc.* **2004**, *126*, 14366.

(144) Gibb, C. L. D.; Sundaresan, A. K.; Ramamurthy, V.; Gibb, B. C. *J. Am. Chem. Soc.* **2008**, *130*, 4069.

(145) Natarajan, A.; Kaanumalle, L. S.; Jockusch, S.; Gibb, C. L. D.; Gibb, B. C.; Turro, N. J.; Ramamurthy, V. *J. Am. Chem. Soc.* **2007**, *129*, 4132.

(146) Kaanumalle, L. S.; Gibb, C. L. D.; Gibb, B. C.; Ramamurthy, V. *J. Am. Chem. Soc.* **2005**, *127*, 3674.

(147) Liu, S.; Gan, H.; Hermann, A. T.; Rick, S. W.; Gibb, B. C. *Nat. Chem.* **2010**, *2*, 847.

(148) Baldridge, A.; Samanta, S. R.; Jayaraj, N.; Ramamurthy, V.; Tolbert, L. M. *J. Am. Chem. Soc.* **2010**, *132*, 1498.

(149) Baldridge, A.; Samanta, S. R.; Jayaraj, N.; Ramamurthy, V.; Tolbert, L. M. *J. Am. Chem. Soc.* **2011**, *133*.

(150) Porel, M.; Jayaraj, N.; Raghothama, S.; Ramamurthy, V. *Org. Lett* **2010**, *12*, 4544.

(151) Kulasekharan, R.; Jayaraj, N.; Porel, M.; Choudhury, R.; Sundaresan, A. K.; Parthasarathy, A.; Ottaviani, M. F.; Jockusch, S.; Turro, N. J.; Ramamurthy, V. *Langmuir* **2010**, *26*, 6943.

(152) Jayaraj, N.; Maddipatla, M. V. S. N.; Prabhakar, R.; Jockusch, S.; Turro, N. J.; Ramamurthy, V. *J. Phys. Chem. B* **2010**, *114*, 14320.

(153) Jockusch, S.; Zeika, O.; Jayaraj, N.; Ramamurthy, V.; Turro, N. J. *J. Phys. Chem. Lett* **2010**, *1*, 2628.

(154) Podkoscielny, D.; Gadde, S.; Kaifer, A. E. *J. Am. Chem. Soc.* **2009**, *131*, 12876.

(155) Saitoha, M.; Fukaminatoa, T.; Irie, M. *J. Photochem. Photobiol. A–Chem.* **2009**, *207*, 28.

(156) Porel, M.; Jayaraj, N.; Kaanumalle, L. S.; Maddipatla, M. V. S. N.; Parthasarathy, A.; Ramamurthy, V. *Langmuir* **2009**, *25*, 3473.

(157) Jayaraj, N.; Zhao, Y.; Parthasarathy, A.; Porel, M.; Liu, R. S. H.; Ramamurthy, V. *Langmuir* **2009**, *25*, 10575.

(158) Chen, J. Y.-C.; Jayaraj, N.; Jockusch, S.; Ottaviani, M. F.; Ramamurthy, V.; Turro, N. J. *J. Am. Chem. Soc.* **2008**, *130*, 7206.

(159) Podkoscielny, D.; Hooley, R. J.; Rebek, J. J.; Kaifer, A. E. *Org. Lett* **2008**, *10*, 2865.

(160) Sundaresan, A. K.; Ramamurthy, V. *Photochem. Photobiol. Sci.* **2008**, *7*, 1555.

(161) Kaanumalle, L. S.; Ramamurthy, V. *Chem. Commun.* **2007**, 1062.

(162) Sundaresan, A. K.; Ramamurthy, V. *Org. Lett.* **2007**, *9*, 3575.

(163) Parthasarathy, A.; Kaanumalle, L. S.; Ramamurthy, V. *Org. Lett.* **2007**, *9*, 5059.

(164) Karthikeyan, S.; Ramamurthy, V. *J. Org. Chem.* **2006**, *71*, 6409.

(165) Giles, M. D.; Liu, S.; Emanuel, R. L.; Gibb, B. C.; Grayson, S. M. *J. Am. Chem. Soc.* **2008**, *130*, 14430.

(166) Ludlow, R. F.; Otto, S. *Chem. Soc. Rev.* **2008**, *37*, 101.

(167) *Molecular Switches*; Wiley-VCH: Weinheim, 2001.

(168) Tian, H.; Wang, Q. C. *Chem. Soc. Rev.* **2006**, *35*, 361.

(169) Liu, S.; Whisenhunt-Ioup, S. E.; Gibb, C. L. D.; Gibb, B. C. *Supramol. Chem* **2011**, *24*, 480.

(170) Cohen, Y.; Avram, L.; Frish, L. *Angew. Chem. Int. Ed.* **2005**, *44*, 520.

(171) Houk, K. N.; Leach, A. G.; Kim, S. P.; Zhang, X. *Angew. Chem. Int. Ed.* **2003**, *42*, 4872.

(172) Fake, I. **1984**.

(173) Pal, A.; Karthikeyan, S.; Sijbesma, R. P. *J. Am. Chem. Soc.* **2010**, *132*, 7842.

(174) Liu, S.; Ruspic, C.; Mukhopadhyay, P.; Chakrabarti, S.; Zavalij, P. Y.; Isaac, L. *J. Am. Chem. Soc.* **2005**, *127*, 15959.

(175) Schmittel, M.; Mahata, K. *Chem. Commun.* **2010**, *46*, 4163.

(176) Brizard, A.; Stuart, M.; van Bommel, K.; Friggeri, A.; de Jong, M.; van Esch, J. *Angew. Chem. Int. Ed.* **2008**, *120*, 2063.

(177) Cicchi, S.; Ghini, G.; Lascialfari, L.; Brandi, A.; Betti, F.; Berti, D.; Baglioni, P.; Bari, L. D.; Pescitelli, G.; Mannini, M.; Canneschi, A. *Soft Matter* **2010**, *6*, 1655.

(178) Heeres, A.; van der Pol, C.; Stuart, M.; Friggeri, A.; Feringa, B. L.; van Esch, J. *J. Am. Chem. Soc.* **2003**, *125*, 14252.

(179) Moffat, J. R.; Smith, D. K. *Chem. Commun* **2009**, 316.

(180) Xu, H.; Hong, R.; Lu, T. X.; Uzun, O.; Rotello, V. M. *J. Am. Chem. Soc.* **2006**, *128*, 3162.

(181) Jiang, W.; Winkler, H. D. F.; Schalley, C. A. *J. Am. Chem. Soc.* **2008**, *130*, 13852.

(182) Jiang, W.; Schäfer, A.; Mohr, P. C.; Schalley, C. A. *J. Am. Chem. Soc.* **2010**, *132*, 2309.

(183) Jiang, W.; Schalley, C. A. *Proc. Nat. Acad. Sci. U.S.A.* **2009**, *106*, 10425.

(184) Mahata, K.; Schmittel, M. *J. Am. Chem. Soc.* **2009**, *131*, 16544.

(185) Mahata, K.; Saha, M. L.; Schmittel, M. *J. Am. Chem. Soc.* **2010**, *132*, 15933.

(186) Scarso, A.; Trembleau, L.; Rebek, J. J. *J. Am. Chem. Soc.* **2004**, *126*, 13512.

(187) Gan, H.; Benjamin, C. J.; Gibb, B. C. *J. Am. Chem. Soc.* **2011**, *133*, 4770.

(188) Turnbull, W. B.; Daranas, A. H. *J. Am. Chem. Soc.* **2003**, *125* 14859.

(189) Tellinghuisen, J. *J. Phys. Chem.* **2007**, *111*, 11531.

(190) MacGillivray, L. R.; Atwood, J. L. *Nature* **1997**, *389*, 469.

(191) Hiraoka, S.; Nakamura, T.; Shiro, M.; Shionoya, M. *J. Am. Chem. Soc* **2010**, *132*, 13223.

(192) Hofmeister, F. *Arch. Exp. Pathol. Pharmakol.* **1888**, *24*, 247.

(193) Kunz, W.; Henle, J.; Ninham, B. W. *Curr. Opin. Colloid In.* **2004**, *9*, 19.

(194) Kalra, A.; Tugcu, N.; Cramer, S. M.; Garde, S. *J. Phys. Chem. B* **2001**, *105*, 6380.

(195) Collins, K. D.; Washabaugh, M. W. *Q. Rev. Biophys.* **1985**, *18*, 323.

(196) Cacace, M. G.; Landau, E. M.; Ramsden, J. J. *Quarterly Reviews of Biophysics* **1997**, *30*, 241.

(197) McDevit, W. F.; Long, F. A. *J. Am. Chem. Soc.* **1952**, *74*, 1773.

(198) Poiseuille, J. M. L. *Ann. Chim. Phys* **1847**, *21*, 76.

(199) Pegram, L. M.; Record, M. T. J. *J. Phys. Chem. B* **2007**, *111*, 5411.

(200) Pegram, L. M.; Record, M. T. J. *Chem. Phys. Lett.* **2008**, *467*, 1.

(201) Pegram, L. M.; Wendorffa, T.; Erdmanna, R.; Shkela, I.; Bellissimoa, D.; Felitskya, D. J.; Record, M. T. J. *Proc. Nat. Acad. Sci. U.S.A.* **2010**, *107*, 7716.

(202) Baldwin, R. L. *Biophys. J.* **1996**, *71*, 2056.

(203) Zangi, R.; Hagen, M.; Berne, B. J. *J. Am. Chem. Soc.* **2007**, *129*, 4678.

(204) Smith, J. D.; Saykally, R. J.; Geissler, P. L. *J. Am. Chem. Soc.* **2007**, *129*, 13847.

(205) Gibb, C. L. D.; Gibb, B. C. *J. Am. Chem. Soc.* **2011**, *133*, 7344.

(206) Collins, K. D. *Biophys. J.* **1997**, *72*, 65.

(207) Frish, L.; Matthews, S. E.; Böhmer, V.; Cohen, Y. *J. Chem. Soc. Perkin Trans 2* **1999**, 669.

(208) Frank, H.; Evans, M. W. *J. Phys. Chem.* **1945**, *13*, 507.

(209) Dill, K. A.; Truskett, T. M.; Vlachy, V.; Hribar-Lee, B. *Annu. Rev. Biophys. Biomol. Struct.* **2005**, *34*, 173.

(210) Slusher, J. T.; Cummings, P. T. *J. Phys. Chem. B* **1997**, *101*, 3818.

(211) Kustov, A. V.; Smirnova, N. L. *J. Phys. Chem. B* **2011**, ASAP.

(212) Jain, S.; Ahluwalia, J. C. *Biophys. Chem.* **1996**, *59*, 171.

(213) Gurney, R. W. *Ionic Process in Solution*; McGraw-Hill: New York, 1953.

(214) Desnoyers, J. E.; Pelletier, G. E.; Jolicoeur, C. *Can. J. Chem* **1965**, *43*, 3232.

Vita

Haiying Gan was born in Xi'An, Shaanxi, P. R. of China. She received a B.S. degree of Orgainic Chemistry in 2001 from the Northwest University of China. She entered the Departemnt of Chemistry of the University of New Orleans in 2005 and studied in Physical Organic and Supramolecular under the guidance of Prof. Bruce C. Gibb.